Supplementary Material File ESI1

DETAILED EXPERIMENTAL
Chemical and biochemical reactivity of the reduced forms of nicotinamide riboside

Mikhail V. Makarov[*], Faisal Hayat[*], Briley Graves, Manoj Sonavane, Edward A. Salter, Andrzej Wierzbicki, Natalie R. Gassman and Marie E. Migaud[$]

[$]Corresponding author: mmigaud@southalabama.edu
*Joint first authorship.

Table of contents

General remarks. NMR spectra were recorded on a Bruker Avance III HD 400 spectrometer (^{1}H, 400.11; ^{19}F, 376.44; and ^{13}C, 100.62 MHz) using residual proton signal (^{1}H) and that of carbon atom (^{13}C) of a deuterated solvent as an internal standard relative to TMS, and $CFCl_3$ (^{19}F) as an external standard. Column chromatography was performed on silica gel columns using Teledyne medium pressure liquid chromatography system with UV monitoring of eluted fractions (at 280 nm and 350 nm). Analytical TLCs were performed with Merck silica gel 60 F254 plates; visualization of TLCs was accomplished by UV light. HRMS spectra were obtained on LTQ Orbitrap XL Mass Spectrometer (HESI source, positive polarity, capillary temp 200°C, source voltage 3.0 kV).

All commercial reagents were purchased from VWR and used without further purification. Anhydrous DCM was obtained by distillation of commercial DCM (from VWR) over calcium hydride. Anhydrous commercial DMF was kept over calcinated molecular sieves. Anhydrous MeOH was prepared by distillation over Mg in the presence of iodine according to standard procedure and kept afterward over molecular sieves (*cf.*: W.L.F. Armarego and C.L.L. Chai, *Purification of Laboratory Chemicals*, 6th Ed., Butterworth-Heinemann/Elsevier, Burlington/Oxford, **2009**).

Reduction of pyridinium salts, including *N*-alkylated nicotinamide salts, to mixtures of corresponding isomeric 1,2-, 1,4-, and 1,6-dihydropyridines, in anhydrous DMF at 0°C along with the assignment of proton signals for the 1,2-, 1,4-, and 1,6-dihydropyridine core in the ^{1}H NMR spectra was previously described in the literature and relied upon in this work (*cf.*: R.B. Schmidt, G. Berger, *Chem. Ber.* **1976**, *109*, 2936–2947).

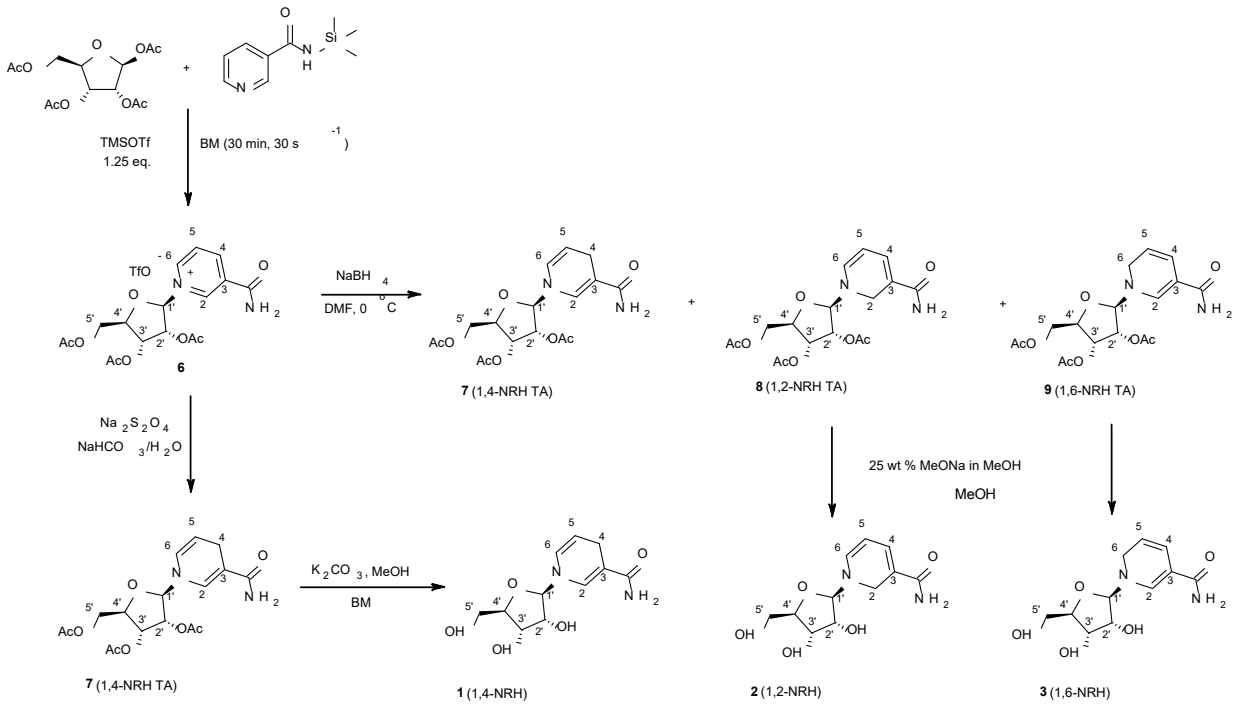

Scheme S1. Synthesis of 1,2-NRH, 1,4-NRH and 1,6-NRH.

***N*-(Trimethylsilyl)nicotinamide.** A 250 mL round-bottom two-neck flask equipped with a reflux condenser was charged with nicotinamide (5.00 g; 0.041 mol) followed by the addition of HMDS (45 mL; 34.6 g; 0.215 mol; 5.2 equiv.) and TMSCl (10.4 mL; 8.9 g; 0.082 mol; 2 equiv.) *via* a syringe in one portion. The reaction mixture was heated in an oil bath to 105°C (oil bath temperature) at stirring and was left under these conditions overnight. The next day, a clear, colorless solution formed; the flask was taken from the heating oil bath and the warm reaction solution was transferred into a round-bottom single-neck flask through a cannula. The solution was evaporated to dryness on a rotary evaporator followed by drying under high vacuum to give colorless crystalline product, 7.95 g (100%). ^{1}H NMR (C_6D_6), δ, ppm: 0.00 (br s, 9H, $SiMe_3$), 5.89 (br s, 1H, NH), 6.38 (dd, 1H, $^{3}J_{HH}$= 4.9 Hz, $^{3}J_{HH}$= 8.0 Hz, H5), 7.62 (d, 1H, $^{3}J_{HH}$= 8.0 Hz, H4), 8.12 (d, 1H, $^{3}J_{HH}$= 4.7 Hz, H6), 8.82 (br s, 1H, H2). ^{13}C NMR ($CDCl_3$), δ, ppm: 0.22 ($SiMe_3$), 124.10 (C5), 131.81 (C3), 136.22 (C4), 149.88 (C2), 153.07 (C6), 171.35 (CO).

3-Carbamoyl-1-((2*R*,3*R*,4*R*,5*R*)-3,4-diacetoxy-5-(acetoxymethyl)tetrahydrofuran-2-yl)pyridin-1-ium trifluoromethanesulfonate (6). A PTFE jar was charged with *N*-(trimethylsilyl)nicotinamide (0.80 g; 0.004 mol), 1,2,3,5-tetra-*O*-acetyl-D-β-ribofuranose (1.31 g; 0.004 mol) and anhydrous DCM (0.4 mL; 0.006 mol) was added, followed by addition of TMSOTf (1.13 g; 0.005 mol). The reagents were subjected to ball-milling on a Retsch MM400 miller for 30 min at 30 Hz. The jar was allowed to cool down to room temperature. The content of the jar was dissolved in DCM (2×10 mL) and the yellow solution was transferred into a round bottom flask. Volatiles were removed on a rotary evaporator to dryness to give a yellow foam (2.92 g; ca. quantitative yield as calculated on N-silylated form of **6**) triturated by a spatula resulting in a yellow powder. The product containing residues of acetic acid and silylated residues was used on the next step without additional purification. ^{19}F NMR (D_2O), δ, ppm: -78.83. ^{1}H NMR (D_2O), δ, ppm: 1.95 (Me from acetic acid residue), 2.02 (s, 3H, Me), 2.06 (s, 3H, Me), 2.09 (s, 3H, Me), 4.42–4.50 (m, 2H, H5′), 4.80–4.83 (m, 1H, H4′), 5.38 (apparent t, 1H, $^{3}J_{HH}$= 5.4 Hz, H3′), 5.49 (dd, 1H, $^{3}J_{HH}$= 3.8 Hz, $^{3}J_{HH}$= 5.8 Hz, H2′), 6.51 (d, 1H, $^{3}J_{HH}$= 3.7 Hz, H1′), 8.21 (dd, 1H, $^{3}J_{HH}$= 6.5 Hz, $^{3}J_{HH}$= 8.7 Hz, H5), 8.92 (d, 1H, $^{3}J_{HH}$= 8.0 Hz, H4), 9.13 (d, 1H, $^{3}J_{HH}$= 6.4 Hz, H6), 9.37 (s, 1H, H2). ^{13}C NMR (D_2O), δ, ppm: 19.92 (Me), 19.97 (Me), 20.31 (Me), 20.52 (Me from acetic acid residue), 62.77 (C5′), 69.54 (C3′), 76.50 (C2′), 82.78 (C4′), 97.48 (C1′), 119.77 (CF_3, $^{1}J_{CF}$=316 Hz), 128.78 (C5), 134.36 (C3), 140.58 (C2), 143.23 (C6), 146.39 (C4), 165.60 ($CONH_2$), 172.53 (CO), 172.58 (CO), 173.48 (CO), 176.77 (CO from acetic acid residue). MS: found m/z = 380.84 (M). HRMS found: 381.12965. Calculated for $C_{17}H_{21}N_2O_8$ (M): 381.12924.

(2*R*,3*R*,4*R*,5*R*)-2-(Acetoxymethyl)-5-(3-carbamoylpyridin-1(4*H*)-l)tetrahydrofuran-3,4-diyl diacetate (7). In a round bottom flask flushed with nitrogen, compound **6** (2.85 g, ca. 0.004 mol) was dissolved in a nitrogen-purged DCM (40 mL) and 13 mL of saturated aqueous $NaHCO_3$ solution were added, followed by addition of solid sodium dithionite (ca. 85%; 4.27 g; 0.021 mol) and 7 mL of water at stirring and at room temperature. The biphasic reaction mixture was stirred at room temperature for 4 h, and then brine (30 mL) and DCM (40 mL) were added. Yellow organic phase was separated, washed twice with brine, dried over Na_2SO_4, filtered and evaporated under reduced pressure to give light yellow foam (1.35 g; 84% based on compound **3**). ^{1}H NMR ($CDCl_3$), δ, ppm: 2.02 (s, 3H, Me), 2.04 (s, 3H, Me), 2.10 (s, 3H, Me), 3.06 (q, 2H, $^{3}J_{HH}$= 1.4 Hz, H4), 4.11 (dd, 1H, $^{3}J_{HH}$= 4.7 Hz, $^{3}J_{HH}$= 3.2 Hz, H4′), 4.20–4.21 (m, 2H, H5′), 4.80 (dt, 1H, $^{3}J_{HH}$= 3.4 Hz, $^{3}J_{HH}$= 8.2 Hz, H5), 4.89 (d, 1H, $^{3}J_{HH}$= 7.0 Hz, H1′), 5.11 (t, 1H,

$^{3}J_{HH}$= 6.4 Hz, H2′), 5.18 (dd, 1H, $^{3}J_{HH}$= 2.8 Hz, $^{3}J_{HH}$= 5.8 Hz, H3′), 5.27 (br s, 2H, NH_2), 5.88 (dd, 1H, $^{4}J_{HH}$= 1.7 Hz, $^{3}J_{HH}$= 8.2 Hz, H6), 7.09 (s, 1H, H2). ^{13}C NMR ($CDCl_3$), δ, ppm: 18.47 (Me), 18.59 (Me), 18.79 (Me), 21.22 (C4), 61.60 (C5′), 68.87 and 68.91 (C3′ and C2′), 77.05 (C4′), 91.36 (C1′), 100.38 (C3), 102.49 (C5), 123.07 (C6), 134.36 (C2), 167.52 (two overlapped CO), 167.53 (CO), 168.55 (CO). MS: found m/z = 382.96 (M+1). HRMS found: 383.14530. Calculated for $C_{17}H_{23}N_2O_8$ (M+1): 383.14489.

1-((2*R*,3*R*,4*S*,5*R*)-3,4-Dihydroxy-5-(hydroxymethyl)tetrahydrofuran-2-yl)-1,4-dihydropyridine-3-carboxamide (1). A PTFE jar was charged with compound **7** (0.50 g; 0.0013 mol), anhydrous potassium carbonate (0.0180 g; 0.00013 mol) and methanol (0.3 mL; 0.238 g; 0.0074 mol) were added. The reagents were subjected to ball-milling on a Retsch MM400 miller for 25 min at 25 Hz. The jar was allowed to cool down to room temperature. The content of the jar was dissolved in methanol (2×10 mL) and the yellow solution was transferred into a round bottom flask. Volatiles were removed on a rotary evaporator to dryness to give a yellow foam that was triturated with diethyl ether resulting in a yellow powder. Diethyl ether was removed by decantation and the product was dried under reduced pressure at 34°C. Yield: 0.34 g (ca. 100%). ^{1}H NMR (D_2O), δ, ppm: 2.98 (q, 2H, $^{3}J_{HH}$= 1.5 Hz, H4), 3.26 (s, 1.5H, 0.5 MeOH), 3.60 and 3.66 (AB part of ABX system, 2H, J_{AB}=12.5 Hz, J_{BX}= 4.8 Hz, J_{AX}= 3.6 Hz, H5′$_A$ and H5′$_B$), 3.88 (dd, 1H, $^{3}J_{HH}$= 6.8 Hz, $^{3}J_{HH}$= 3.5 Hz, H4′), 4.04 (dd, 1H, $^{3}J_{HH}$= 2.9 Hz, $^{3}J_{HH}$= 5.6 Hz, H3′), 4.11 (t, 1H, $^{3}J_{HH}$= 6.3 Hz, H2′), 4.66 (OH, NH_2 overlapped with D_2O), 4.79 (d, 1H, $^{3}J_{HH}$= 7.0 Hz, H1′), 4.90 (dt, 1H, $^{3}J_{HH}$= 3.4 Hz, $^{3}J_{HH}$= 8.2 Hz, H5), 6.01 (dd, 1H, $^{4}J_{HH}$= 1.5 Hz, $^{3}J_{HH}$= 8.2 Hz, H6), 7.06 (s, 1H, H2). ^{13}C NMR (D_2O), δ, ppm: 22.07 (C4), 49.00 (MeOH), 61.63 (C5′), 70.21 (C3′), 71.11 (C2′), 83.56 (C4′), 95.03 (C1′), 101.08 (C3), 105.20 (C5), 125.37 (C6), 137.80 (C2), 172.96 (CO). MS: found m/z = 257.21 (M+1). HRMS found: 257.11376. Calculated for $C_{11}H_{17}N_2O_5$ (M+1): 257.11320

Reduction of NRTA OTf (6) with sodium borohydride in DCM/water: Synthesis of 1,2-NRH TA (8) and 1,6-NRH TA (9). Compound **6** (4.25 g; prepared from 1.43 g (0.0074 mol) of silylated nicotinamide and 2.35 g (0.0074 mol) of 1,2,3,5-tetra-*O*-acetyl-D-β-ribofuranose in a yield of ca. 96% as calculated on N-silylated form of **6**) was dissolved in a mixture of 25 mL of water and 75 mL of DCM. The biphasic mixture was cooled in an ice bath at stirring, and 5 mL of an aqueous solution of freshly prepared sodium borohydride (0.133 g, 0.0035 mol) were added. The reaction mixture was stirred at cooling for 2 hours with monitoring by ^{1}H NMR (acetone-d_6); at the 2 h time point, the ^{1}H NMR indicated an incomplete reduction of starting compound **6**. Additional 0.266 g of sodium borohydride in 4 mL of water were added (0.39 g of $NaBH_4$; 0.010 mol in total) and stirring of the reaction mixture was continued at r.t. for 1 h. At this time point, ^{1}H NMR (acetone-d_6) of the reaction mixture indicated a complete reduction of compound **6**. Organic phase was separated, washed with brine, dried over Na_2SO_4, filtered and evaporated to give a yellow solid foam, 2.30 g (85%). According to ^{1}H NMR, the foam contained a mixture of 1,2-NRH TA, 1,4-NRH TA, and 1,6-NRH TA in a ratio of ca. 0.9:0.8:1.0 (**Fig. 24S**). To isolate 1,2- and 1,6-isomers of NRH TA, the reaction product was subjected to silica gel column chromatography using a Teledyne chromatography system (RediSep® Flash Column, 40 gram). Fractions were UV monitored at 254 and 350 nm. Chromatography parameters: flow rate, 25 mL/min; fractions volume, 20 mL. Fraction 1 was eluted with hexanes, fraction 2 was eluted with a 45:55 hexanes/EtOAc mixture, fractions 3–30 were eluted with EtOAc, fractions 31–34 were eluted with a 5:95 EtOH/EtOAc mixture, and further elution was continued with a 10:90 EtOH/EtOAc mixture. 1,2-NRH TA was eluted in fractions 12–16 (UV absorption at 350 nm, **Fig. 26S**), and after evaporation of the fractions, 0.27 g (ca. 10% yield) of 1,2-NRH TA were obtained (portion A). Mixtures of 1,4-NRH TA and 1,6-NRH TA were eluted in fractions 41–46, with the content of 1,6-NRH TA being maximal in fraction 46. UV monitoring of the fractions during chromatography indicated two absorption peaks at 254 nm which were partially overlapping (**Fig. 25S**). Based on the absorbance pattern, fractions 41–43 were combined and evaporated to afford 0.51 g (ca. 19% yield) of portion B. Fractions 44–46 were combined and evaporated to give 0.38 g (ca. 14% yield) of portion C. Each

of portions A–C was analyzed by ^{1}H NMR (acetone-d_6), and it was found that portion A was composed of 1,2-NRH TA (with some residual DCM and EtOAc being present) (**Figs. 26S** and **27S**). According to integration of the ^{1}H NMR (and ^{13}C NMR) spectra, portion B was composed of a ca. 1.0:0.6 1,4-NRH TA/1,6-NRH TA mixture (**Fig. 32S**); portion C was composed of a ca. 0.2:1.0 1,4-NRH TA/1,6-NRH TA mixture (**Figs. 33S** and **34S**).

Reduction of NRTA OTf (6) with sodium borohydride in DMF: Synthesis of compounds 8 (1,2-NRH TA) and 9 (1,6-NRH TA). Compound **6** (8.50 g; prepared from 2.65 g (0.0137 mol) of silylated nicotinamide and 4.35 g (0.0137 mol) of 1,2,3,5-tetra-*O*-acetyl-D-β-ribofuranose in a yield of ca. 100% as calculated on N-silylated form of **6**) was dissolved in 55 mL of anhydrous DMF. The solution was cooled in an ice bath (0 ºC) at stirring and a solution of sodium borohydride (0.54 g, 0.0143 mol) in 25 mL of anhydrous DMF was added to the stirred and cooled solution. The reaction mixture was stirred at cooling for 30 min and monitored by ^{1}H NMR (acetone-d_6) at this time point, indicating the complete reduction of starting compound **3** and formation of a mixture of 1,2-, 1,4-, and 1,6-isomeric mixture of NRH TA. The reaction was quenched with brine (ca. 70 mL), and the aqueous phase was repeatedly (8×) extracted with EtOAc (500 mL total volume). The organic phase was washed with brine (8×40 mL), dried over Na_2SO_4, filtered, and evaporated. To remove residual DMF, the product was dissolved in ca. 150 mL of EtOAc and extracted with brine (5×30 mL); the organic phase was dried over Na_2SO_4, filtered, and evaporated to give yellow solid foam in the amount of 3.61 g (69%). According to ^{1}H NMR, the foam contained a mixture of 1,2-NRH TA, 1,4-NRH TA, and 1,6-NRH TA in the ratio of ca. 1.0:0.44:1.0, respectively (**Fig. 40S**). To isolate 1,2- and 1,6-isomers of NRH TA, the reaction product was subjected to silica gel column chromatography using Teledyne chromatography system (RediSep® Flash Column 80 gram, catalog # 69-2203-380). Fractions were UV monitored at 254 and 350 nm. Chromatography parameters: flow rate, 30 mL/min; fractions volume 20 mL. Fractions 1–4 were eluted with hexanes, fractions 5–9 were eluted with a 40:60 hexanes/EtOAc mixture, after which elution was continued with EtOAc (fractions 10–68), 5:95 EtOH/EtOAc (fractions 69–79) and 10:90 EtOH/EtOAc (fractions 80–85) mixtures. 1,2-NRH TA was eluted in fractions 23–35 (UV absorption at 350 nm). Fractions 24–28 were combined and evaporated to give portion A (0.51 g, 9.7 %); fractions 29–35 were combined and evaporated to give portion B (0.245 g; 4.7 %). Mixtures of 1,4-NRH TA and 1,6-NRH TA were eluted in fractions 51–85, with last fractions containing mostly 1,6-NRH TA. In particular, fractions 51–58 were combined and evaporated to give portion C (0.404 g, 7.7 %); fractions 59–70 were combined and evaporated to give portion D (0.323 g, 6.2 %); fractions 71–79 were combined and evaporated to give portion E (0.226 g, 4.3 %); and fractions 80–85 were combined and evaporated to give portion F (0.108 g, 2.1 %). The total amount of eluted compounds was 1.82 g (35 %). Each of portions A–F was analyzed by ^{1}H NMR (acetone-d_6) and it was found that portions A, B were composed of 1,2-NRH TA (with some residual DCM and EtOAc being present), resulting in the isolated yield of 1,2-NRH TA being equal ca. 0.75 g (14.3 %). According to the ^{1}H NMR spectral data (**Fig. 41S**), portion C was composed of a ca. 1.0:0.5 1,4-NRH TA/1,6-NRH TA mixture; portion D was composed of a ca. 0.4:1.0 1,4-NRH TA/1,6-NRH TA mixture; portion E was composed of a ca. 0.12:1.0 1,4-NRH TA/1,6-NRH TA mixture; and portion E was composed of 1,6-NRH TA, with all the listed portions containing some residual EtOAc. For full characterization, portions A+B and F were analyzed by ^{1}H and ^{13}C NMR (acetone-d_6) (**Figs. 42S–45S** and **Figs. 46S–50S,** respectively).

(2*R*,3*R*,4*R*,5*R*)-2-(acetoxymethyl)-5-(3-carbamoylpyridin-1(2*H*)-yl)tetrahydrofuran-3,4-diyl diacetate (8, 1,2-NRH TA). ^{1}H NMR (acetone-d_6, 400 MHz), δ, ppm: 1.90 (s, 3H, Me), 1.95 (s, 3H, Me), 2.04 (s, 3H, Me), 3.90–3.93 (dd, 1H, $^3J_{HH}$= 13.2 Hz, $^4J_{HH}$= 1.1 Hz, 1/2H2), 4.07–4.10 (m, 2H, H4′+1/2H5′), 4.14–4.20 (m, 2H, 1/2H2+1/2H5′), 4.76 (dd, 1H, $^3J_{HH}$= 6.0 Hz, $^3J_{HH}$= 7.0 Hz, H5), 4.94 (d, 1H, $^3J_{HH}$= 7.0 Hz, H1′), 5.15 (dd, $^3J_{HH}$= 2.8 Hz, $^3J_{HH}$= 5.8 Hz, 1H, H3′), 5.27 (t, 1H, $^3J_{HH}$= 6.4 Hz, H2′), 6.23 (br s, 2H, NH_2), 6.40 (d, 1H, $^3J_{HH}$= 7.2 Hz, H4), 6.58 (d, 1H, $^3J_{HH}$= 5.9 Hz, H6). ^{13}C NMR

(acetone-d_6, 100 MHz), δ, ppm: 19.46 (Me), 19.63 (Me), 19.83 (Me), 40.81 (C2), 63.41 (C5′), 68.52 (C2′), 71.02 (C3′), 78.72 (C4′), 94.99 (C1′), 96.54 (C5), 116.04 (C3), 128.72 (C6), 140.70 (C4), 167.60 (CO), 169.11 (CO), 169.33 (CO), 170.03 (CO). MS: found m/z = 383.07 (M+1). HRMS: found m/z = 383.1453; calculated for M+1 ($C_{17}H_{23}N_2O_8$) m/z = 383.1454.

(2*R*,3*R*,4*R*,5*R*)-2-(acetoxymethyl)-5-(5-carbamoylpyridin-1(2*H*)-yl)tetrahydrofuran-3,4-diyl diacetate (9, 1,6-NRH TA). 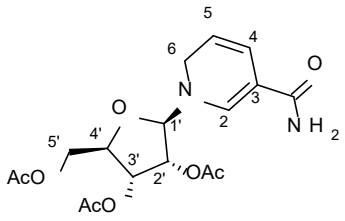 ^{1}H NMR (acetone-d_6, 400 MHz), δ, ppm: 2.04 (s overlapped with acetone-d_6, 3H, Me), 2.07 (s, 3H, Me), 2.08 (s, 3H, Me), 4.10–4.12 (m, 2H, H6), 4.20–4.23 (m, 1H, H4′), 4.23–4.29 (m, 2H, H5′), 5.06 (d, 1H, $^3J_{HH}$= 6.7 Hz, H1′), 5.18 (dt, 1H, $^3J_{HH}$= 3.7 Hz, $^3J_{HH}$= 9.9 Hz, H5), 5.23 (dd, 1H, $^3J_{HH}$= 3.4 Hz, $^3J_{HH}$= 5.7 Hz, H3′), 5.36 (t, 1H, $^3J_{HH}$= 6.3 Hz, H2′), 6.09 (br s, 2H, NH_2), 6.29 (dd, 1H, $^4J_{HH}$= 1.5 Hz, $^3J_{HH}$= 10.0 Hz, H4), 7.24 (s, 1H, H2). ^{13}C NMR (acetone-d_6, 100 MHz), δ, ppm: 19.46 (Me), 19.63 (Me), 19.83 (Me), 42.33 (C6), 63.24 (C5′), 68.63 (C2′), 70.57 (C3′), 78.67 (C4′), 95.20 (C1′), 104.07 (C3), 111.91 (C5), 122.21 (C4), 142.06 (C2), 167.14 (CO), 169.32 (CO), 169.82 (CO), 169.93 (CO). MS: found m/z = 383.09 (M+1). HRMS: found m/z = 383.1455; calculated for M+1 ($C_{17}H_{23}N_2O_8$) m/z = 383.1454.

General procedure for the synthesis of 1,2-NRH (2) and 1,6-NRH (3). Under an argon atmosphere and at room temperature, isomeric NRH triacetate (compound **8** or **9**) (0.38 g; 1 mmol) was dissolved in anhydrous and degassed MeOH (7 mL) and 25 wt. % solution of sodium methoxide in methanol (60 μL; 0.26 mmol) was added at stirring thereto. The reaction solution was stirred under these conditions for ca. 30 min (TLC control in 10:3 EtOAc/EtOH mixture) and evaporated under reduced pressure at room temperature. Anhydrous DCM was added to the residue and evaporated to afford the corresponding deacetylated product (compound **2** (1,2-NRH) or compound **3** (1,6-NRH)) as a yellow solid in virtually quantitative yield (0.26 g).

1-((2*R*,3*R*,4*S*,5*R*)-3,4-dihydroxy-5-(hydroxymethyl)tetrahydrofuran-2-yl)-1,2-dihydropyridine-3-carboxamide (2, 1,2-NRH). 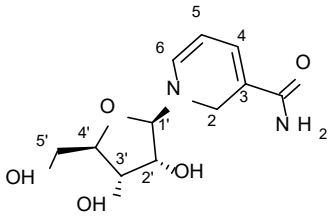 ^{1}H NMR (D_2O, 400 MHz), δ, ppm: 3.25 (0.78 Me from MeOH), 3.60 and 3.67 (AB part of ABX system, 2H, J_{AB}=12.4 Hz, J_{BX}= 3.7 Hz, J_{AX}= 5.0 Hz, H5′$_A$ and H5′$_B$), 3.85–3.88 (m, 1H, H4′), 3.91 (d, 1H, $^3J_{HH}$= 12.8 Hz, 1/2H2), 4.02 (dd, 1H, $^3J_{HH}$= 3.4 Hz, $^3J_{HH}$= 5.7 Hz, H3′), 4.08 (d, 1H, $^3J_{HH}$= 12.8 Hz, 1/2H2), 4.19 (t, 1H, $^3J_{HH}$= 6.2 Hz, H2′), 4.81 (d, $^3J_{HH}$= 3.4 Hz, 1H, H1′), 5.02 (t, 1H, $^3J_{HH}$= 6.6 Hz, H5), 6.57 (d, 1H, $^3J_{HH}$= 7.0 Hz, H4), 6.77 (d, 1H, $^3J_{HH}$= 6.1 Hz, H6). ^{13}C NMR (D_2O, 100 MHz), δ, ppm: 40.83 (C2), 48.83 (MeOH), 61.57 (C5′), 69.36 (C2′), 70.24 (C3′), 83.08 (C4′), 96.48 (C1′), 97.36 (C5), 111.89 (C3), 133.22 (C6), 142.57 (C4), 171.19 (CO). HRMS: found m/z = 257.1137; calculated for M+1 ($C_{11}H_{17}N_2O_5$) m/z = 257.1132.

1-((2*R*,3*R*,4*S*,5*R*)-3,4-dihydroxy-5-(hydroxymethyl)tetrahydrofuran-2-yl)-1,6-dihydropyridine-3-carboxamide (3, 1,6-NRH). 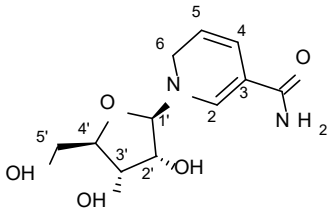 ^{1}H NMR (D_2O, 400 MHz), δ, ppm: 3.25 (1.27 Me from MeOH), 3.58 and 3.66 (AB part of ABX system, 2H, J_{AB}=12.2 Hz, J_{BX}= 3.9 Hz, J_{AX}= 5.8 Hz, H5′$_A$ and H5′$_B$), 3.87–3.90 (m, 1H, H4′), 3.98 (dd, 1H, $^3J_{HH}$= 3.6 Hz, $^3J_{HH}$= 5.7 Hz, H3′), 4.01–4.03 (m, 2H, H6), 4.18 (t, 1H, $^3J_{HH}$= 6.0 Hz, H2′), 4.82 (d, 1H, $^3J_{HH}$= 6.4 Hz, H1′), 5.20 (dt, 1H, $^3J_{HH}$= 3.7 Hz, $^3J_{HH}$= 10.0 Hz, H5), 6.10 (dd, 1H, $^4J_{HH}$= 1.4 Hz, $^3J_{HH}$= 10.0 Hz, H4), 7.24 (s, 1H, H2). ^{13}C NMR (D_2O, 100 MHz), δ, ppm: 42.37 (C6), 48.83 (MeOH), 61.51 (C5′), 69.55 (C2′), 70.37 (C3′), 83.47 (C4′), 97.31 (C1′), 100.42 (C3), 112.84 (C5), 120.54 (C4), 145.18 (C2), 171.44 (CO). HRMS: found m/z = 257.1140; calculated for M+1 ($C_{11}H_{17}N_2O_5$) m/z = 257.1132.

Table S1. ^{1}H NMR data of compounds **7**, **8**, **9** and **1**, **2**, **3**.

Compound (Solvent)	Chemical shifts, number of protons, multiplicity of peaks (J values in Hz)								
	H2	H4	H5	H6	H1’	H2’	H3’	H4’	H5’
7 ($CDCl_3$)	7.09, 1H, s	3.06, 2H, q (J = 1.4)	4.80, 1H, dt (J = 3.4; 8.2)	5.88, 1H, dd (J = 1.7; 8.2)	4.89, 1H, d (J = 7.0)	5.11, 1H, t (J = 6.4)	5.18, 1H, dd (J = 2.8; 5.8)	4.11, 1H, dd (J = 3.2; 4.7)	4.20–4.21, 2H, m
8 (acetone-d_6)	3.90–3.93, 1H (1/2H2), dd (J = 1.1; 13.2) 4.14–4.20,* 1H (1/2H2), m	6.40, 1H, d (J = 7.2)	4.76, 1H, dd (J = 6.0; 7.0)	6.58, 1H, d (J = 5.9)	4.94, 1H, d (J = 7.0)	5.27, 1H, t (J = 6.4)	5.15, 1H, dd (J = 2.8; 5.8)	4.07–4.10, 2H (H4’+1/2H5’), m	
9 (acetone-d_6)	7.24, 1H, s	6.29, 1H, dd (J = 1.5; 10.0)	5.18, 1H, dt (J = 3.7; 9.9)	4.10–4.12, 2H, m	5.06, 1H, d (J = 6.7)	5.36, 1H, t (J = 6.3)	5.23, 1H, dd (J = 3.4; 5.7)	4.20–4.23, 1H, m	4.23–4.29, 2H, m
1 (D_2O)	7.06, 1H, s	2.98, 2H, q (J = 1.5)	4.90, 1H, dt (J = 3.4; 8.2)	6.01, 1H, dd (J = 1.5; 8.2)	4.79, 1H, d (J = 7.0)	4.11, 1H, t (J = 6.3)	4.04, 1H, dd (J = 2.9; 5.6)	3.88, 1H, dd (J = 3.5; 6.8)	3.60, 3.66, 2H, AB of ABX (J =12.5; 3.6; 4.8)
2 (D_2O)	3.91, 1H (1/2H2), d (J = 12.8) 4.08, 1H (1/2H), d (J = 12.8)	6.57, 1H, d (J = 7.0)	5.02, 1H, t (J = 6.6)	6.77, 1H, d (J = 6.1)	4.81, 1H, d (J = 3.4)	4.19, 1H, t (J = 6.2)	4.02, 1H, dd (J = 3.4; 5.7)	3.85–3.88, 1H, m	3.60, 3.67, 2H, AB of ABX (J =12.4; 3.7; 5.0)
3 (D_2O)	7.24, 1H, s	6.10, 1H, dd (J = 1.4; 10.0)	5.20, 1H, dt (J = 3.7; 10.0)	4.01–4.03, 2H, m	4.82, 1H, d (J = 6.4)	4.18, 1H, t (J = 6.0)	3.98, 1H, dd (J = 3.6; 5.7)	3.87–3.90, 1H, m	3.58, 3.66, 2H, AB of ABX (J =12.2; 3.9; 5.8)

* Overlapped with 1/2H5’

Table S2. ^{3}C NMR data of compounds **7**, **8**, **9** and **1**, **2**, **3**.

Compound (Solvent)	Chemical shifts									
	C2	C3	C4	C5	C6	C1’	C2’	C3’	C4’	C5’
7 ($CDCl_3$)	134.36	100.38	21.22	102.49	123.07	91.36	68.87, 68.91		77.05	61.60
8 (acetone-d_6)	40.81	116.04	140.70	96.54	128.72	94.99	68.52	71.02	78.72	63.41
9 (acetone-d_6)	142.06	104.07	122.21	111.91	42.33	95.20	68.63	70.57	78.67	63.24
1 (D_2O)	137.80	101.08	22.07	105.20	125.37	95.03	71.11	70.21	85.36	61.63
2 (D_2O)	40.83	111.89	142.57	97.36	133.22	96.48	69.36	70.24	83.08	61.57
3 (D_2O)	145.18	100.42	120.54	112.84	42.37	97.31	69.55	70.37	83.47	61.51

Isomerism of NRH and NR^+:

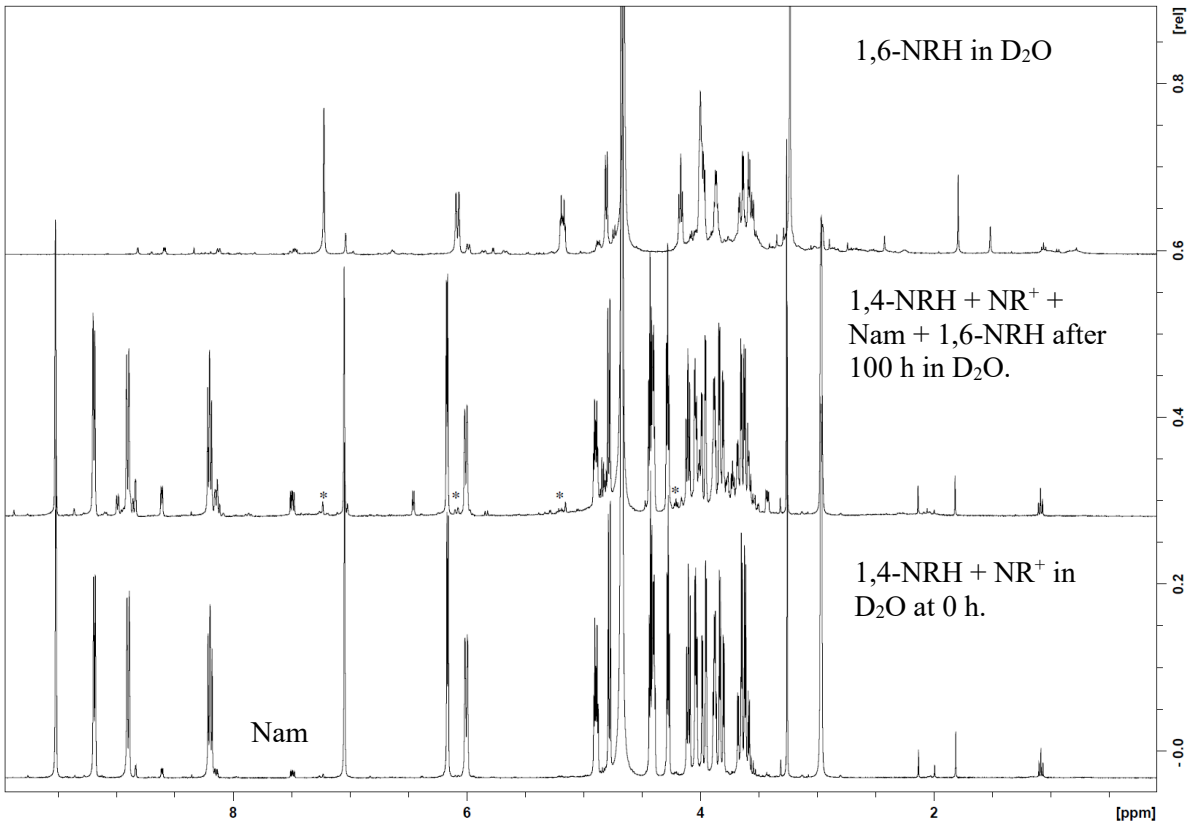

Fig. S1: ESI-NMR1: 1,4-NRH was co-incubated with NR^+ in D_2O (final concentration 10mM of each component). Under these conditions, the 1,6-NRH isomer formed and could be detected after 100 h as indicated by a *.

Products that can readily be identified include alpha and beta-ribose, nicotinamide, NR^+ and 1,6-NRH. The appearance of products with aliphatic hydrogens consistent with structures proposed by Margoli via the intermediacy of NR(OH)H, which can also generate decomposition products as proposed in the scheme below, which remain to be characterized.

Figure S2: Buffer conditions affect the stability of 1,2-, 1,4- and 1,6-NRH in solution in absence of NQO2.

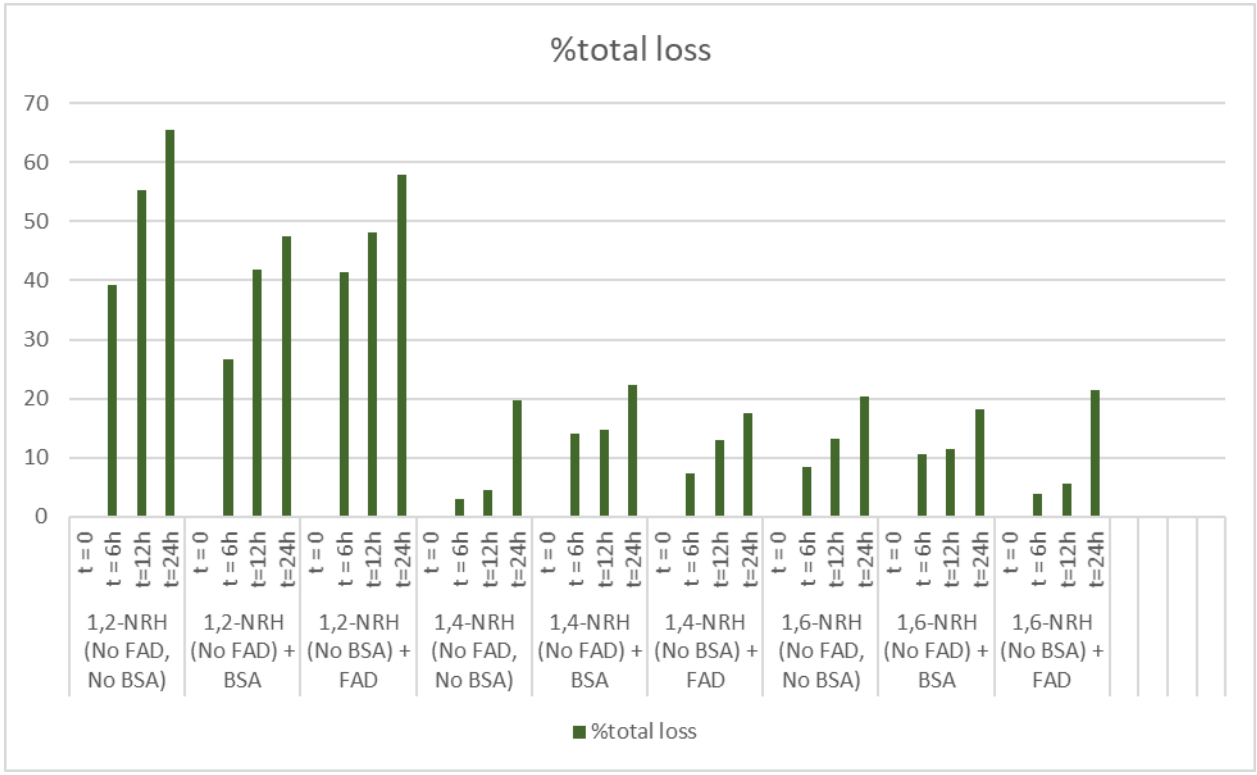

Figure S3: Buffer conditions affect the product distribution of 1,6-NRH in solution in absence of NQO2.

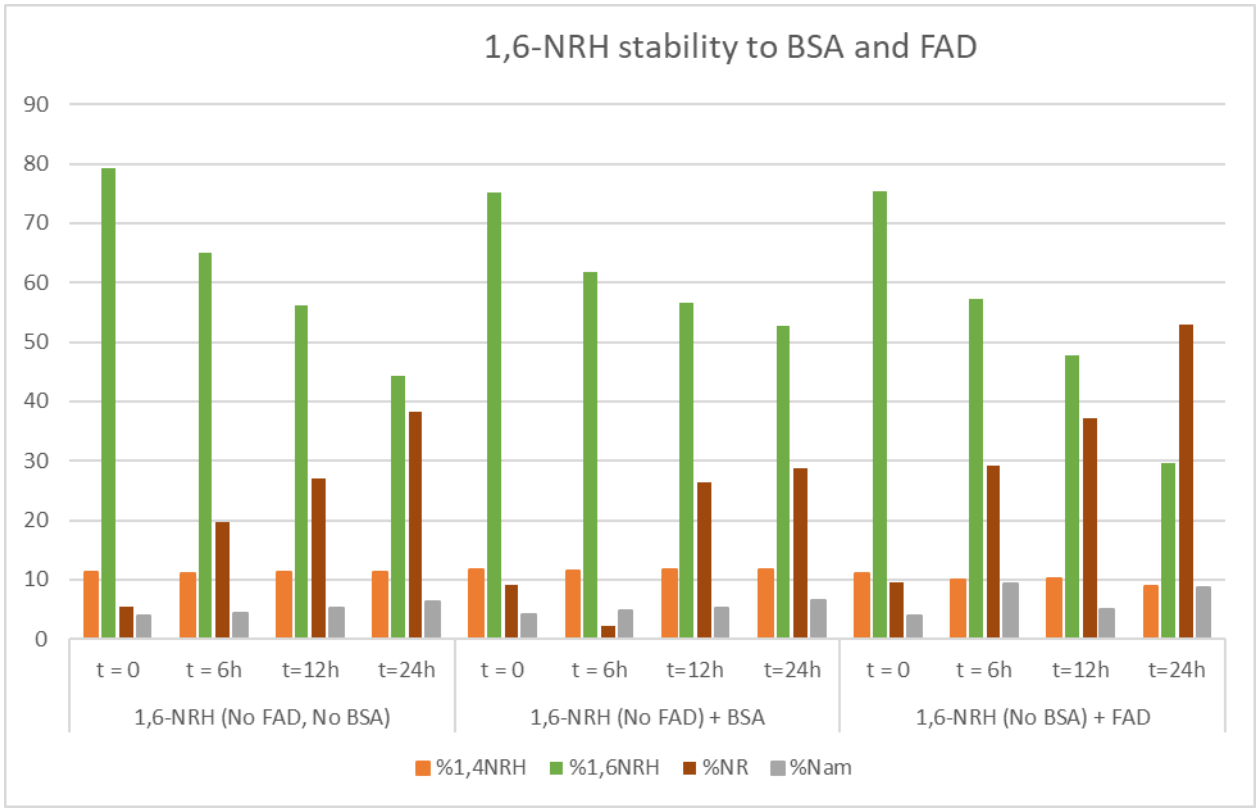

Figure S4: Changes in the product distribution of 1, 2-, 1,4- and 1,6-NRH in solution in absence and presence of NQO2 measured by ^{1}H NMR.

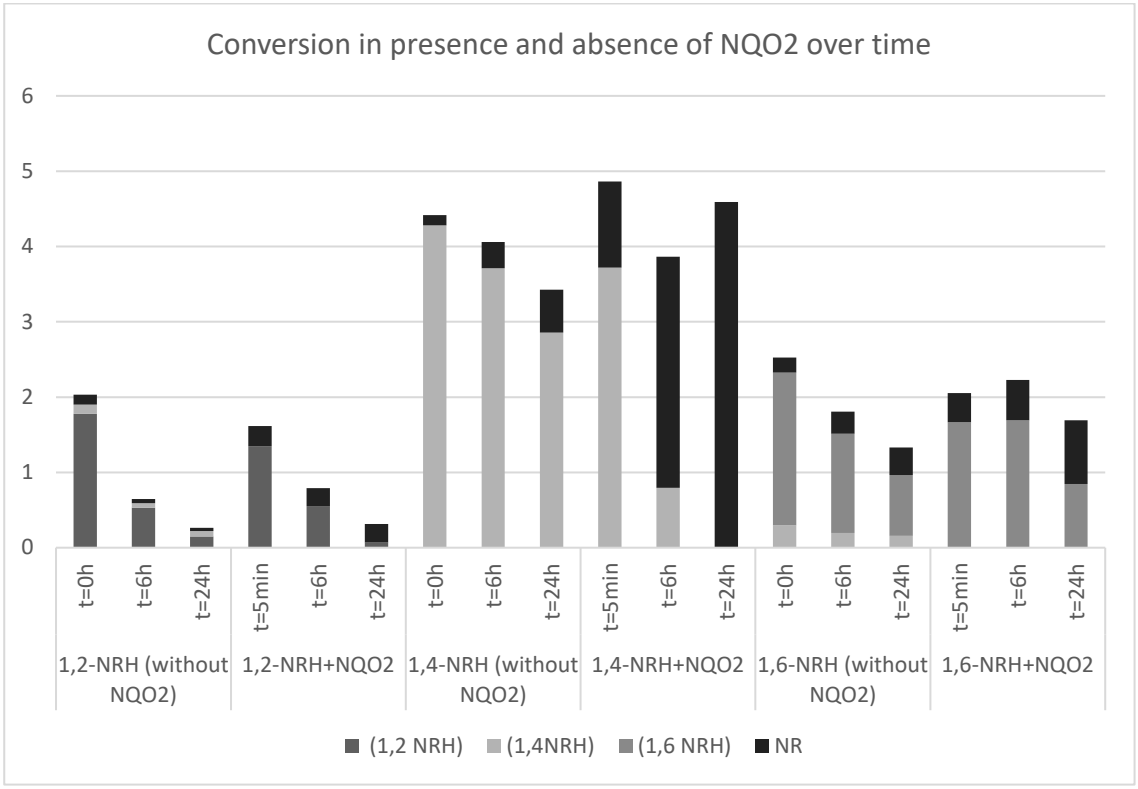

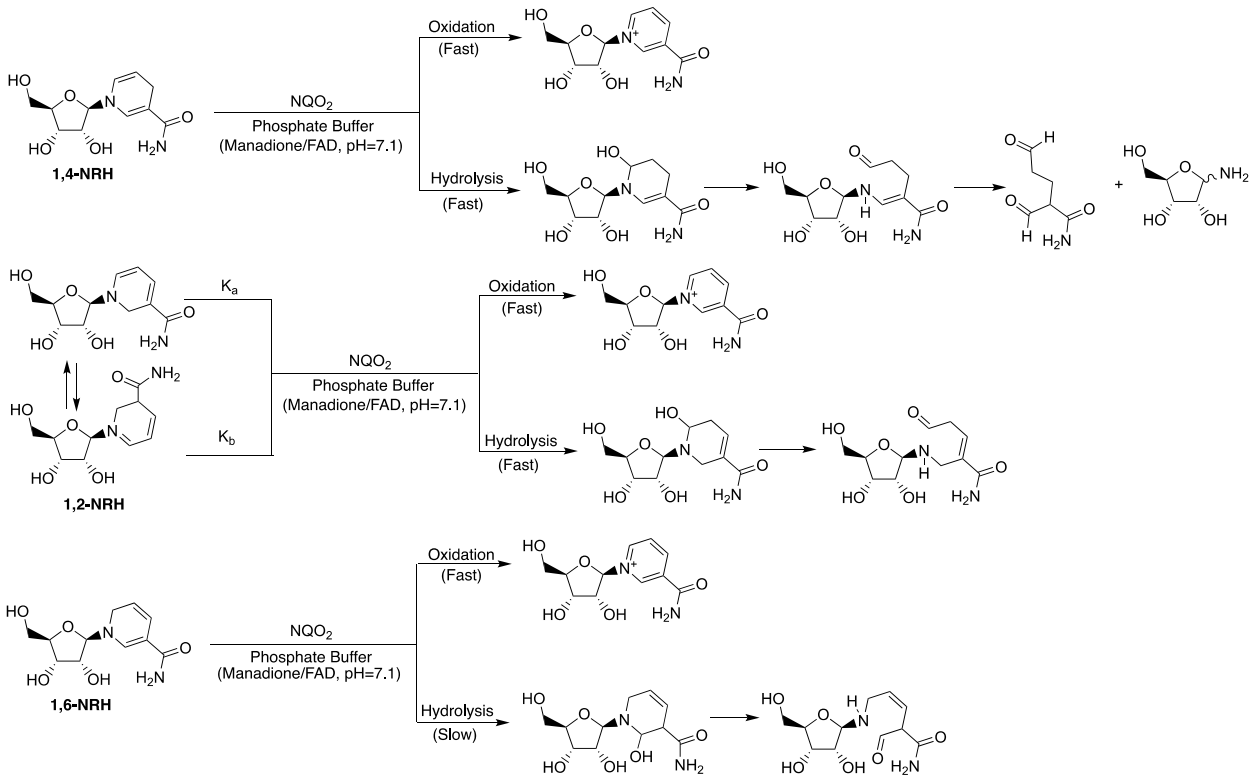

Scheme S1: Stability and reactivity of the three dihydronicotinamide ribosides under NQO2 enzymatic conditions.

Cytotoxicity studies.

HEK293T

Samples	Cell	1,4-NRH	1,6-NRH	1,2-NRH
% Survival	100.00	88.97	86.01	88.01
% SEM	0.00	2.14	2.51	2.92

HepG3

Samples	Cell	1,4-NRH	1,6-NRH	1,2-NRH
% Survival	100.00	92.45	92.68	97.41
% SEM	0.00	0.75	1.95	1.82

Modified peptides identified with high confidence and calculated abundances (based on peak area):

Sequence	Modifications	Abundances:BSA	Abundances: BSA + NRH
LHEKTPVSEKVTK	NRH Adduct C6H9NO2 [K4]	2.61E+08	1.1E+09
SQKFPKAEFVEVTK	NRH Adduct C6H9NO2 [K]	1.42E+08	1.84E+08
QEAKDAFLGSFLYEYSR	NRH [K4]	11990748	15794084
CVLHEKTPVSEKVTK	NRH Adduct C6H9NO2 [K6]	4.39E+08	2.97E+08
HPYFYAPELLYYANKYNGVFQECCQAEDKGACLLP	NRH Adduct C6H9NO2 [K]	68868568	16978286
CTKPESERMPCTEDYLSLILNR	NRH Adduct C11H18N2O5 [K3]	1.87E+08	37090620
HKDDSPDLPK	NRH Adduct C11H18N2O6 [K2]	16943046	28272632
CTKPESERMPCTEDYLSLILNR	NRH Adduct C6H9NO3 [K3]		6.46E+08
YQEAKDAFLGSFLYEYSR	NRH Adduct C11H18N2O5 [K5]	8007322	16282244
CDNQDTISSKLKECCDKPLLEK	NRH Adduct C11H18N2O6 [K12]	2.15E+08	1.35E+08
HLVDEPQNLIKQNCDQF	NRH Adduct C11H18N2O5 [K11]	46415816	25779761
KECCDKPLLEK	NRH Adduct C6H9NO2 [K1]	49370352	51988600
LHEKTPVSEK	NRH Adduct C6H9NO2 [K4]	32803514	88550358
QKFPKAEFVEVTK	NRH Adduct C6H9NO2 [K]; NRH Adduct C6H9NO3 [K]	2.7E+08	2.73E+08
LEECCAKDDPHACYSTVFDKLK	NRH [K7]	30435586	12151486
ADESHAGCEKSLHTLFGDELCK	NRH Adduct C6H9NO2 [K10]	23741036	36932476
TMREKVLASSAR	NRH Adduct C11H18N2O5 [K5]	2958651	1968951
PKIETMREK	NRH [K2]	17969050	48940296

Identified PSMs from BSA without NRH <u>that contain a modification:</u>

High Confidence, Modified Protein Coverage: 37.23%
(94.56% Total coverage regardless of modification)

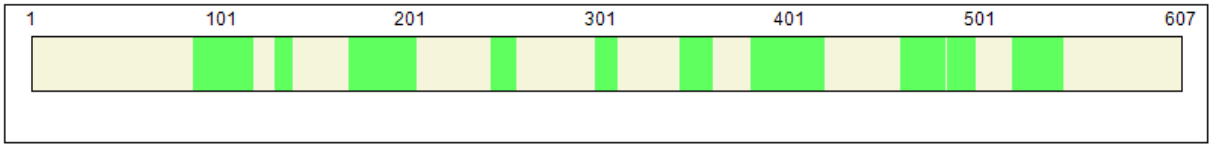

Found Modifications:

C Custom: NRH Adduct C6H9NO2 (K)
D Custom: NRH Adduct C11H18N2O6 (K)
E Custom: NRH Adduct C11H18N2O5 (K)
F Custom: NRH Adduct C6H9NO3 (K)
G Custom:NRH (K)

```
MKWVTFISLL LLFSSAYSRG VFRRDTHKSE IAHRFKDLGE EHFKGLVLIA FSQYLQQCPF DEHVKLVNEL
         D      F         C       D
TEFAKTCVAD ESHAGCEKSL HTLFGDELCK VASLRETYGD MADCCEKQEP ERNECFLSHK DDSPDLPKLK
                          E
                          C       C
PDPNTLCDEF KADEKKFWGK YLYEIARRHP YFYAPELLYY ANKYNGVFQE CCQAEDKGAC LLPKIETMRE
                    E E
```

```
                    C C
KVLASSARQR LRCASIQKFG ERALKAWSVA RLSQKFPKAE FVEVTKLVTD LTKVHKECCH GDLLECADDR
             F
           E   E                          G
ADLAKYICDN QDTISSKLKE CCDKPLLEKS HCIAEVEKDA IPENLPPLTA DFAEDKDVCK NYQEAKDAFL

                    G                F
GSFLYEYSRR HPEYAVSVLL RLAKEYEATL EECCAKDDPH ACYSTVFDKL KHLVDEPQNL IKQNCDQFEK
                         G
                         F               C
LGEYGFQNAL IVRYTRKVPQ VSTPTLVEVS RSLGKVGTRC CTKPESERMP CTEDYLSLIL NRLCVLHEKT
                   F  G
                   E  F
                   D  E
PVSEKVTKCC TESLVNRRPC FSALTPDETY VPKAFDEKLF TFHADICTLP DTEKQIKKQT ALVELLKHKP
KATEEQLKTV MENFVAFVDK CCAADDKEAC FAVEGPKLVV STQTALA
```

Identified PSMs from BSA + NRH <u>that contain a modification:</u>

High Confidence, Modified Protein Coverage: 46.79%

(95.72% Total coverage regardless of modification)

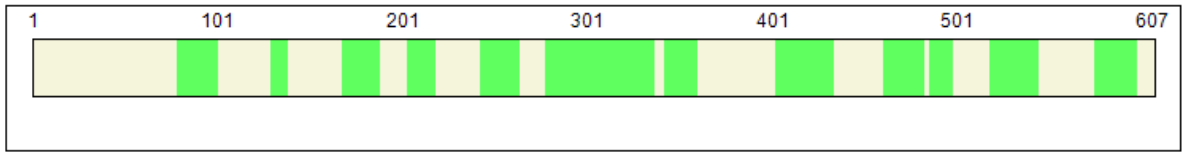

Found Modifications:

C	Custom: NRH Adduct C6H9NO2 (K)
D	Custom: NRH Adduct C11H18N2O6 (K)
E	Custom: NRH Adduct C11H18N2O5 (K)
F	Custom: NRH Adduct C6H9NO3 (K)
G	Custom:NRH (K)

```
MKWVTFISLL LLFSSAYSRG VFRRDTHKSE IAHRFKDLGE EHFKGLVLIA FSQYLQQCPF DEHVKLVNEL
         D                          E
TEFAKTCVAD ESHAGCEKSL HTLFGDELCK VASLRETYGD MADCCEKQEP ERNECFLSHK DDSPDLPKLK
                         G
                         C            G
PDPNTLCDEF KADEKKFWGK YLYEIARRHP YFYAPELLYY ANKYNGVFQE CCQAEDKGAC LLPKIETMRE
                   F F
C                  D D    C
KVLASSARQR LRCASIQKFG ERALKAWSVA RLSQKFPKAE FVEVTKLVTD LTKVHKECCH GDLLECADDR
           E   G                          G

 F       D   C  G     E           E     C
ADLAKYICDN QDTISSKLKE CCDKPLLEKS HCIAEVEKDA IPENLPPLTA DFAEDKDVCK NYQEAKDAFL
                                   C    C
GSFLYEYSRR HPEYAVSVLL RLAKEYEATL EECCAKDDPH ACYSTVFDKL KHLVDEPQNL IKQNCDQFEK
                                      D
                         F             C
LGEYGFQNAL IVRYTRKVPQ VSTPTLVEVS RSLGKVGTRC CTKPESERMP CTEDYLSLIL NRLCVLHEKT
                   E  G
                   C  F
PVSEKVTKCC TESLVNRRPC FSALTPDETY VPKAFDEKLF TFHADICTLP DTEKQIKKQT ALVELLKHKP
               F
           C    D     D
KATEEQLKTV MENFVAFVDK CCAADDKEAC FAVEGPKLVV STQTALA
```

Quantum-based Computational Modeling NQO2[1-9].

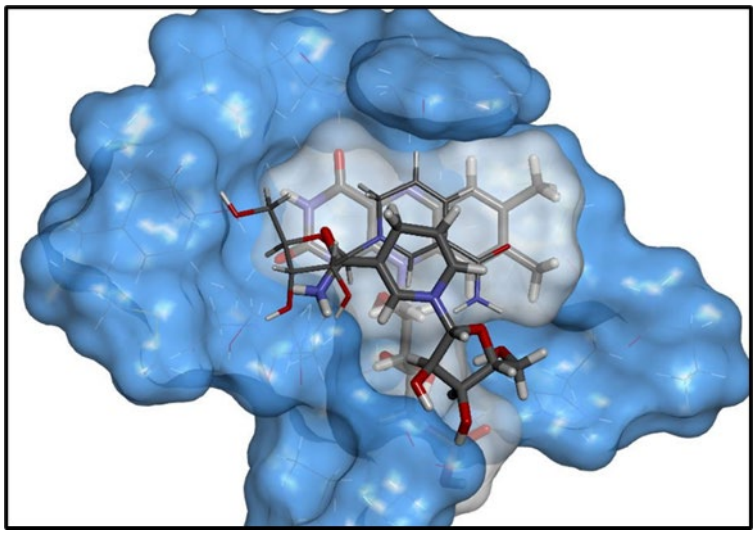

Figure S5: Superposition of 1,4- and 1,6-NRH bound to the face of the flavin moiety of FAD (transparent surface) in FAD-bound NQO2 (blue surface). The 1,4- and 1,6-NRH isomers are represented as thick and thin stick structures, respectively. The computational model of FAD-bound NQO2 is based upon PDB entry 2QX847.

A truncated model of the NQO2(FAD) enzyme (17 amino acid residues) was built from PDB entry 2QX8[1] (res 1.60 Å) using Gaussview 5.0 (Gaussian Inc, Wallingford, CT). The FAD molecule was truncated at the first phosphate to produce a model system with a net charge of -1. In the search for favorable docking poses of the three NRH isomers on the face of FAD, 8 classes of poses of each isomer were considered through manual positioning: 2 positions for the amide moiety x 2 positions for the glycosidic bond x 2 positions for the ribose moiety (left versus right of FAD). Manual docking was followed by semi-empirical PM7 energy optimizations in which only the NRH ligand was permitted to move. The resulting lowest energy structures were selected for follow-up ONIOM[2] hybrid calculations (high-level:B3LYP[3,4]/6-31G(d)[5-7]:low-level:PM7) in order to distinguish them by using an all-electron density functional model (B3LYP) for the high-level region. The ligand positions were reoptimized, ultimately using the ONIOM(wB97XD/6-31G(d):PM7) model in the presence of water using the default SCRF model. The wB97XD model[8] is a density functional method that includes the effects of dispersion. Optimizations were deemed complete when the forces met the default convergence criteria. All calculations were carried out using Gaussian16[9].

1. Calamini, B.; Santarsiero, B.D.; Boutin, J.A.; Mesecar, A.D. Kinetic, thermodynamic and X-ray structural insights into the interaction of melatonin and analogues with quinone reductase 2. *Biochem. J.* **2008**, *413*, 81–91.
2. Dapprich, S.; Komáromi, I.; Byun, K.; Morokuma, K.; Frisch, M.J. A new ONIOM implementation in Gaussian98. Part I. The calculation of energies, gradients, vibrational frequencies and electric field derivatives. *J. Mol. Struct. THEOCHEM* **1999**, *461*, 1–21.
3. Becke, A.D. Density-functional thermochemistry. III. The role of exact exchange. *J. Chem. Phys.* **1993**, *98*, 5648–5652.
4. Lee, C.; Yang, W.; Parr, R.G. Development of the Colle-Salvetti correlation-energy formula into a functional of the electron density. *Phys. Rev. B* **1988**, *37*, 785–789.
5. Ditchfield, R. Self-Consistent Molecular-Orbital Methods. IX. An Extended Gaussian-Type Basis for Molecular-Orbital Studies of Organic Molecules. *J. Chem. Phys.* **1971**, *54*, 724.
6. Hehre, W.J. Self-Consistent Molecular Orbital Methods. XII. Further Extensions of Gaussian-Type Basis Sets for Use in Molecular Orbital Studies of Organic Molecules. *J. Chem. Phys.* **1972**, *56*, 2257.
7. Rassolov, V.A.; Windus, T.L.; Pople, J.A.; Ratner, M.A. 6-31G* basis set for atoms K through Zn. *J. Chem. Phys.* **1998**, *109*, 1223–1229.
8. Chai, J.-D.; Head-Gordon, M. Long-range corrected hybrid density functionals with damped atom-atom dispersion corrections. *Phys. Chem. Chem. Phys.* **2008**, *10*, 6615–20.
9. Frisch, M.J.; Trucks, G.W.; Schlegel, H.B.; Scuseria, G.E.; Robb, M.A.; Cheeseman, J.R.; Scalmani, G.; Barone, V.; Petersson, G.A.; Nakatsuji, H.; et al. Gaussian 16, Revision C.01; Gaussian, Inc.: Wallingford, CT, USA, 2016.

Spectra

NMR, MS and HRMS data

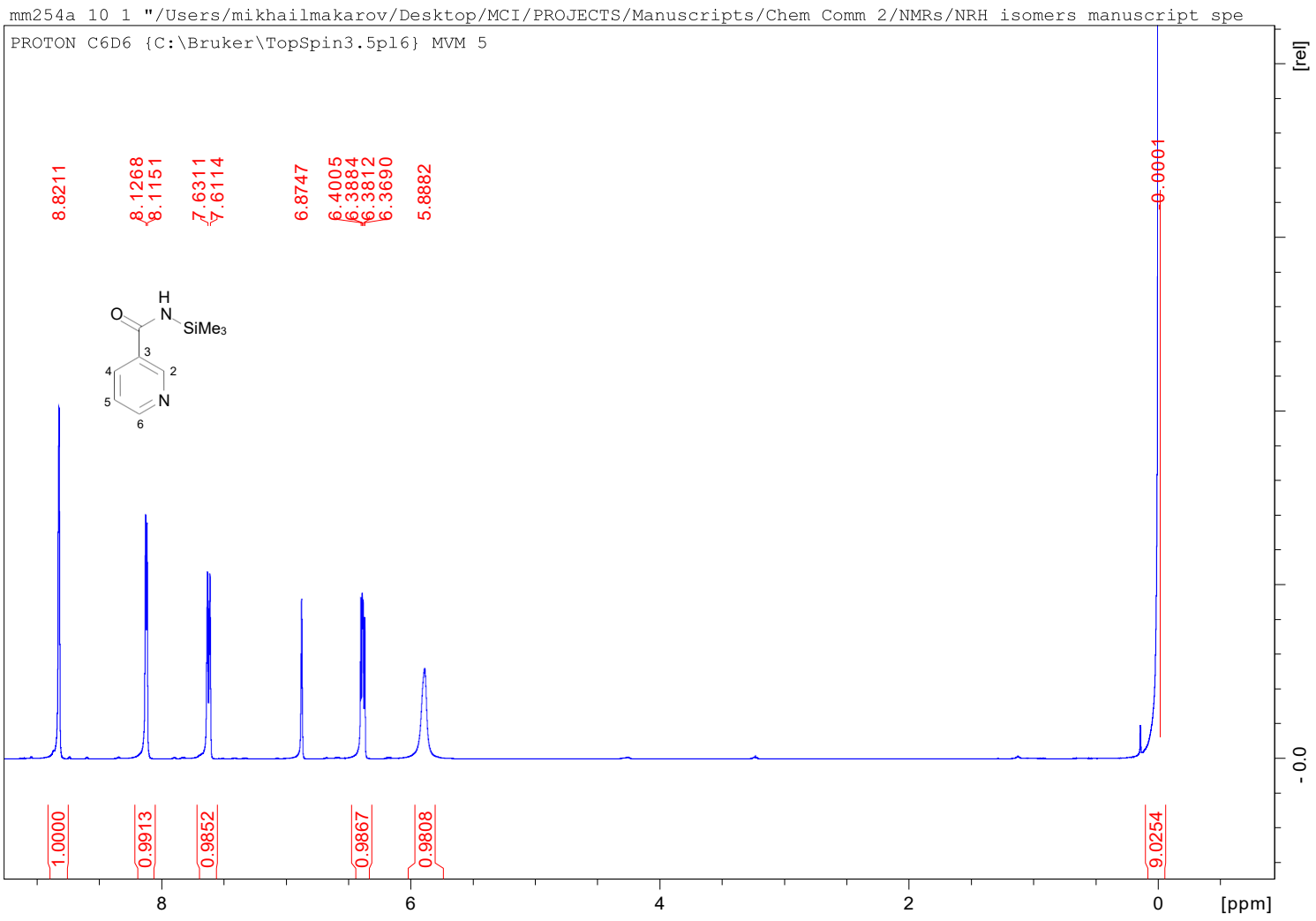

Fig. 3S ^{1}H NMR (C_6D_6) of *N*-(trimethylsilyl)Nam.

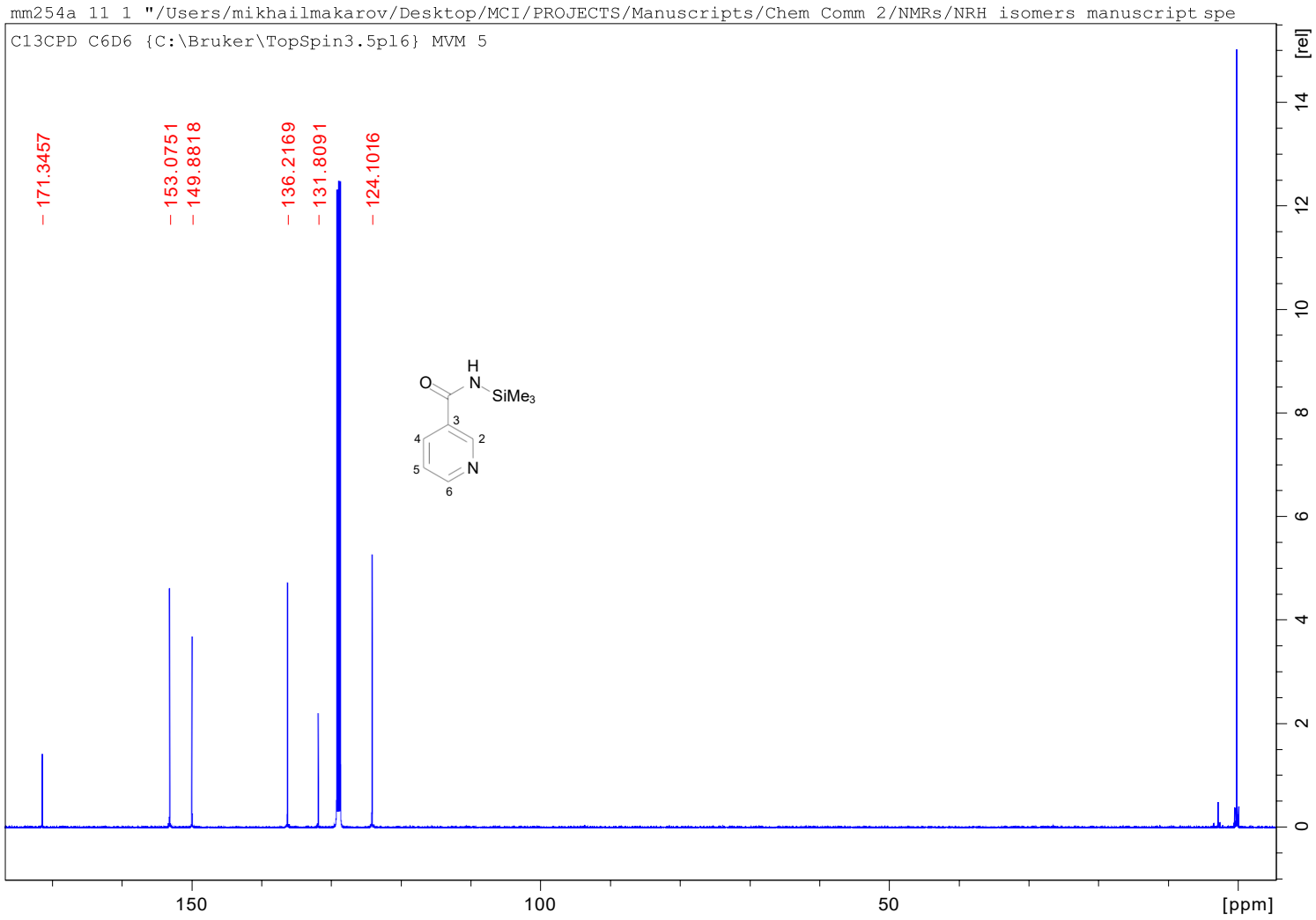

Fig. 4S ^{13}C NMR (C_6D_6) of *N*-(trimethylsilyl)Nam.

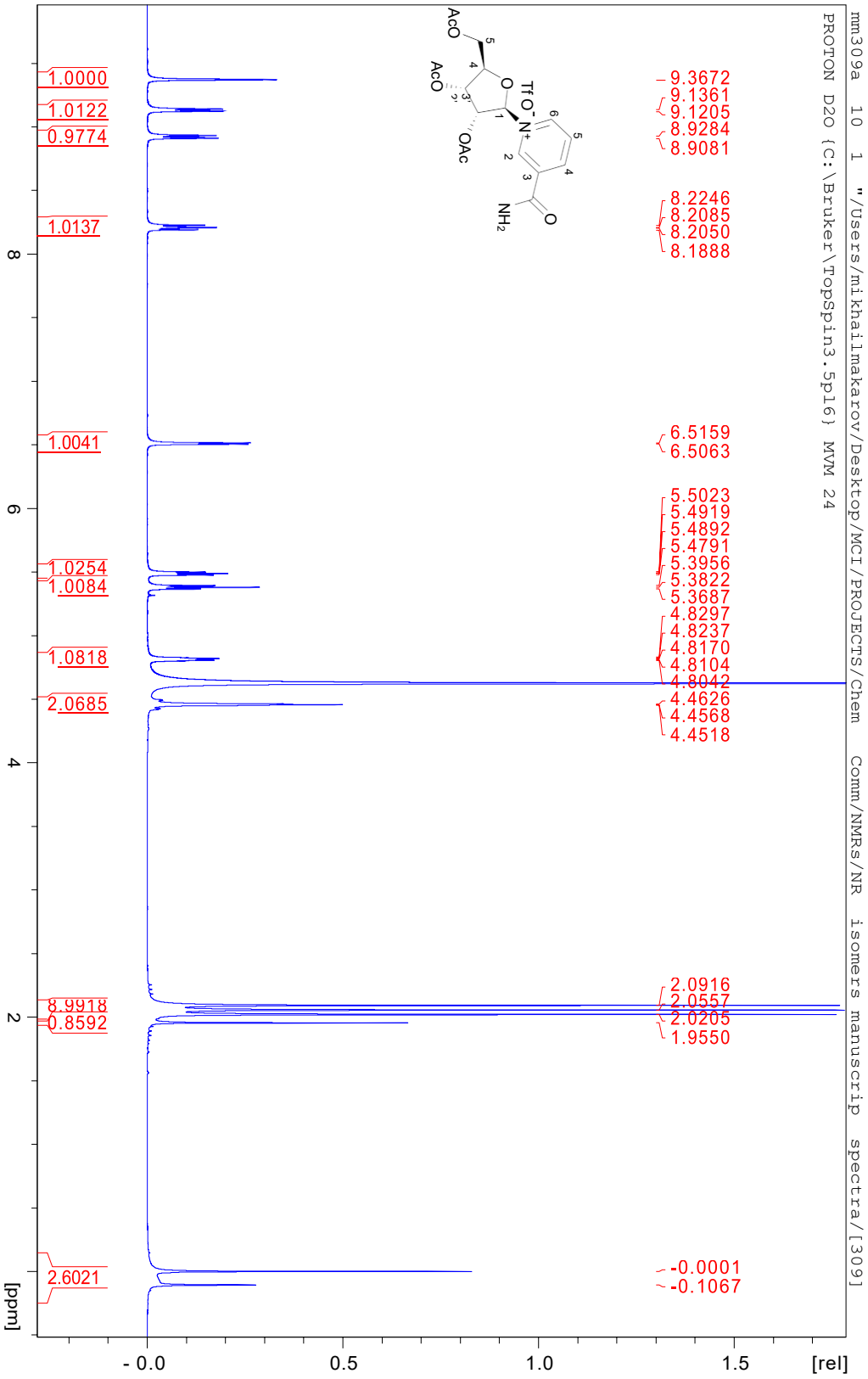

Fig. 5S ^{1}H NMR (D_2O) of NR triacetate triflate (**6**).

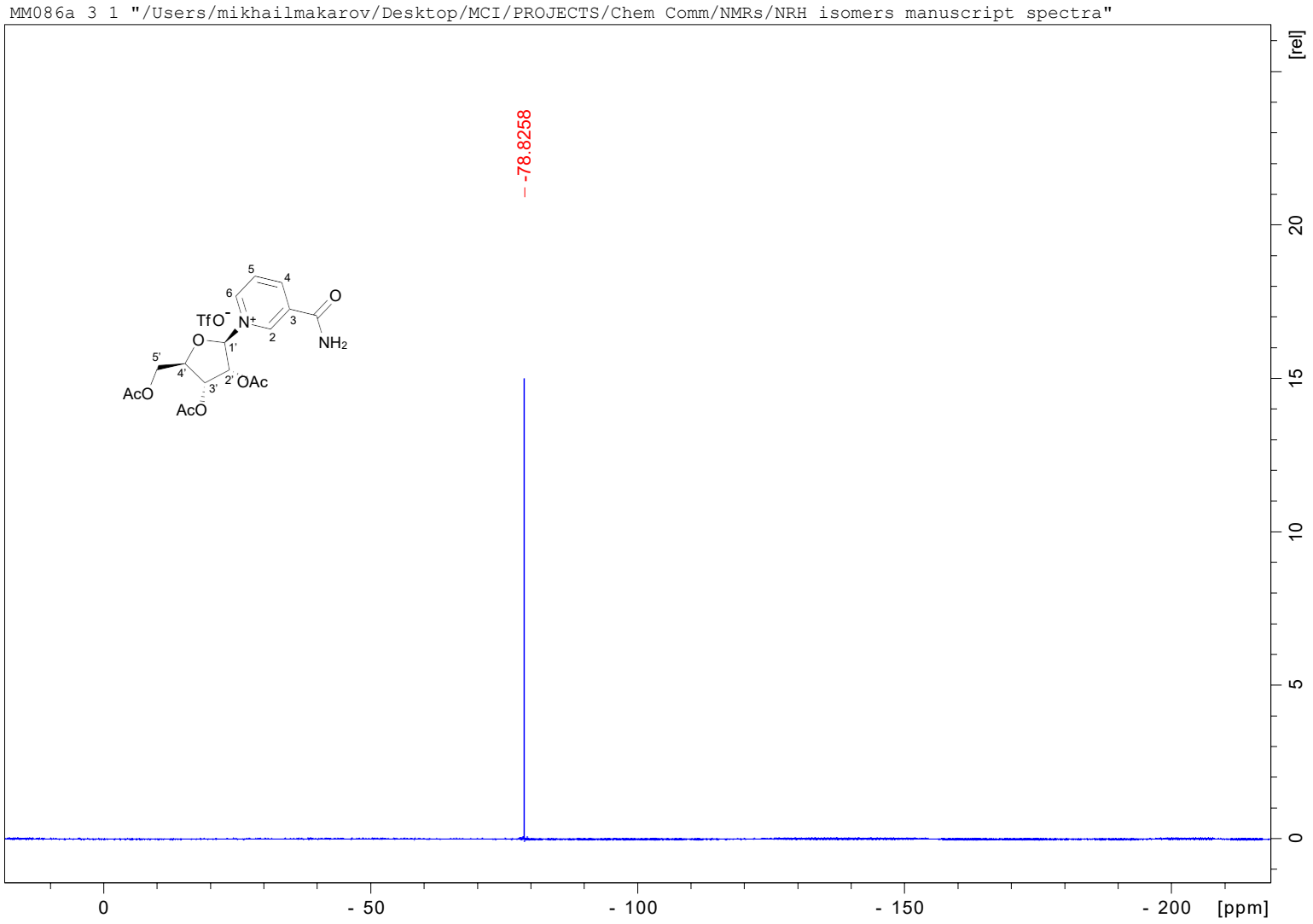

Fig. 6S ^{19}F NMR (D_2O) of NR triacetate triflate (**6**).

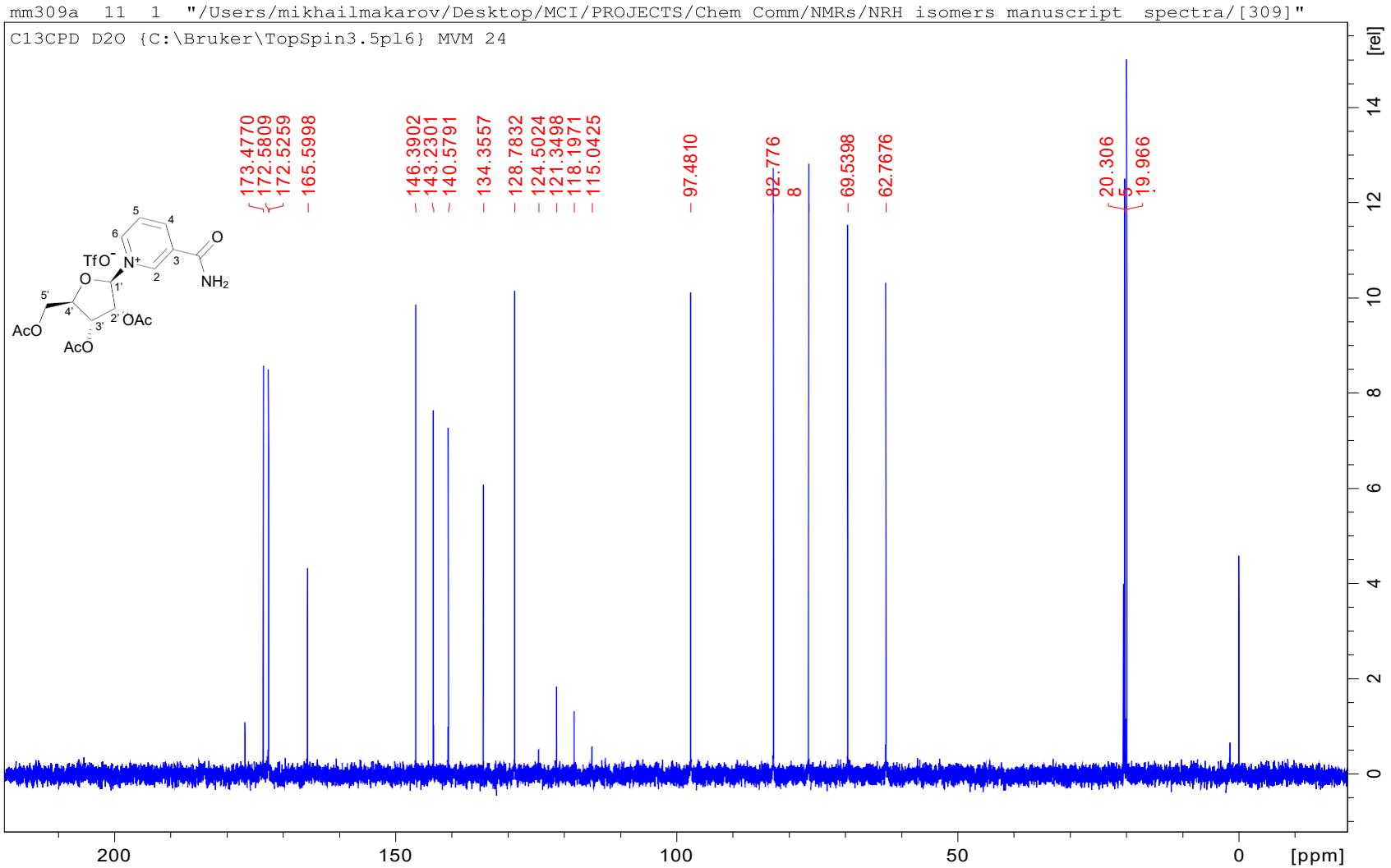

Fig. 7S ^{13}C NMR (D_2O) of NR triacetate triflate (**6**).

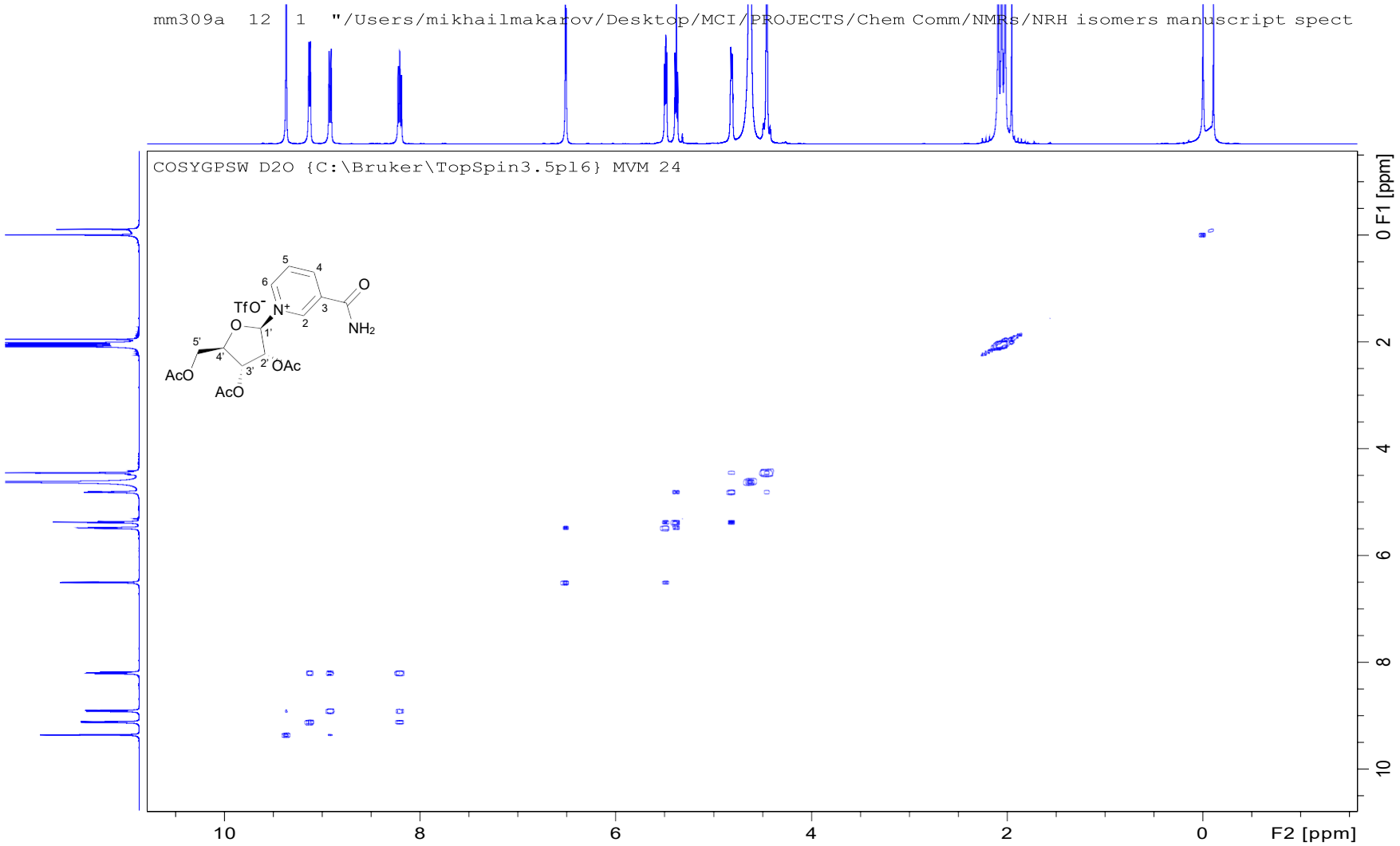

Fig. 8S ^{1}H-^{1}H correlation (COSY) NMR (D_2O) of NR triacetate triflate (**6**).

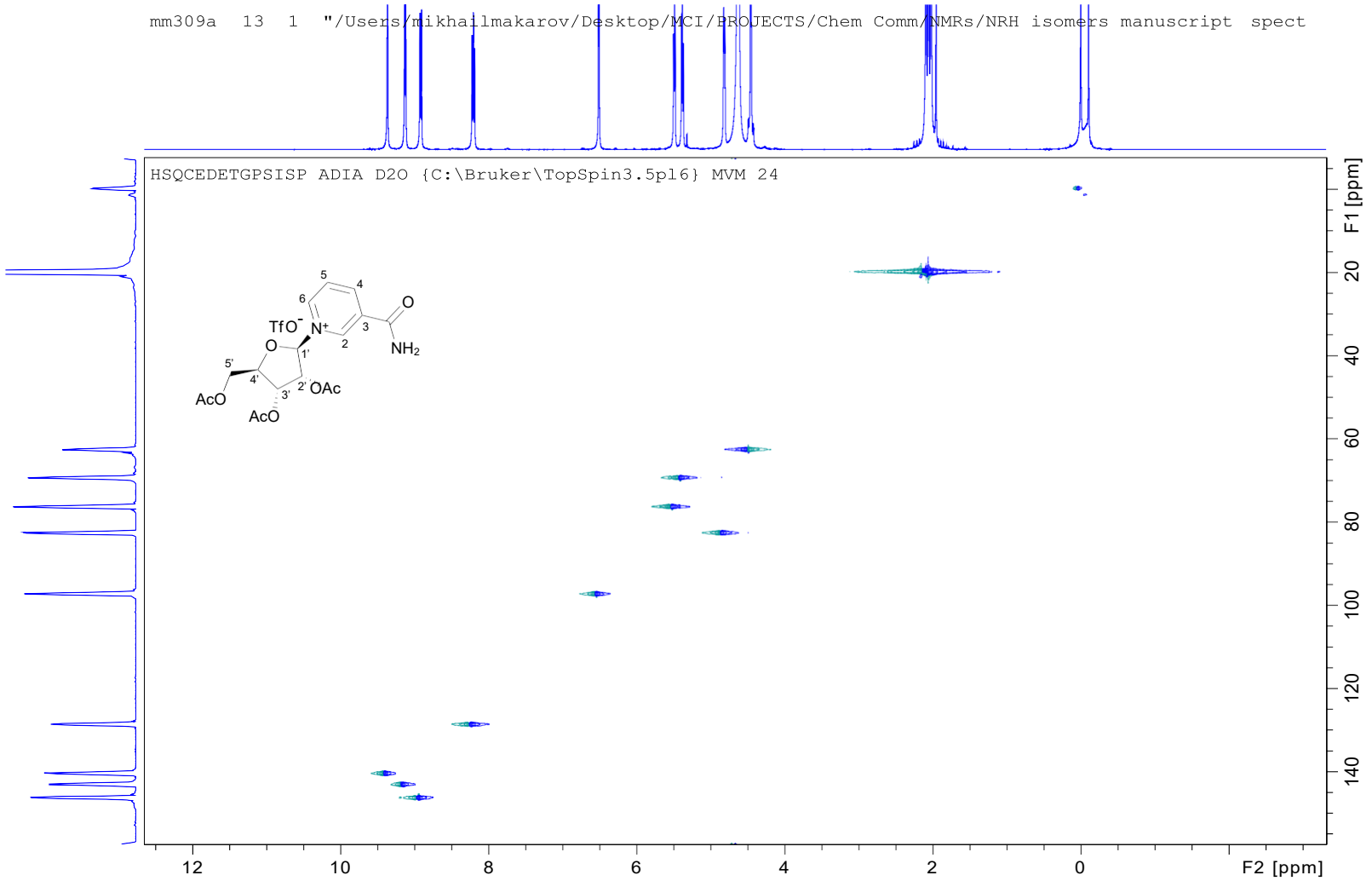

Fig. 9S ^{1}H-^{13}C correlation (HSQC) NMR (D_2O) of NR triacetate triflate (**6**).

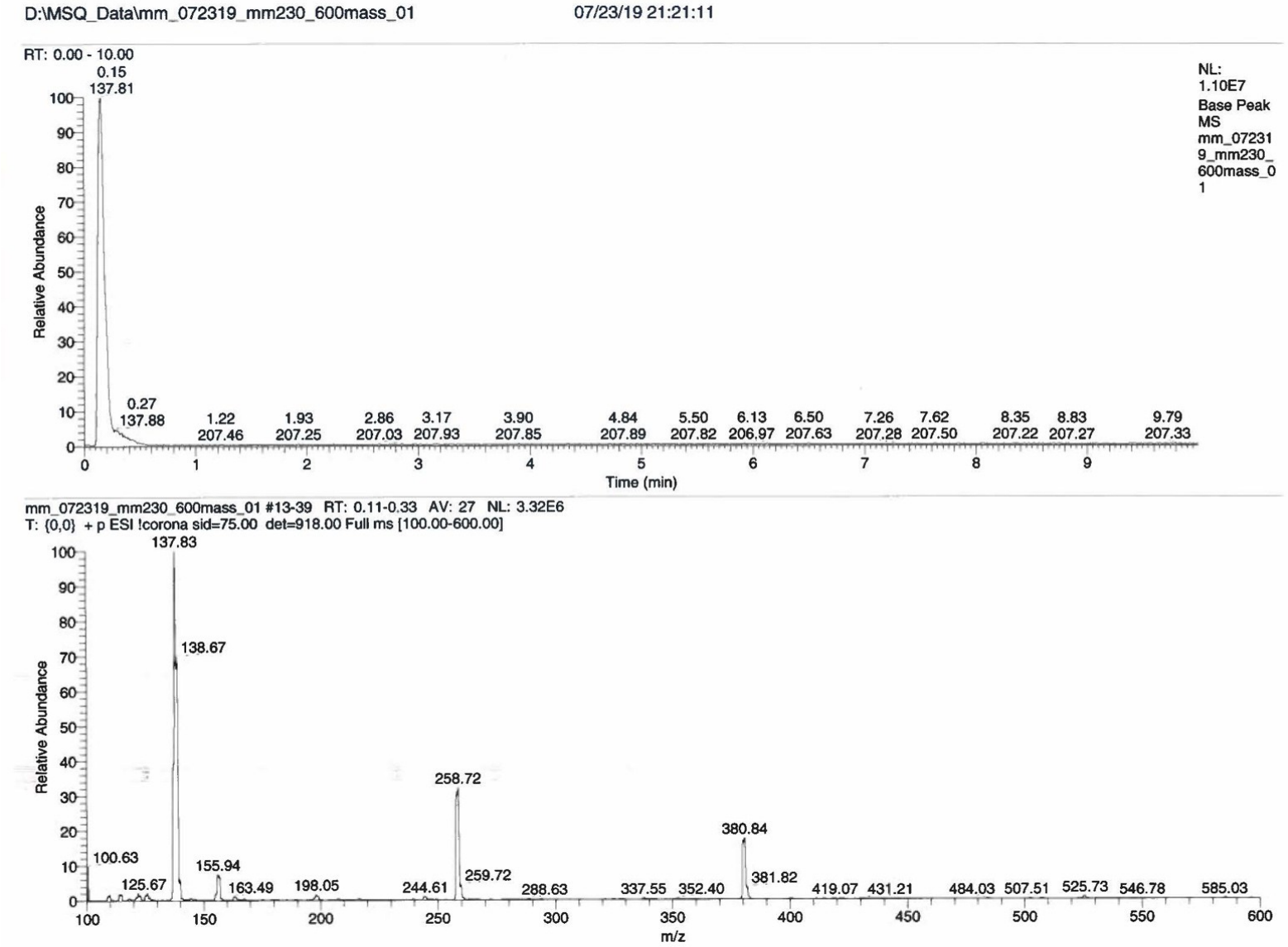

Fig. 10S MS (1:1 H_2O/ACN) of NRTA triflate (**6**).

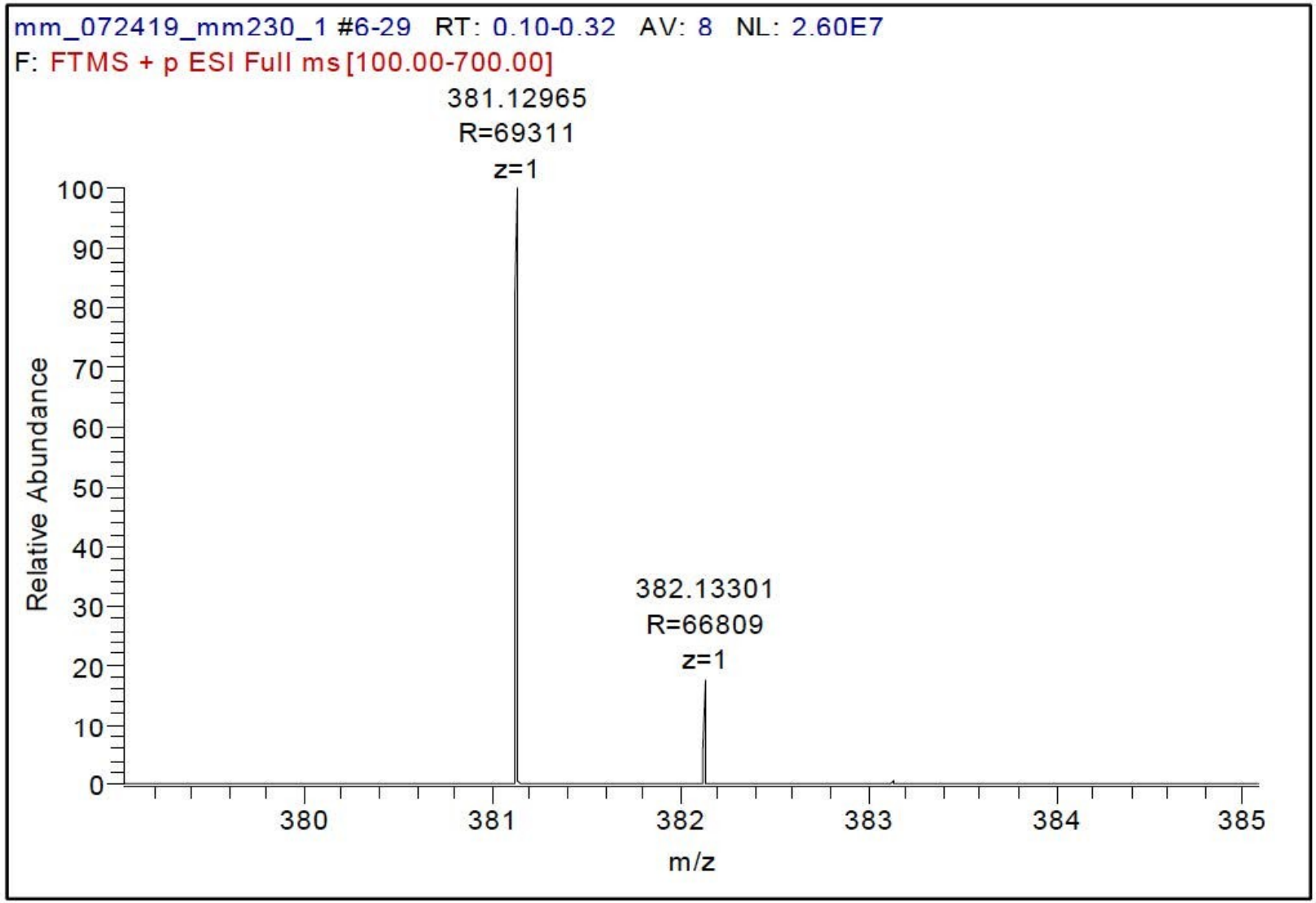

Fig. 11S HRMS (1:1 H_2O/ACN) of NRTA triflate (**3**).

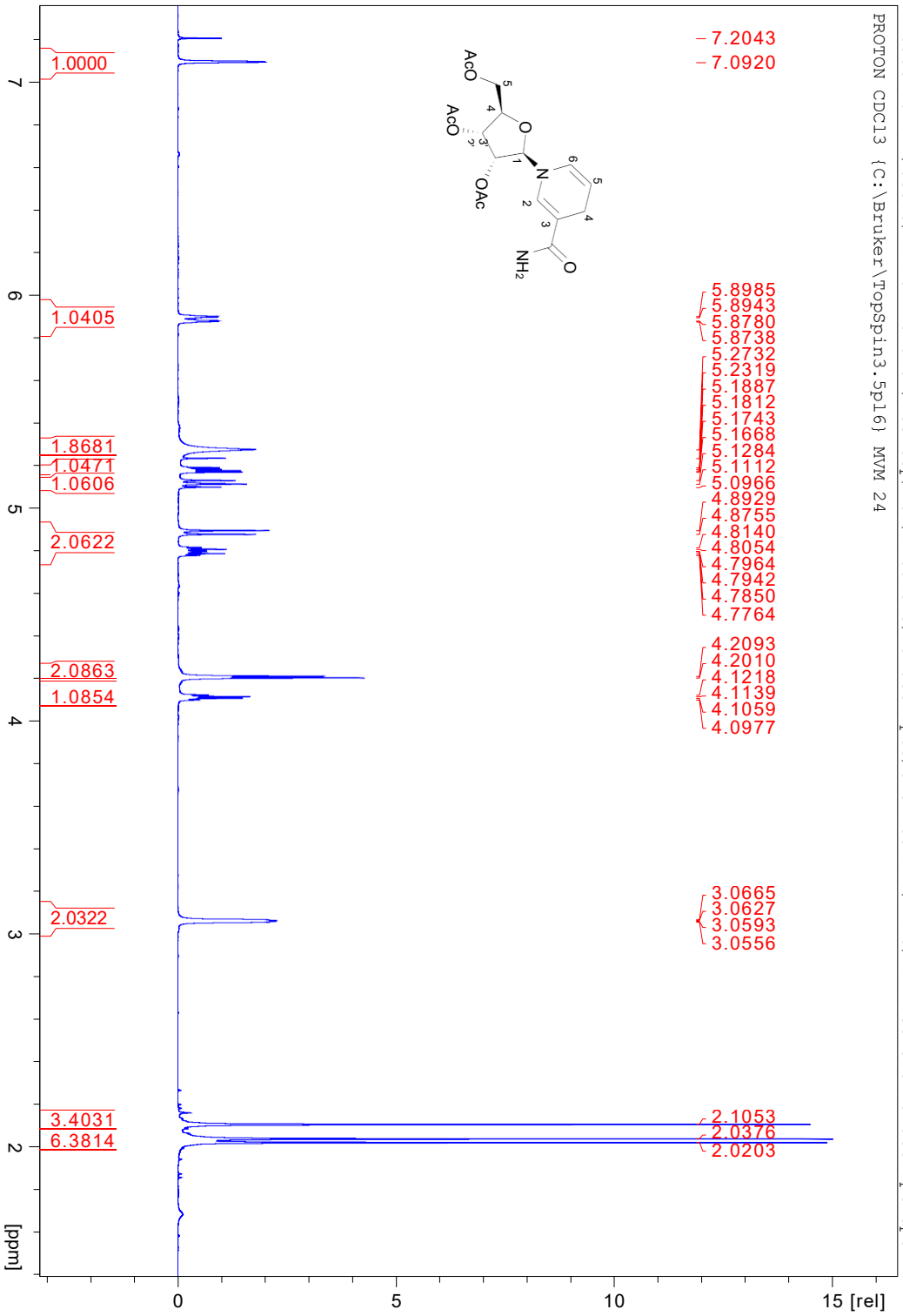

Fig. 12S ^{1}H NMR ($CDCl_3$) of NRH triacetate (7).

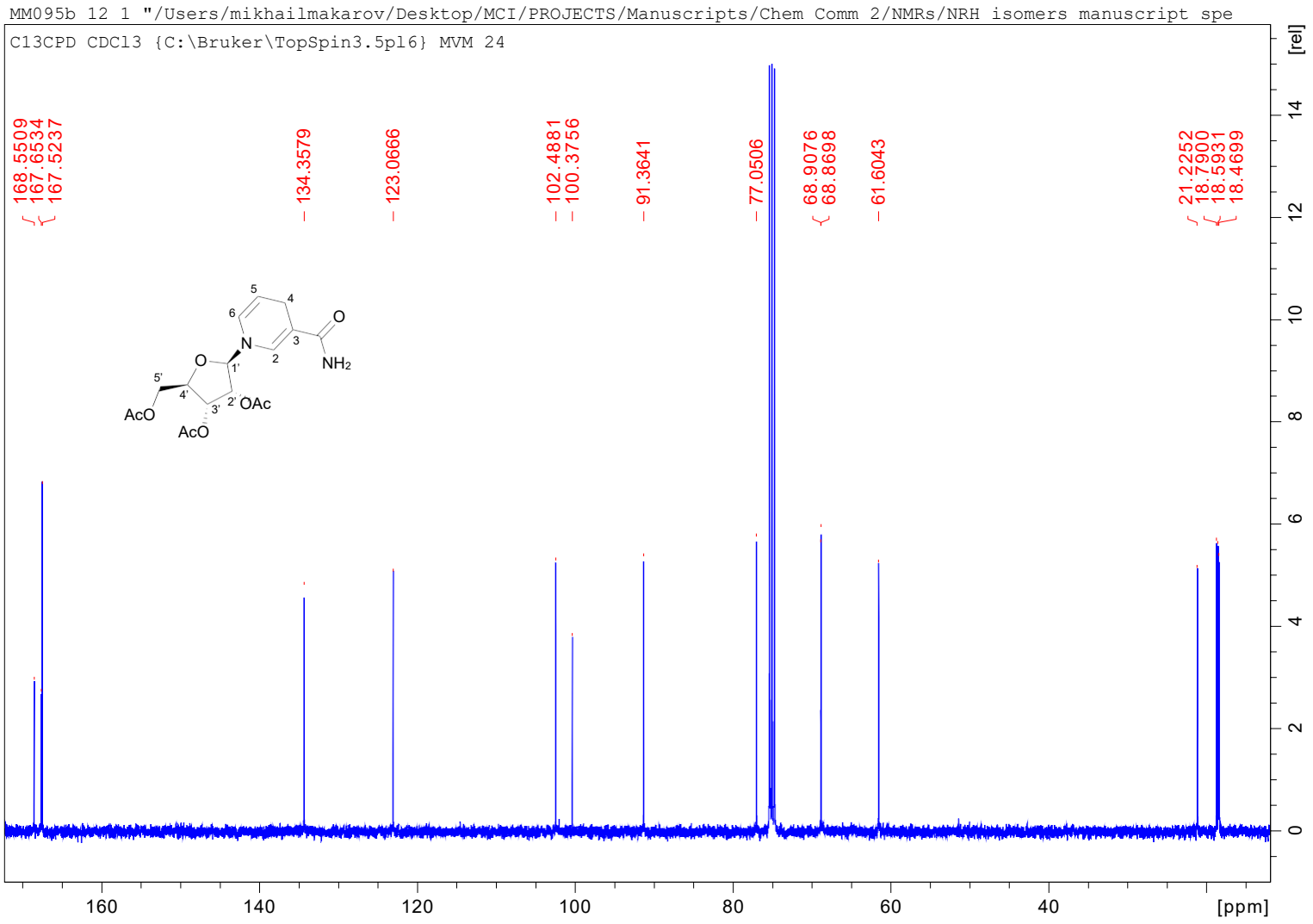

Fig. 13S ^{13}C NMR ($CDCl_3$) of NRH triacetate (**7**).

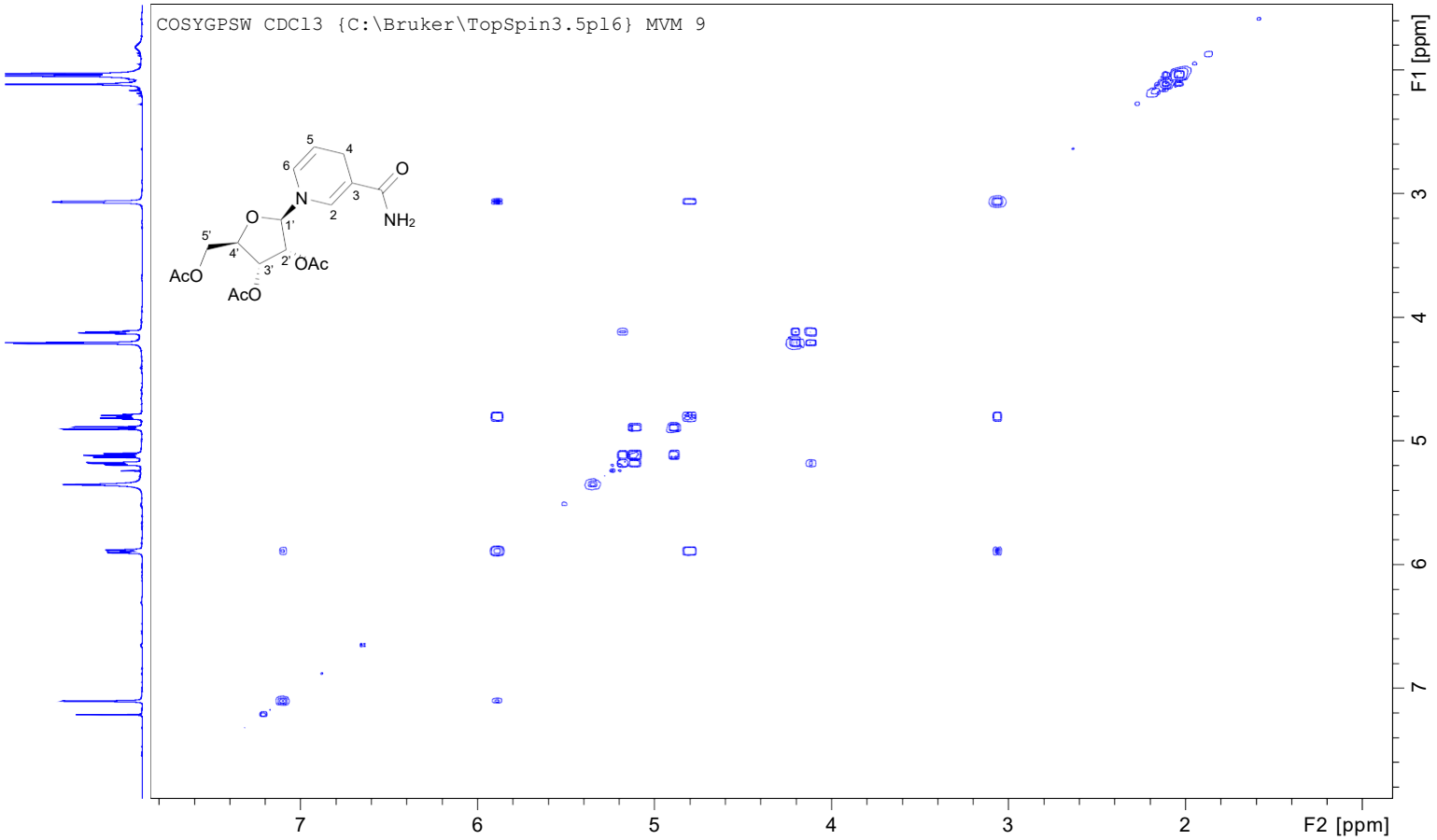

Fig. 14S ^{1}H-^{1}H correlation (COSY) NMR ($CDCl_3$) of NRH triacetate (**7**).

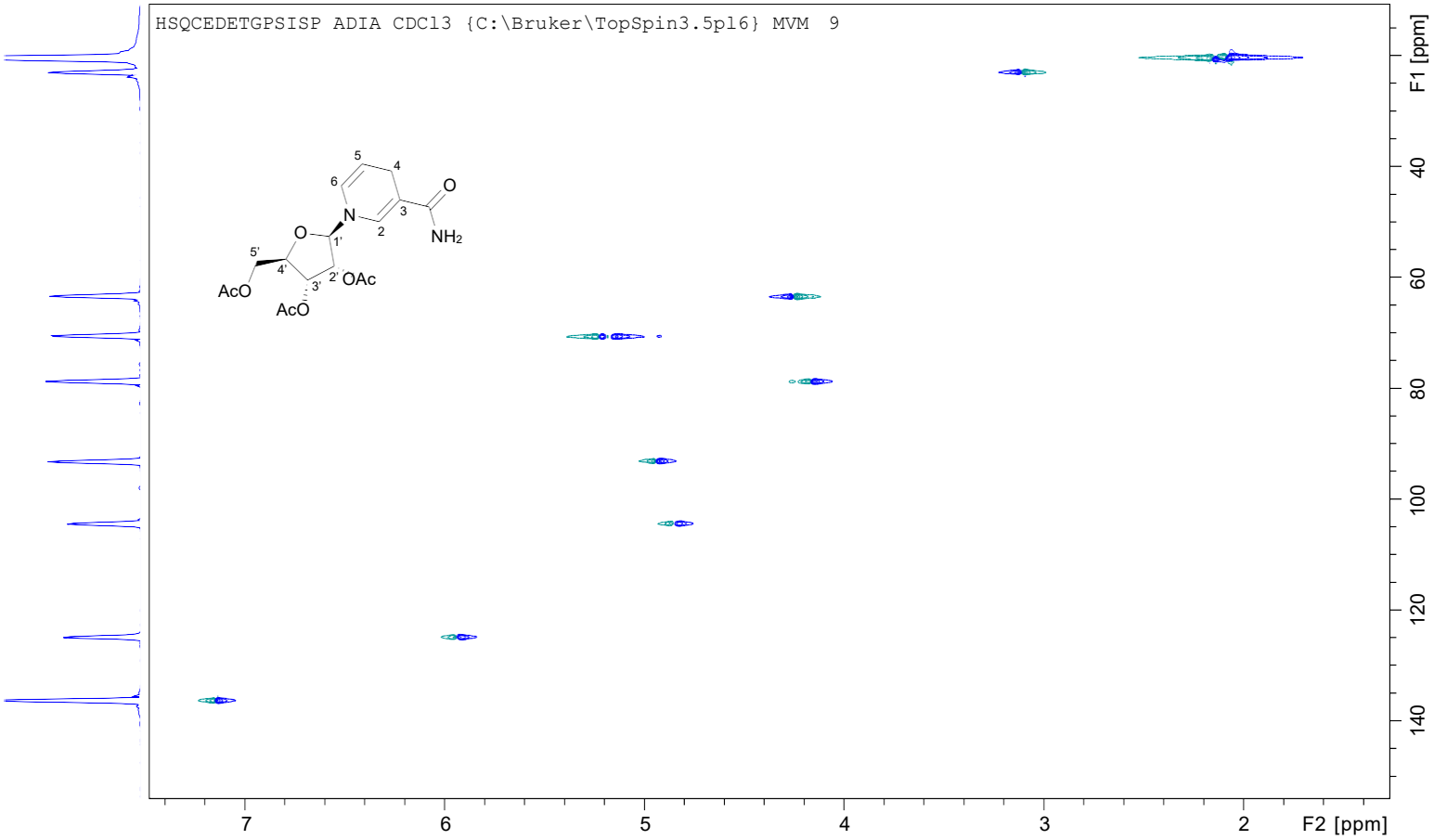

Fig. 15S ^{1}H-^{13}C correlation (HSQC) NMR ($CDCl_3$) of NRH triacetate (**7**).

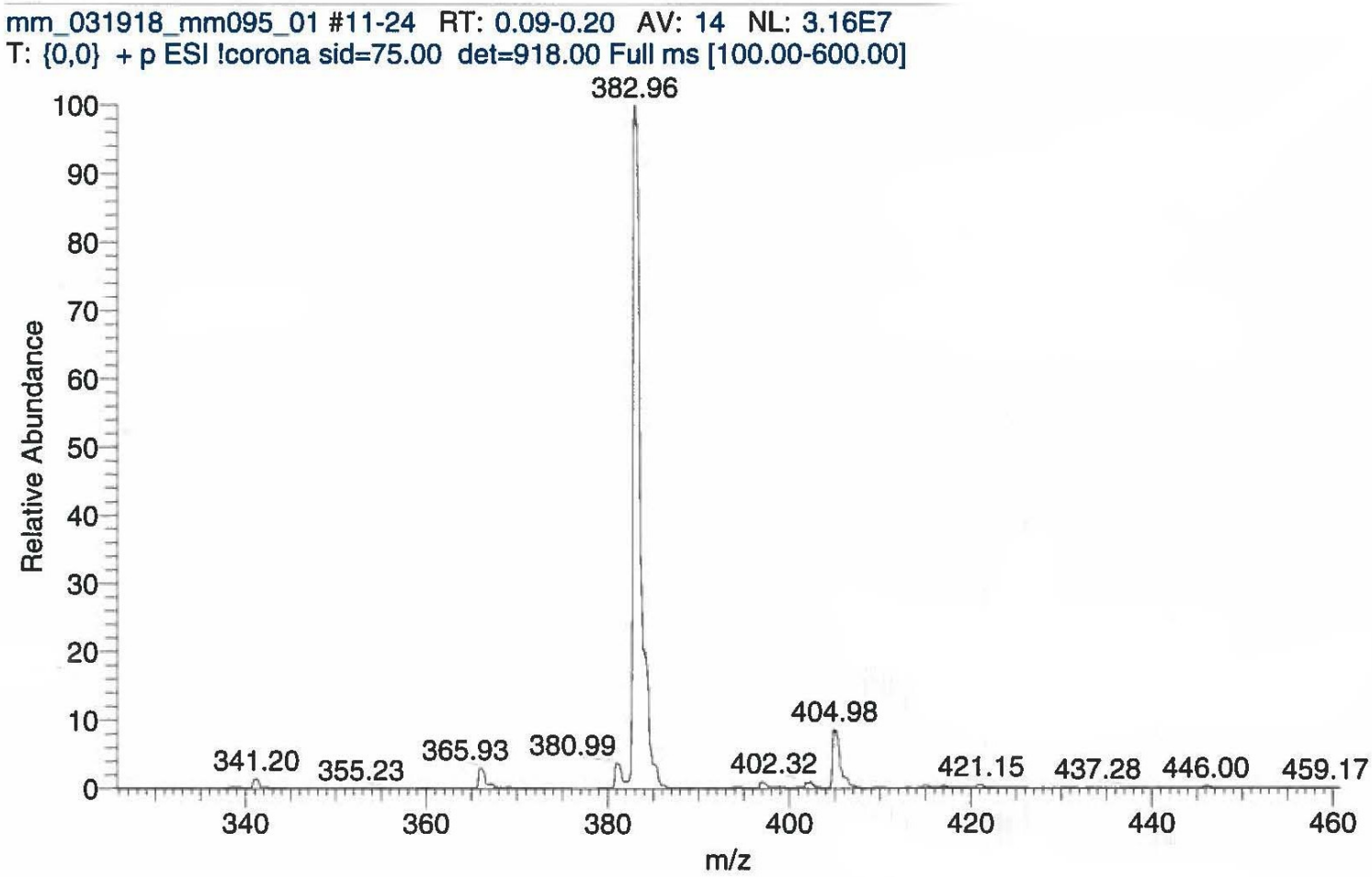

Fig. 16S MS (1:1 H_2O/ACN) of NRH triacetate (**7**).

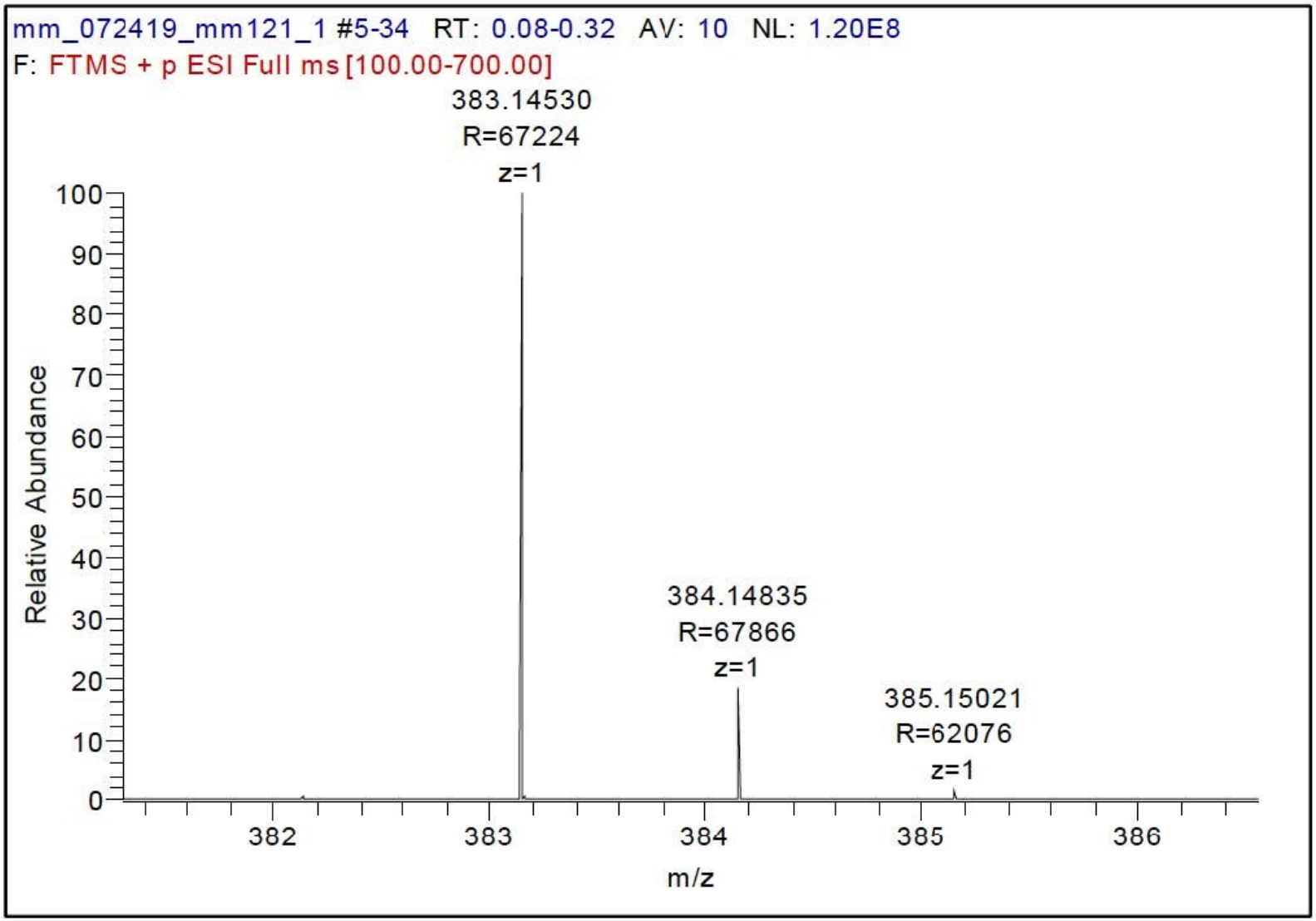

Fig. 17S HRMS (1:1 H_2O/ACN) of NRH triacetate (**7**).

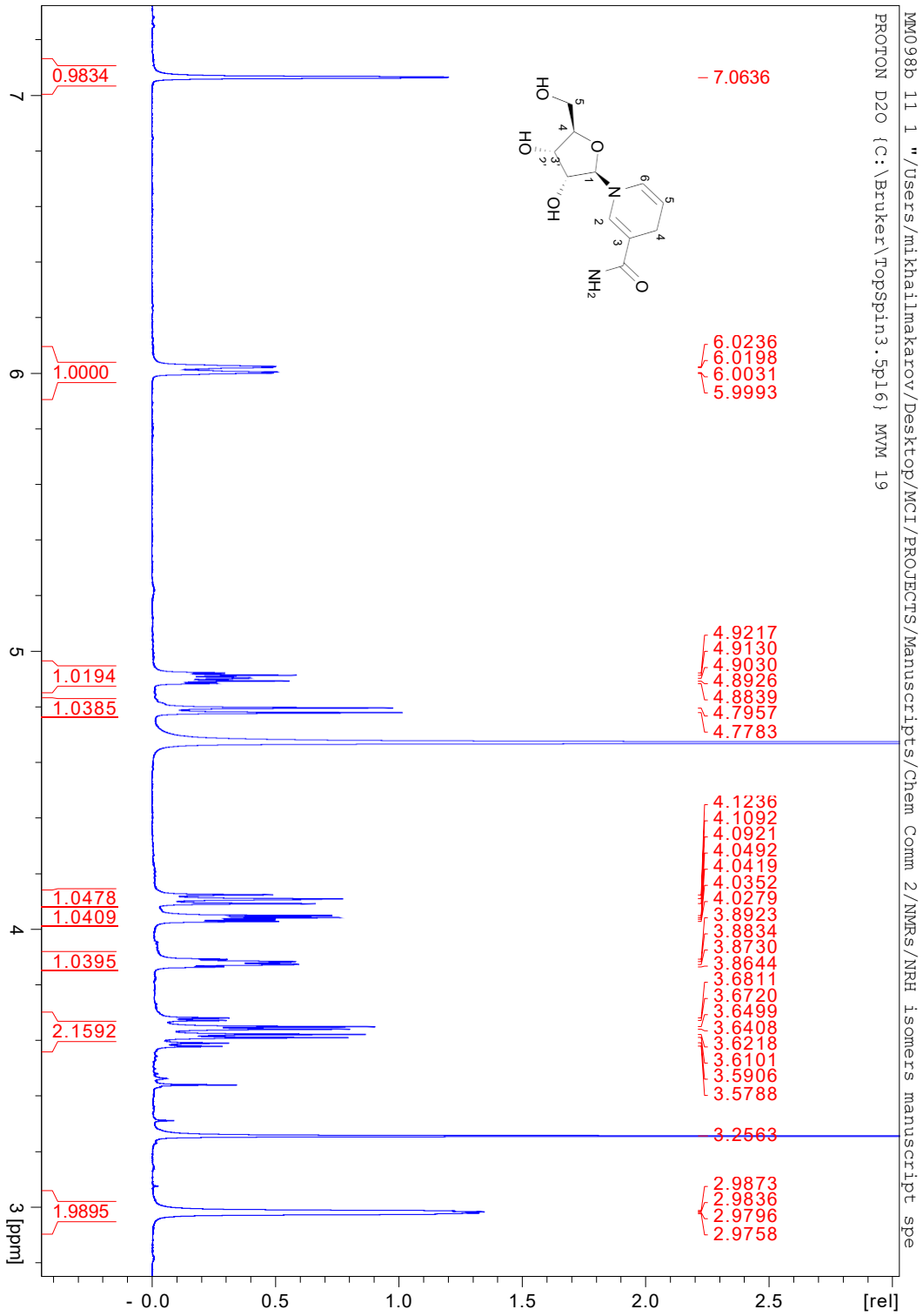

Fig. 18S ^{1}H NMR (D_2O) of NRH (**1**).

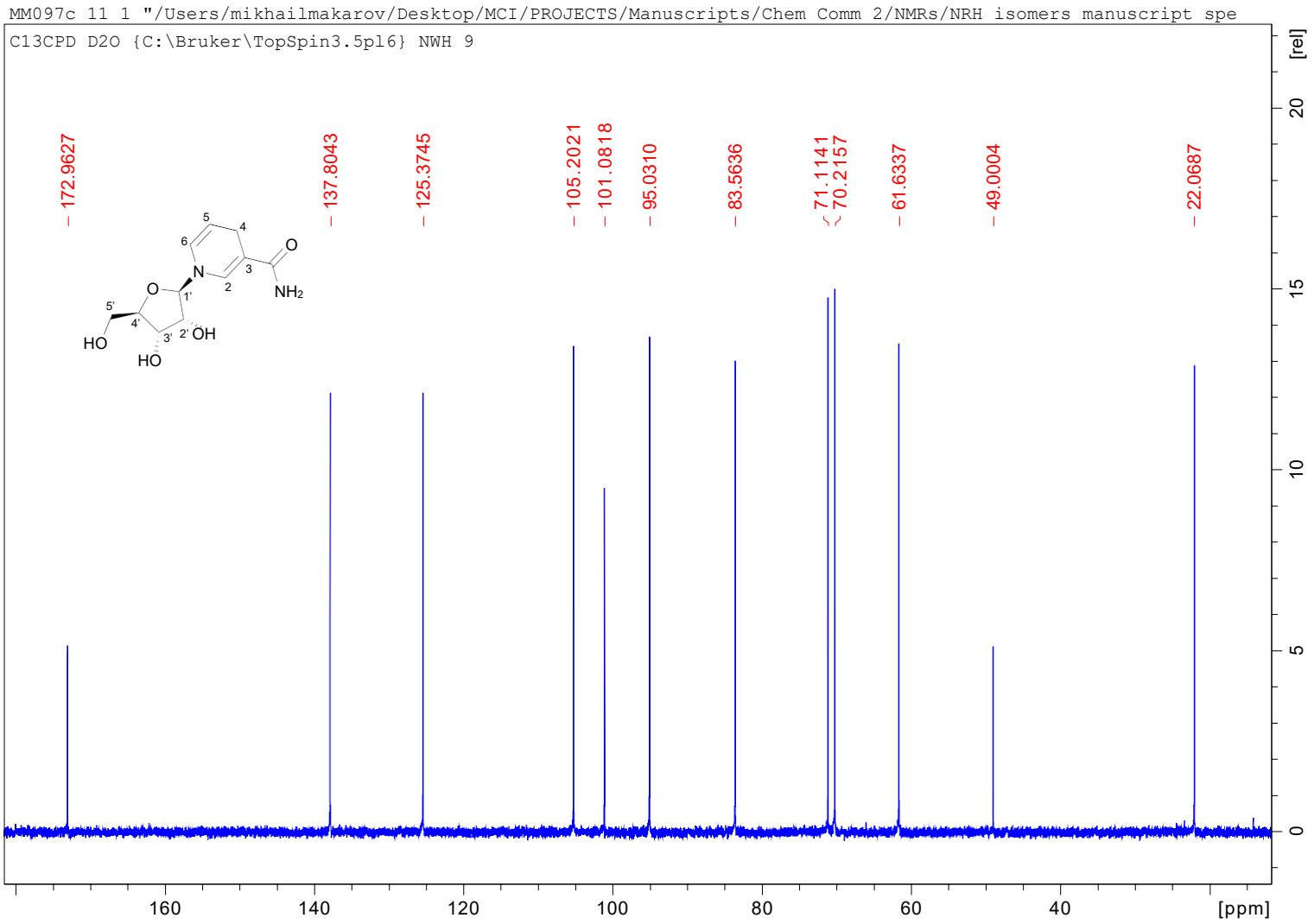

Fig. 19S ^{13}C NMR (D_2O) of NRH (**1**).

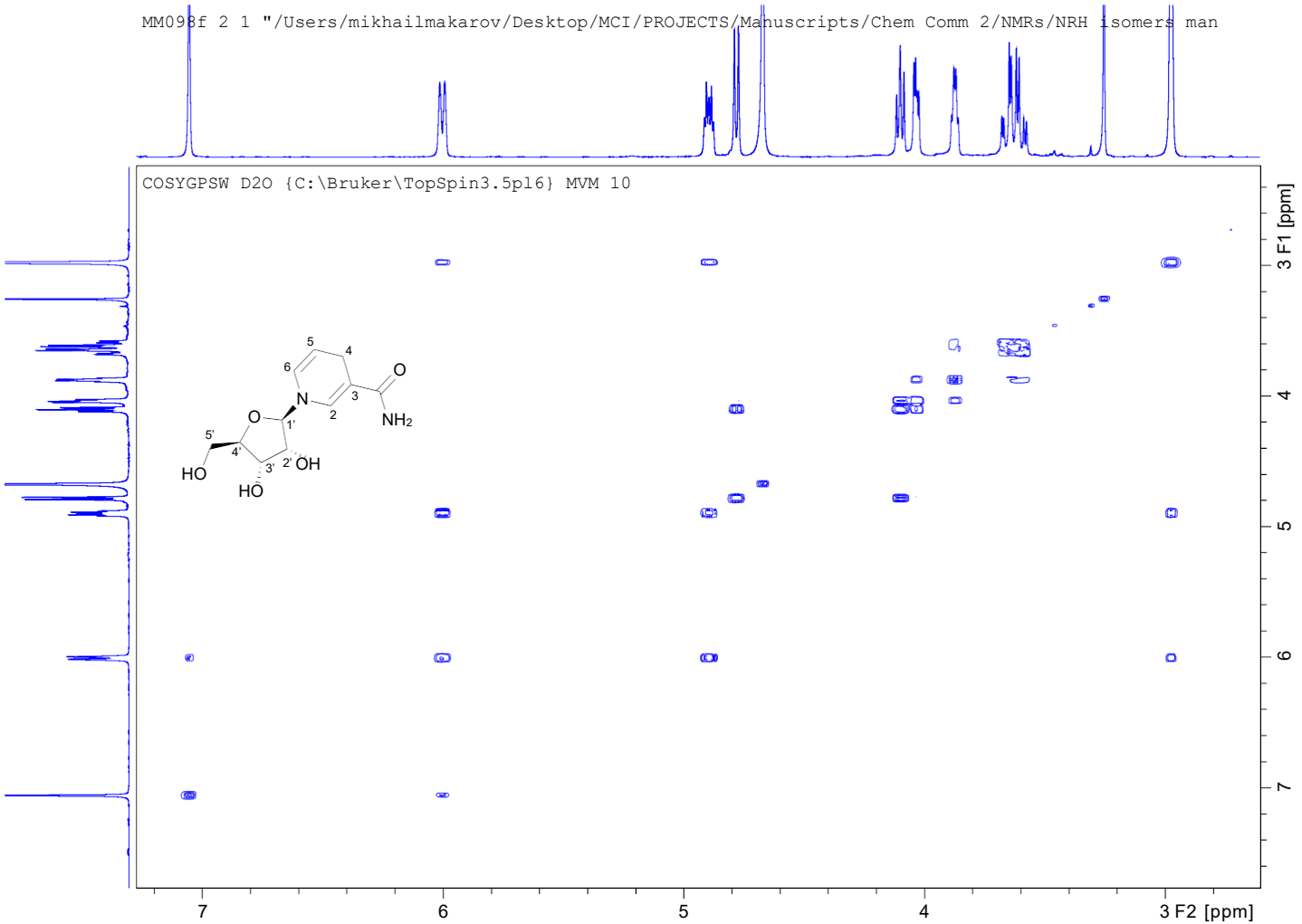

Fig. 20S ^{1}H-^{1}H correlation (COSY) NMR (D_2O) of NRH (**1**).

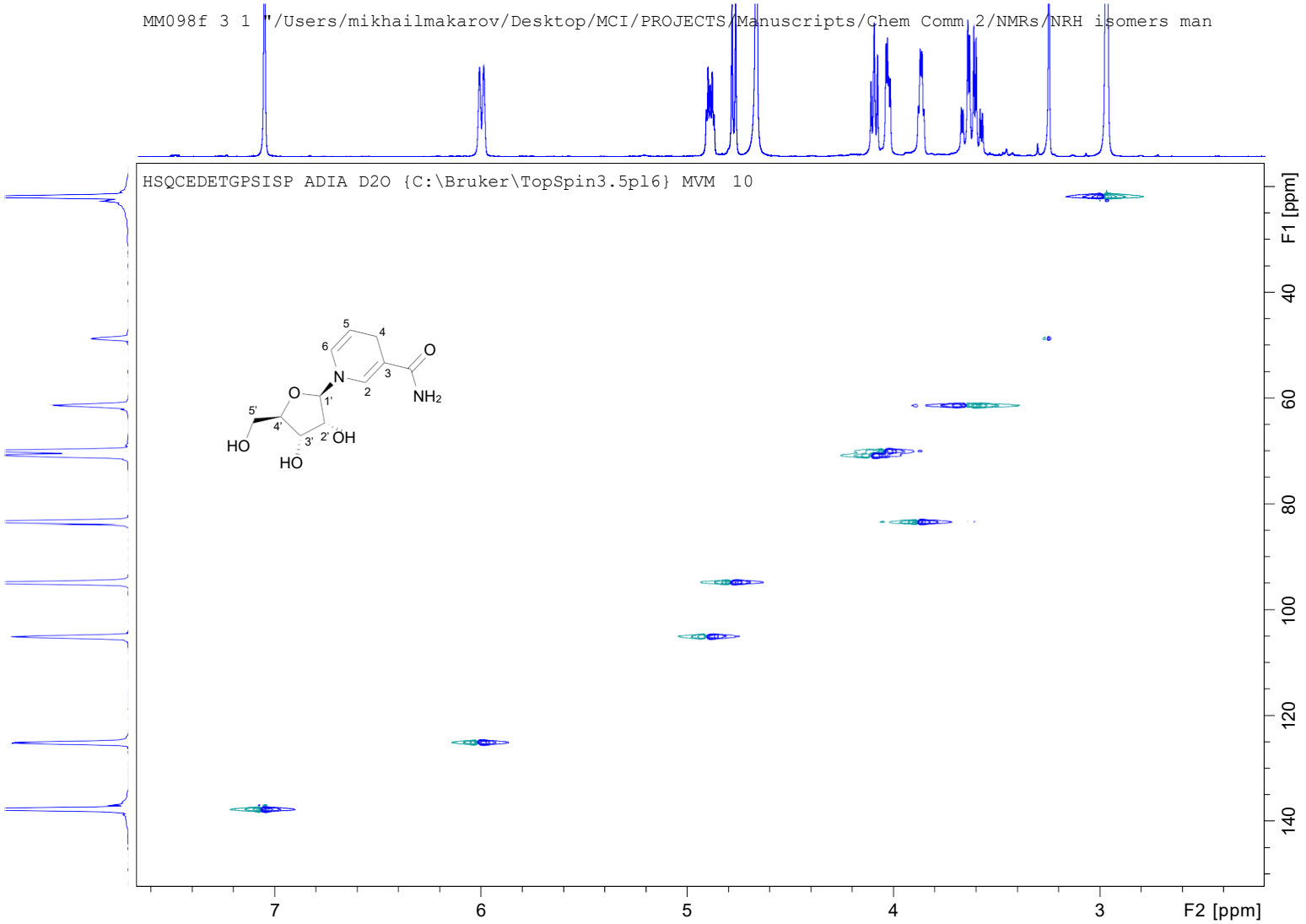

Fig. 21S ^{1}H-^{13}C correlation (HSQC) NMR (D_2O) of NRH (**1**).

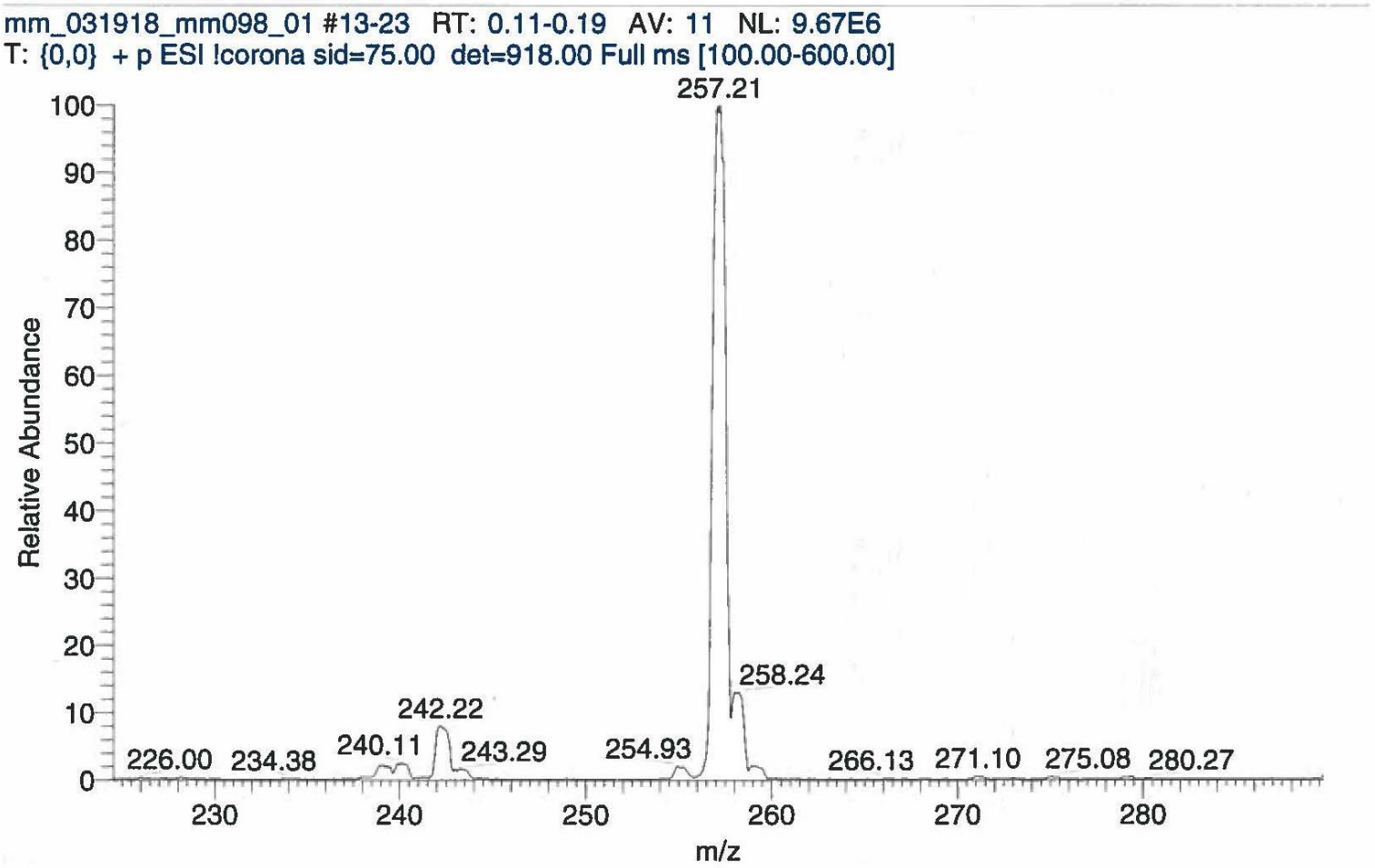

Fig. 22S MS (1:1 H_2O/ACN) of NRH (**1**).

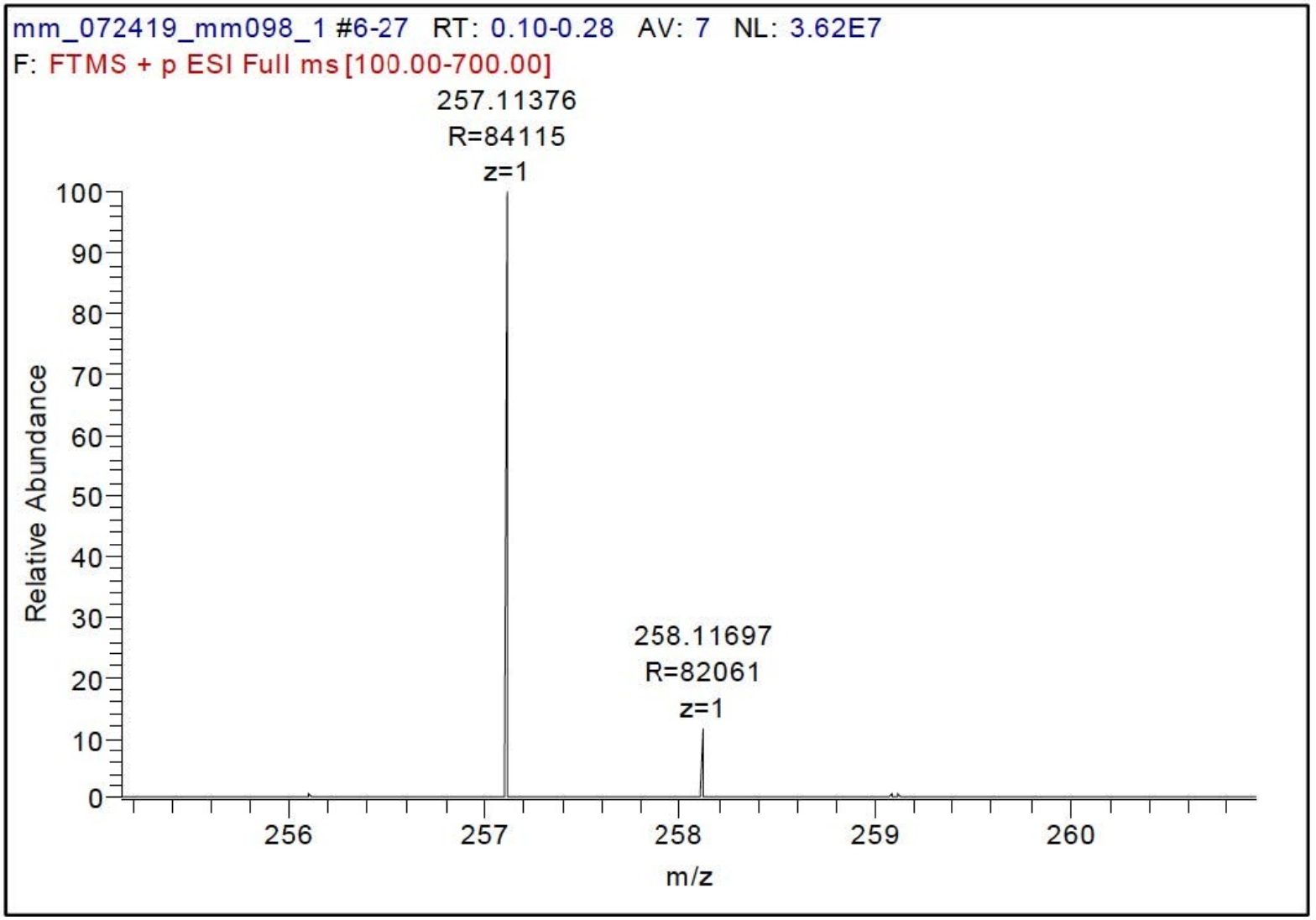

Fig. 23S HRMS (1:1 H_2O/ACN) of of NRH (**1**).

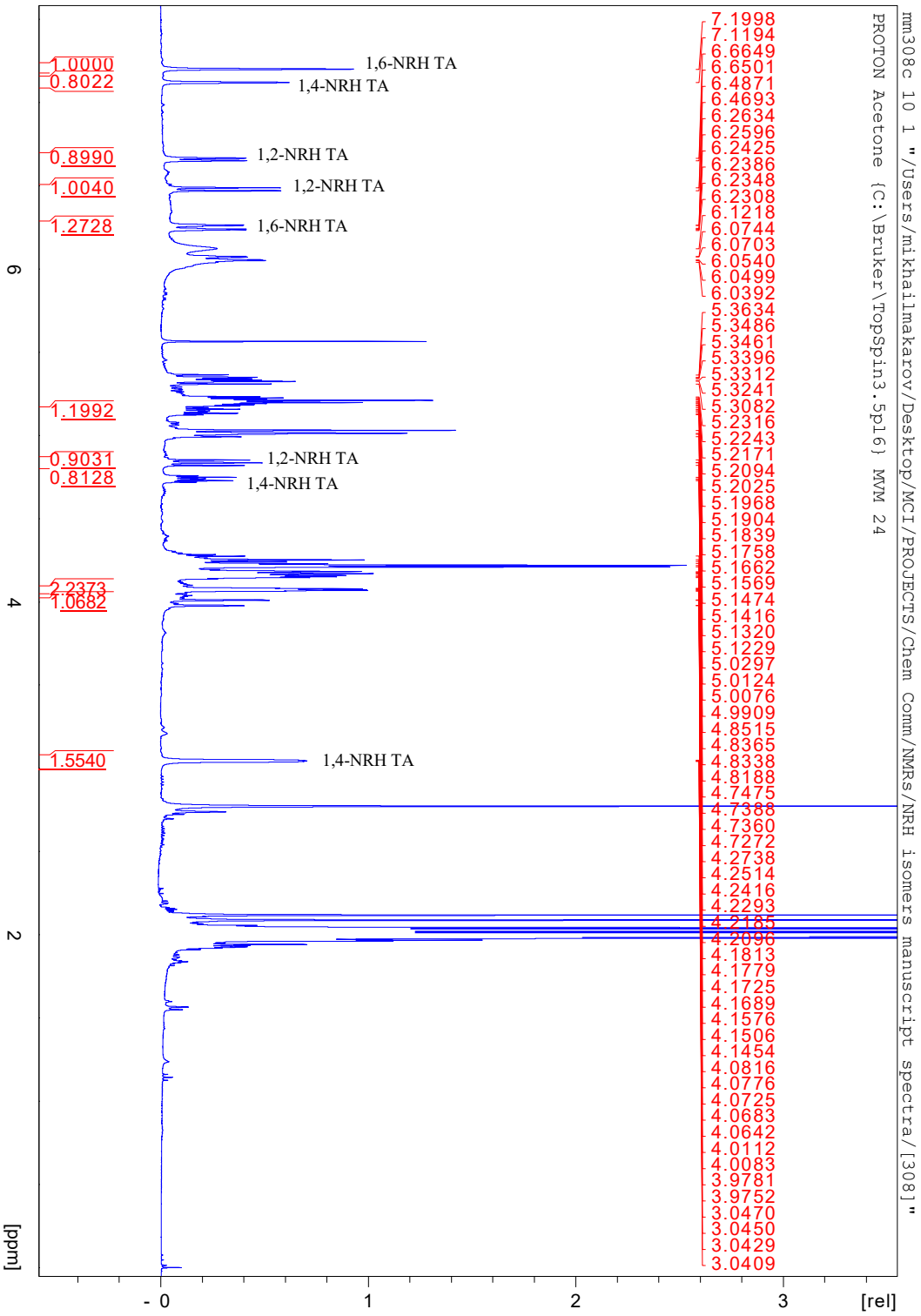

Fig. 24S ^{1}H NMR (acetone-d_6) of crude mixture of 1,2- (**8**), 1,4- (**7**), and 1,6-NRH TA (**9**) (reduction in H_2O/DCM).

Sample: mm308 | **CombiFlash NEXTGEN** | **Friday 26 April 2019 05:21PM**

Column: Silica 40g
Flow Rate: 25 ml/min
Equilibration Volume: 192.2 ml
Initial Waste: 0.0 ml
Air Purge: 0.0 min
Solvent A*: Hexanes, then EtOAc
Solvent B*: EtOAc, then EtOH

Peak Tube Volume: Max.
Non-Peak Tube Volume: Max.
Loading Type: Liquid
Wavelength 1 (red): 254nm
Peak Width: 2 min
Threshold: 0.20 AU
Wavelength 2 (purple): 350nm

***Run Notes:** Chromatography was started with solvent A being hexanes and solvent B being EtOAc up to point X; after this point solvent A was EtOAc and solvent B was EtOH.

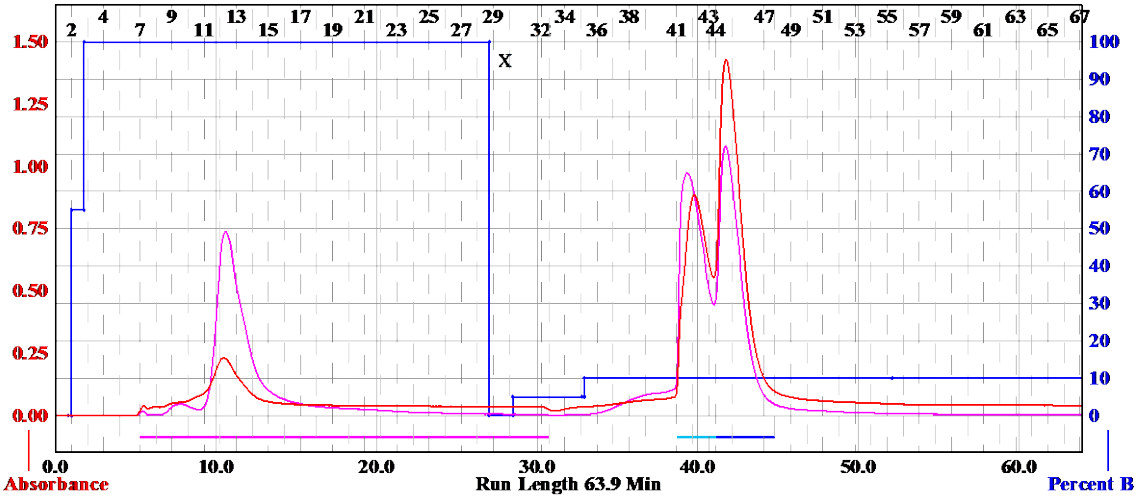

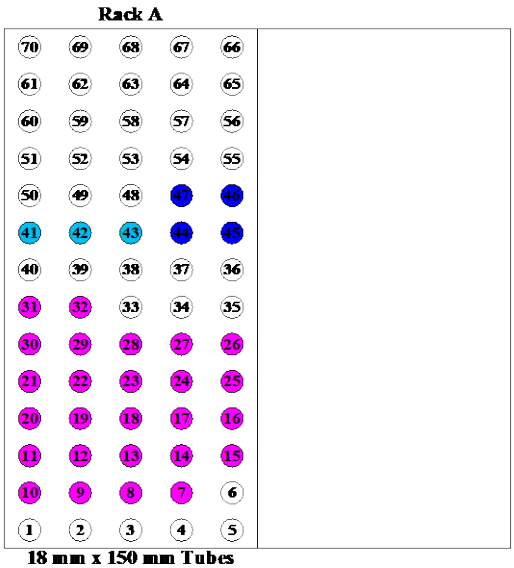

Peak #	Start Tube	End Tube
1	A:7	A:32
2	A:41	A:43
3	A:44	A:47

Duration	%B
0.0	0.0
0.8	0.0
0.2	0.0
0.0	0.0
0.0	55.0
0.8	55.0
0.0	100.0
25.2	100.0
0.0	0.0
1.5	0.0
--	--

Page 1 of 1

Fig. 25S Data on MPLC (Teledyne) chromatographic purification of crude mixture of 1,2- (**8**), 1,4- (**7**), and 1,6-NRH TA (**9**) (reduction in H_2O/DCM).

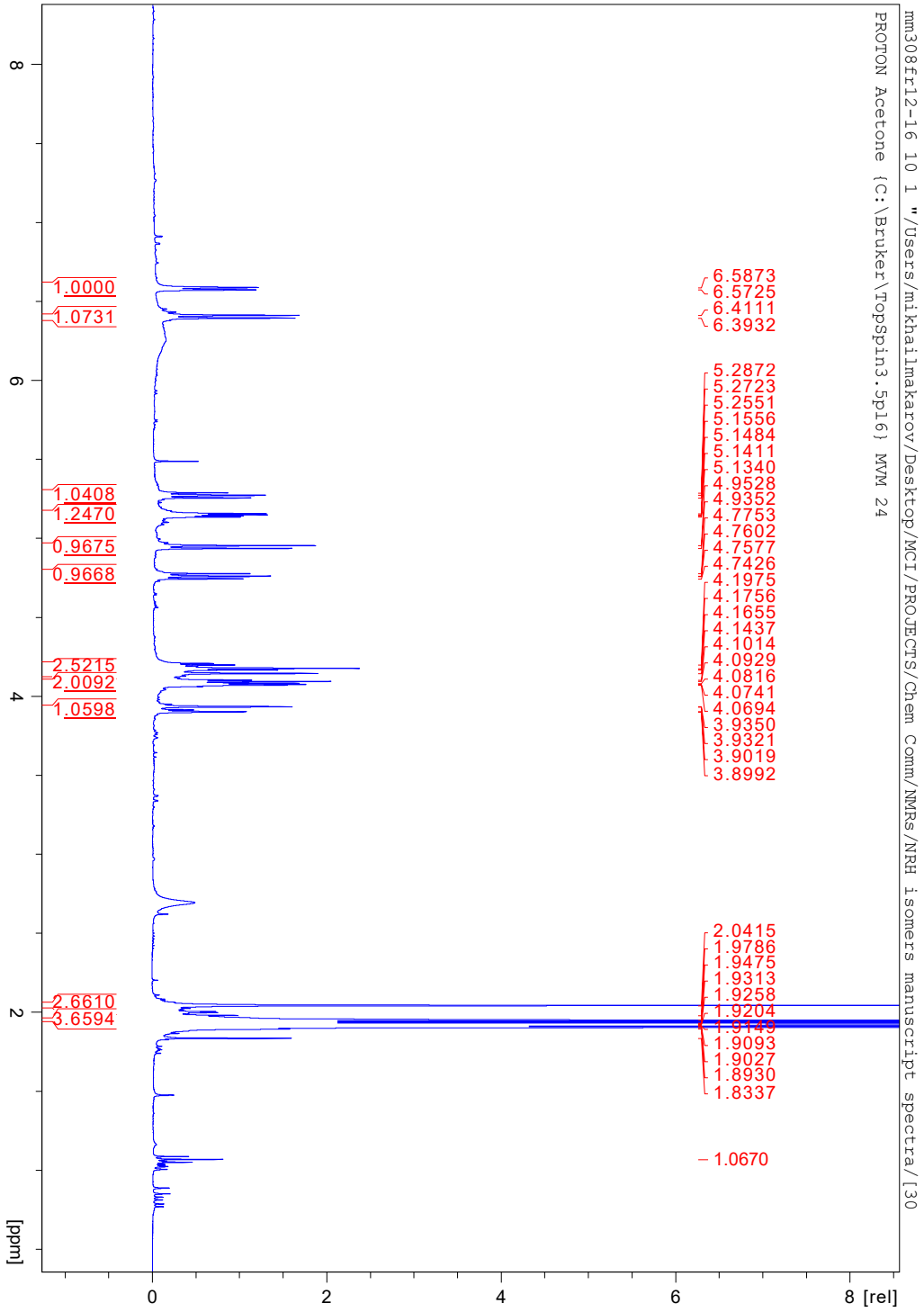

Fig. 26S ^{1}H NMR (acetone-d_6) of 1,2-NRH TA (**8**) (portion A) (reduction in H_2O/DCM).

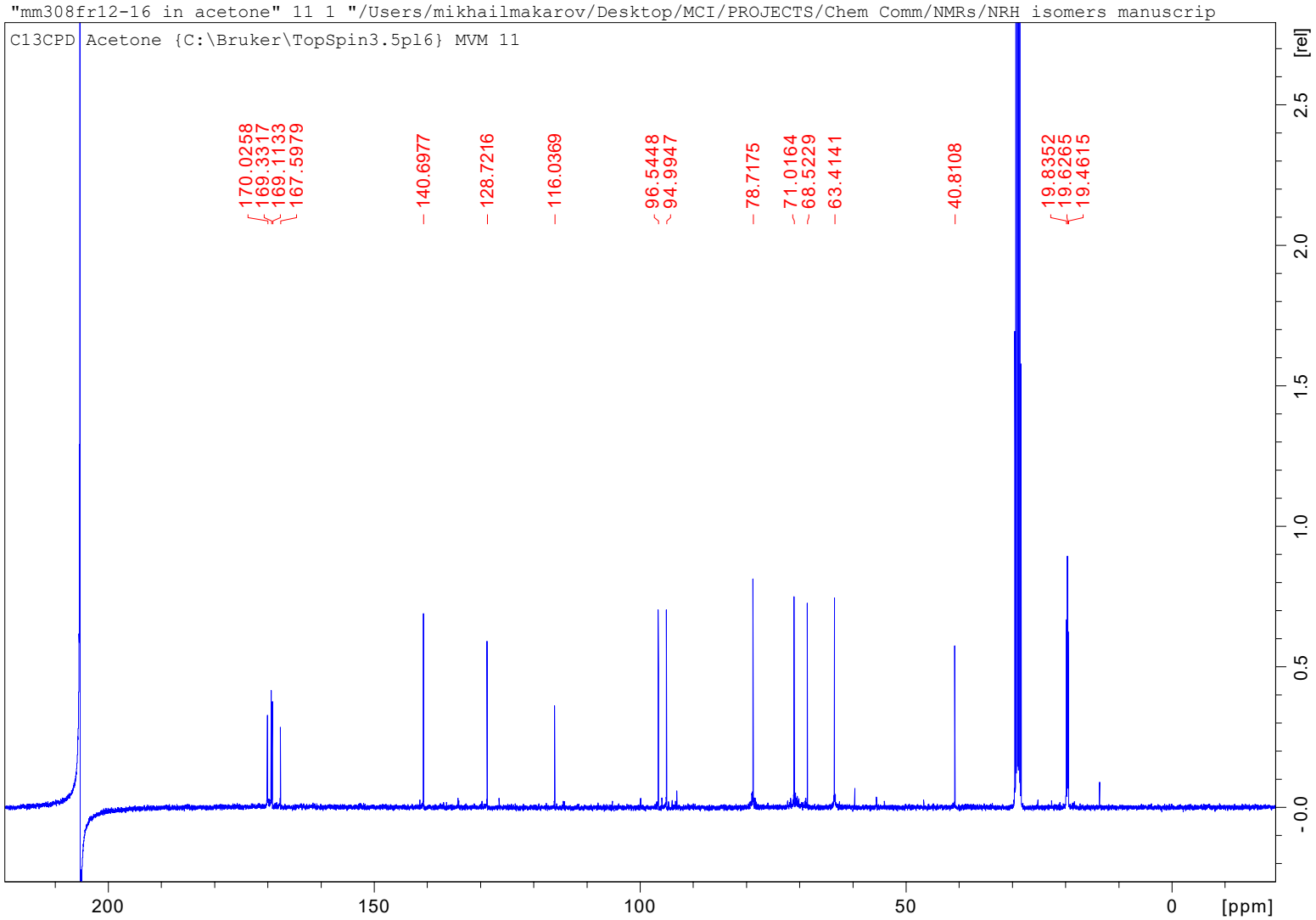

Fig. 27S ^{13}C NMR (acetone-d_6) of 1,2-NRH TA (**8**) (portion A) (reduction in H_2O/DCM).

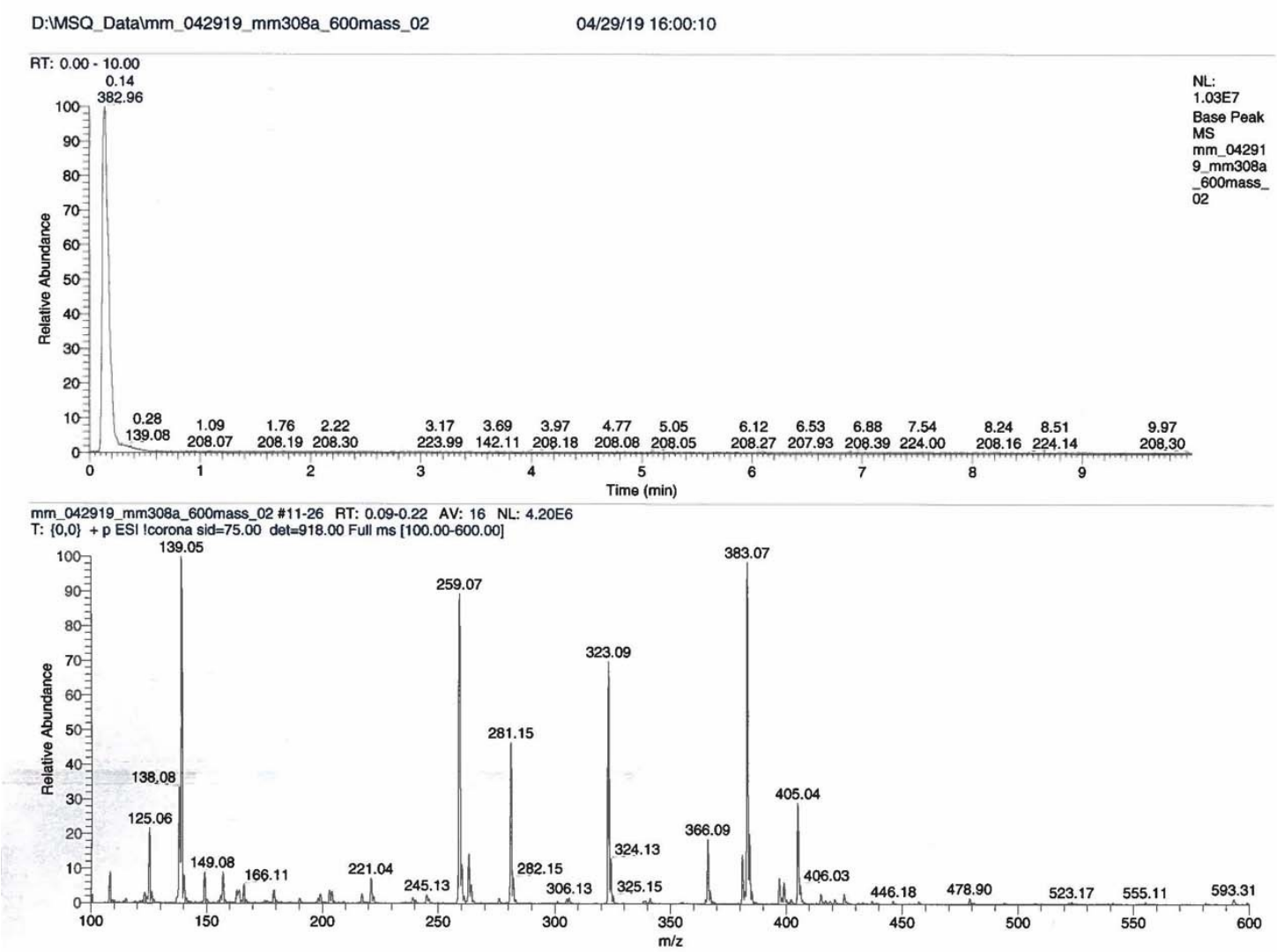

Fig. 28S MS (1:1 H_2O/ACN) of 1,2-NRH TA (**8**)

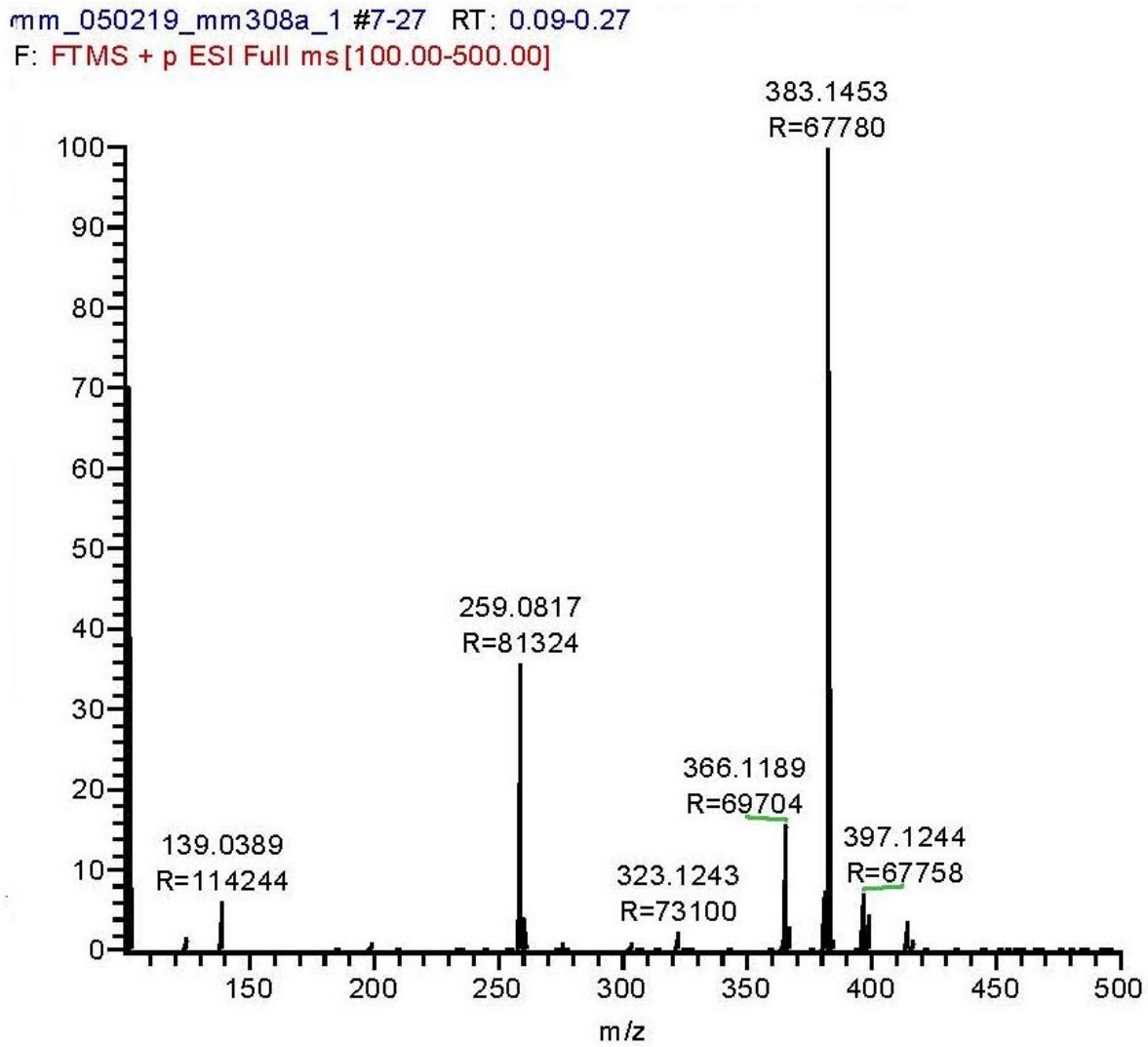

Fig. 29S HRMS (1:1 H_2O/ACN) of 1,2-NRH TA (**8**): full scan.

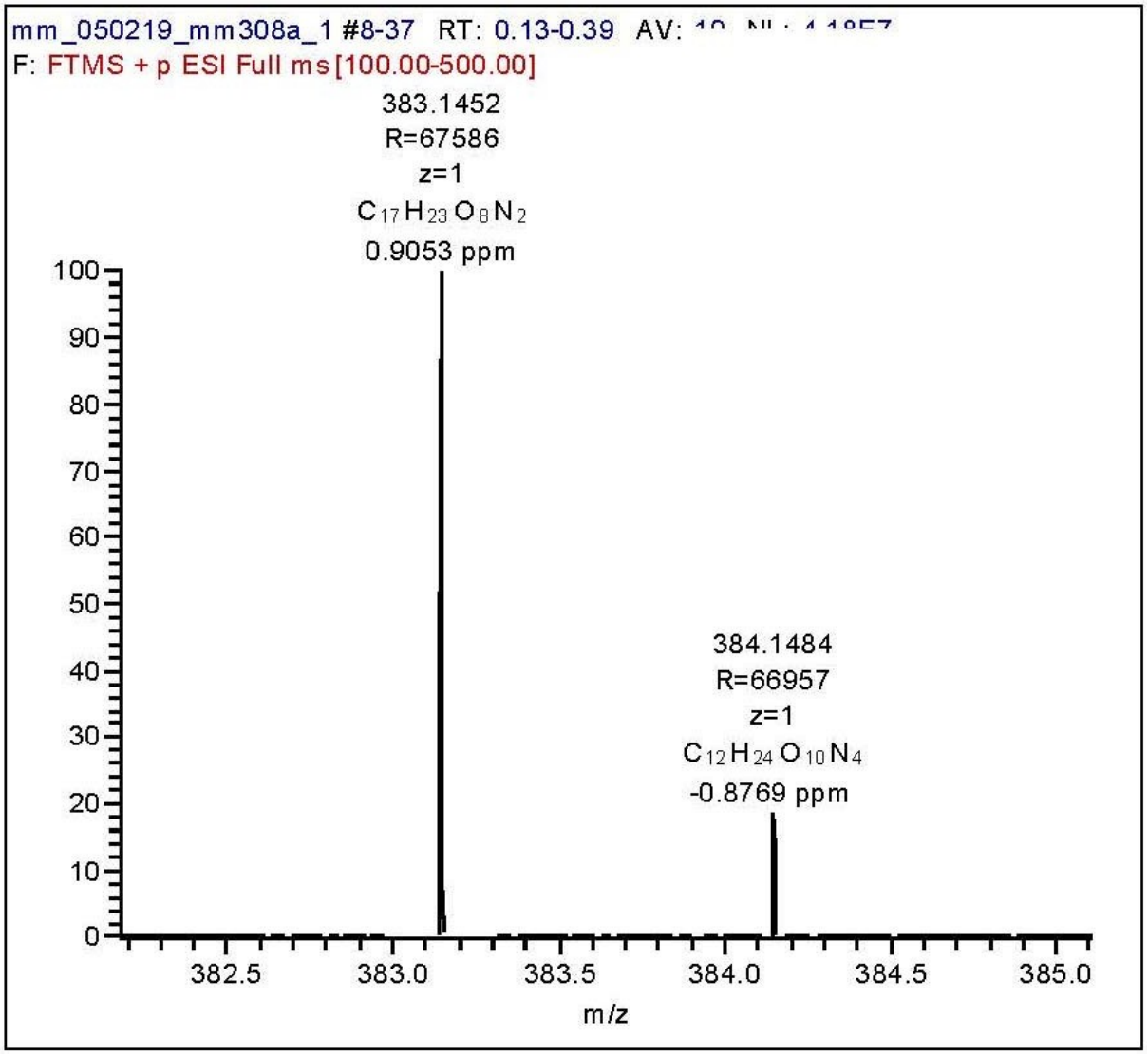

Fig. 30S HRMS (1:1 H_2O/ACN) of 1,2-NRH TA (**8**): parent peak.

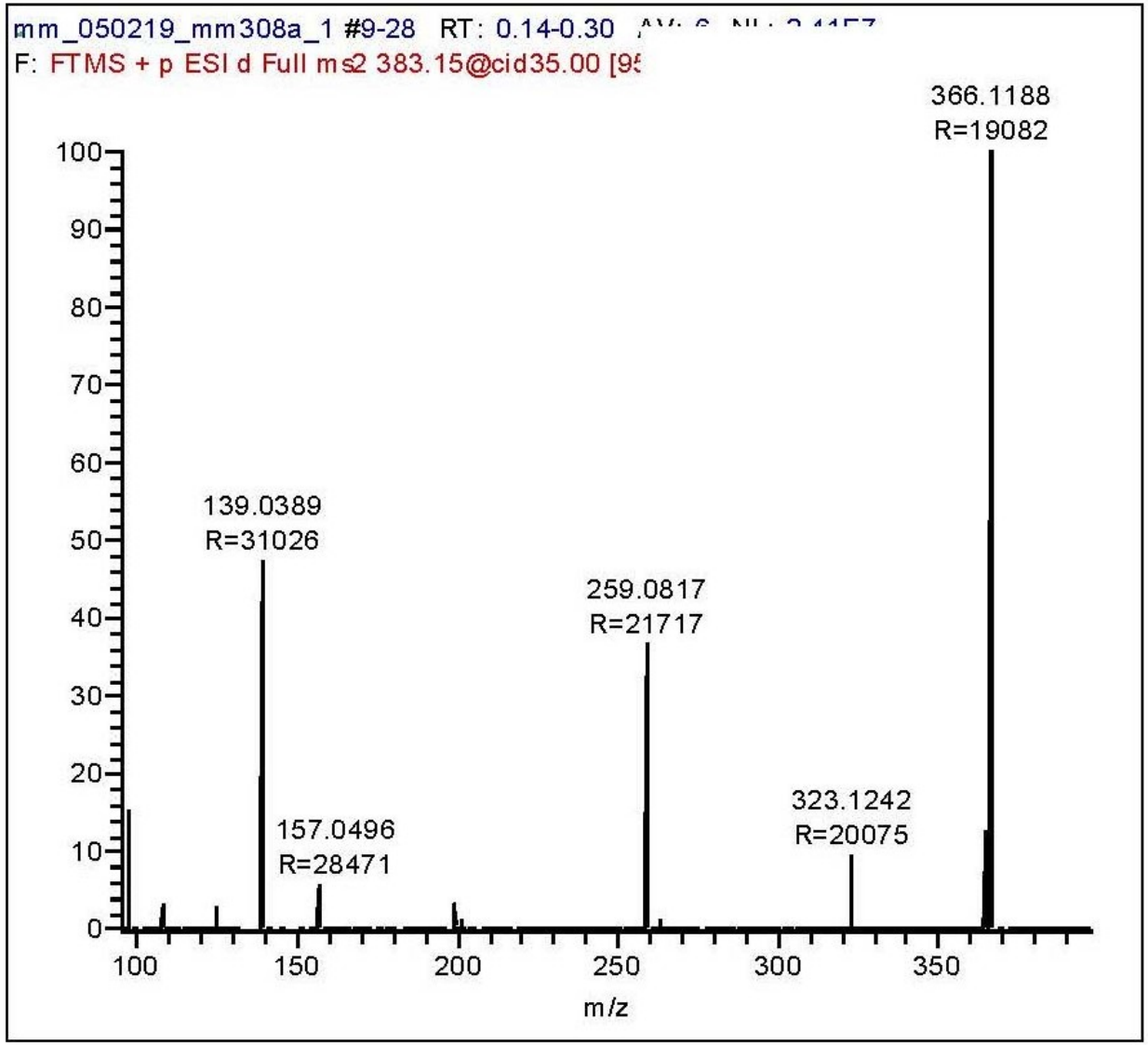

Fig. 31S HRMS (1:1 H_2O/ACN) of 1,2-NRH TA (**8**): fragmentation of parent peak.

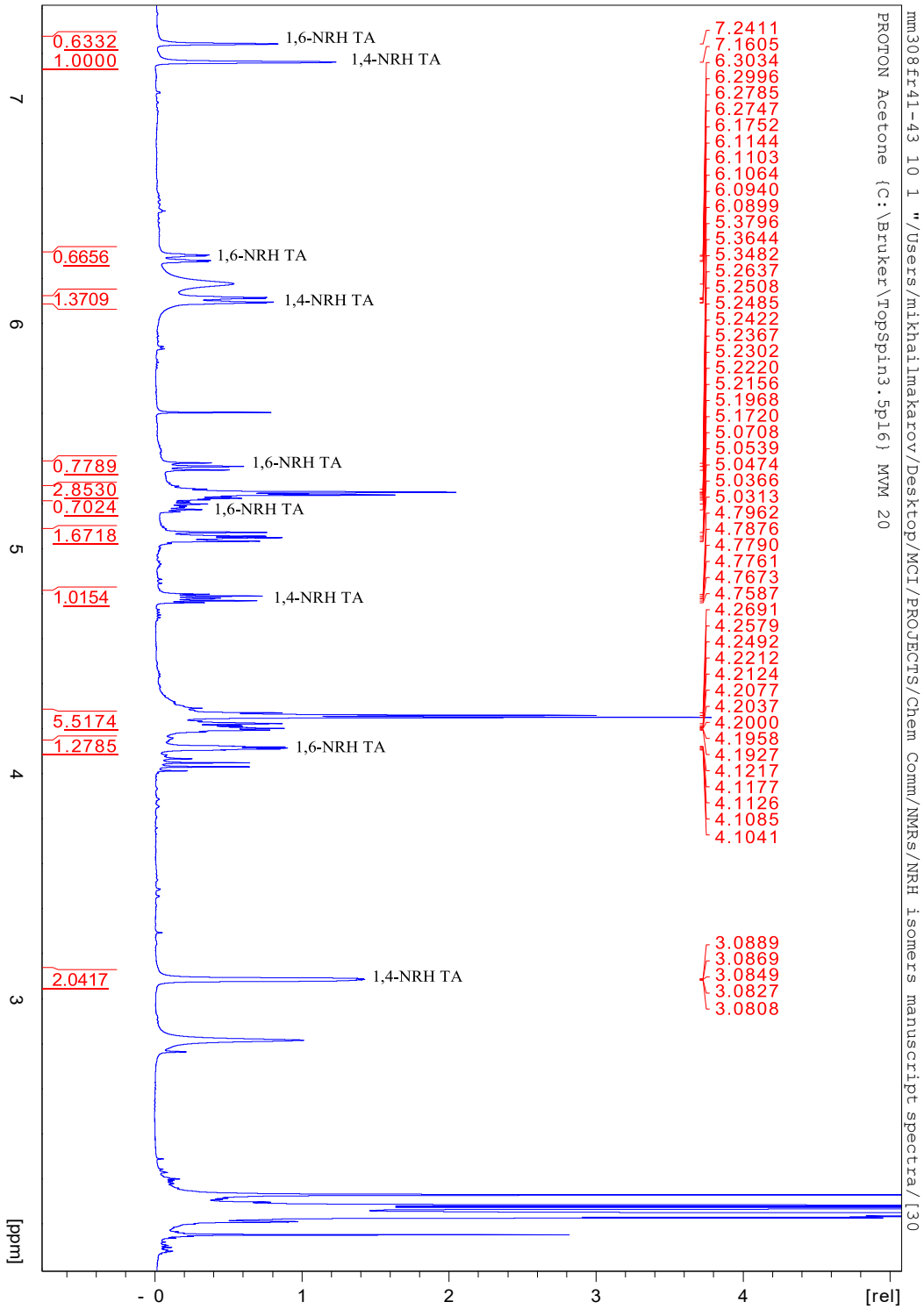

Fig. 32S ^{1}H NMR (acetone-d_6) of 1,4- (**7**) and 1,6-NRH TA (**9**) mixture (portion B) (reduction in

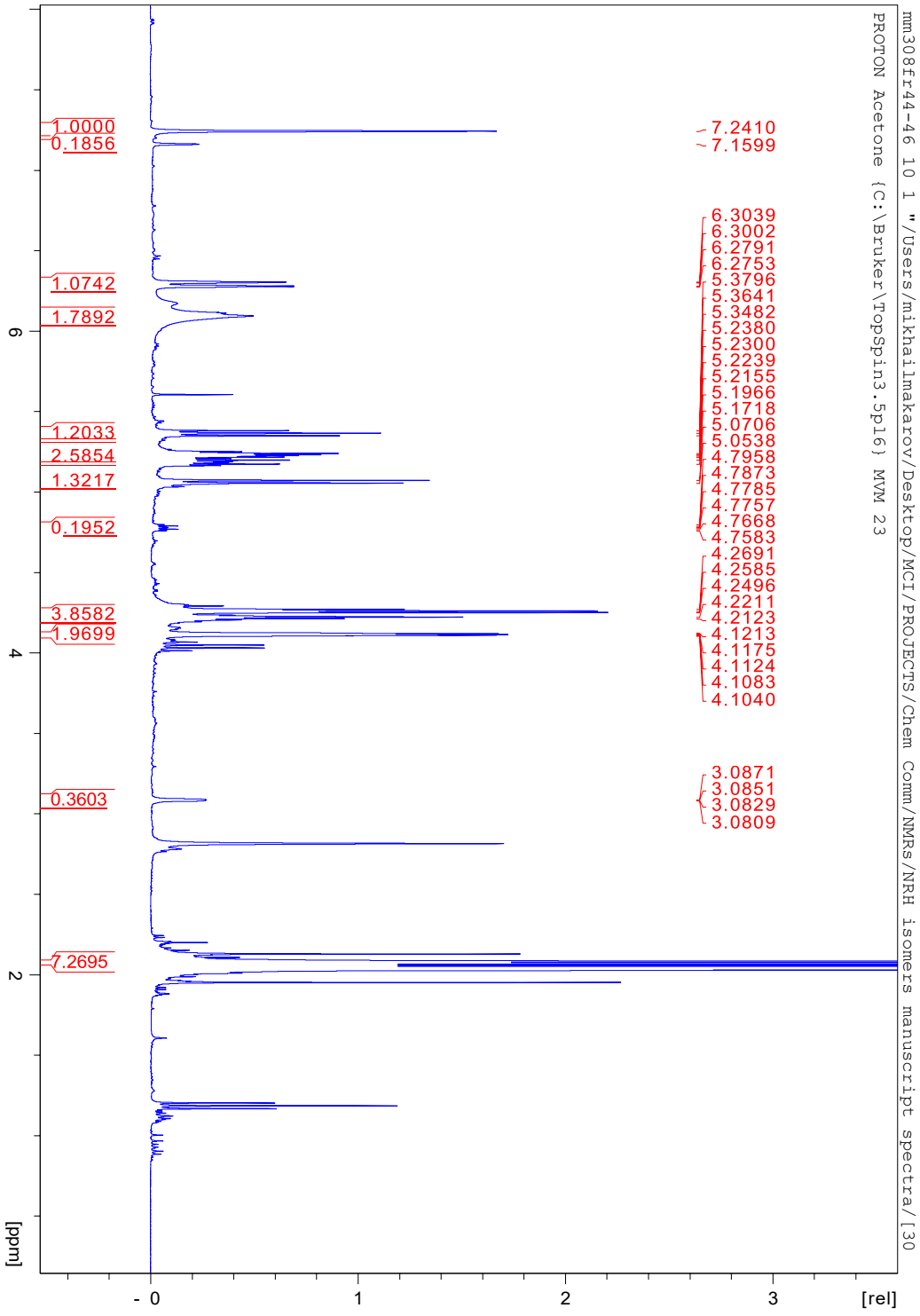

Fig. 33S ^{1}H NMR (acetone-d_6) of 1,6-NRH TA (**9**) containing admixtire of 1,4-NRH TA (**7**) (18– 20 mol%) (portion C) (reduction in

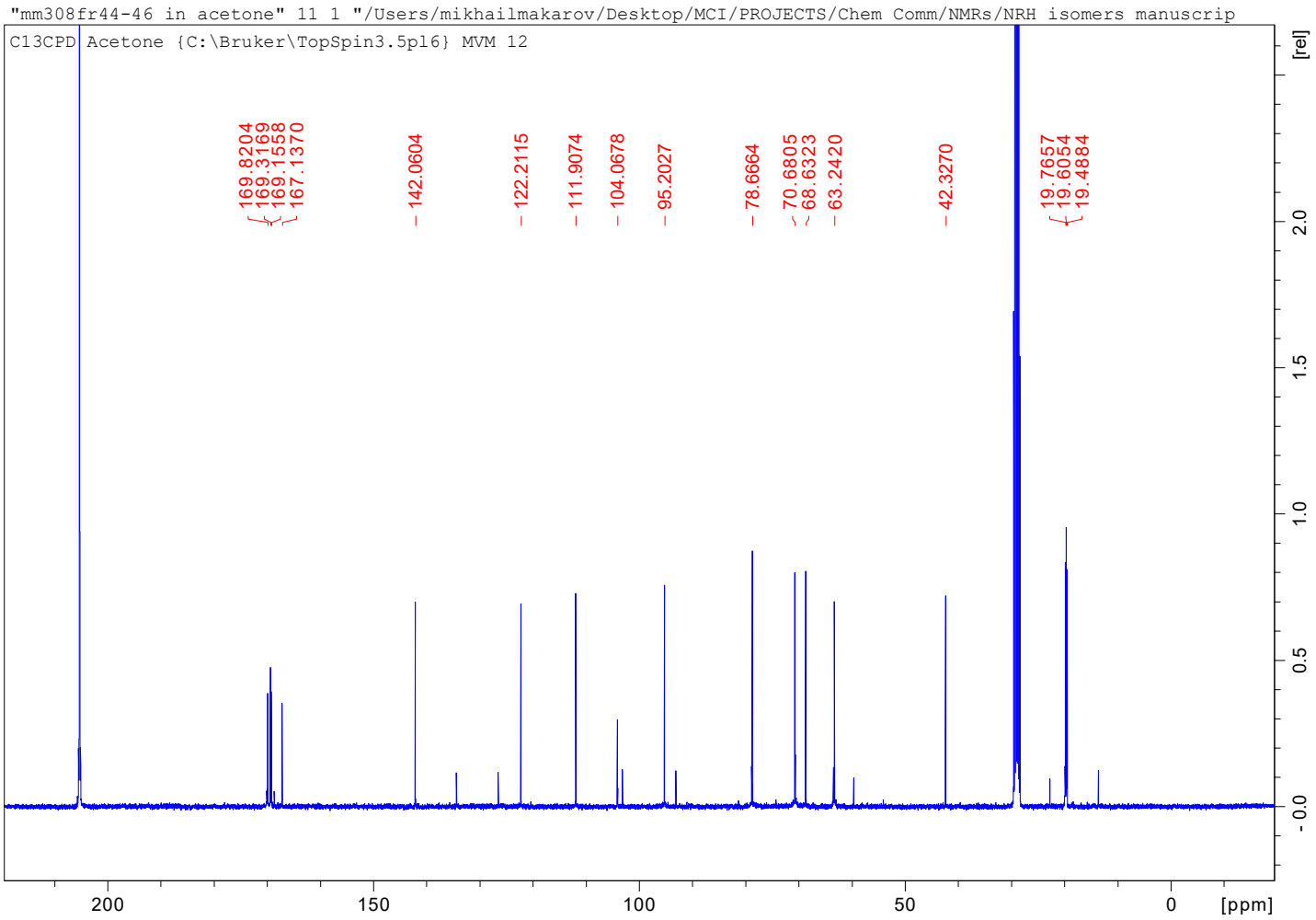

Fig. 34S ^{13}C NMR (acetone-d_6) of 1,6-NRH TA (**9**) containing admixtire of 1,4-NRH TA (**7**) (18–20 mol%) (portion C) (reduction in H_2O/DCM).

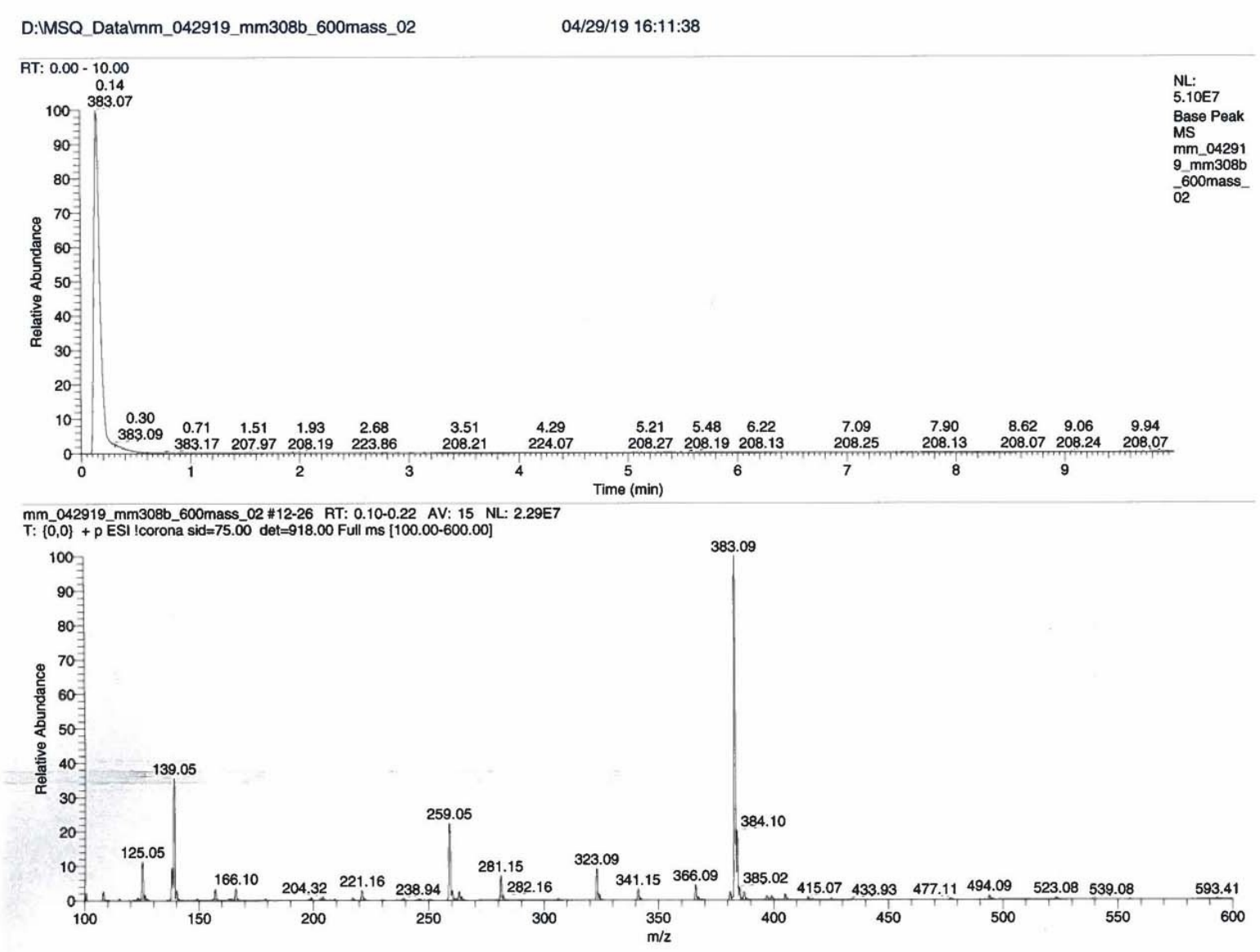

Fig. 35S MS (1:1 H_2O/ACN) 1,6-NRH TA (**9**)

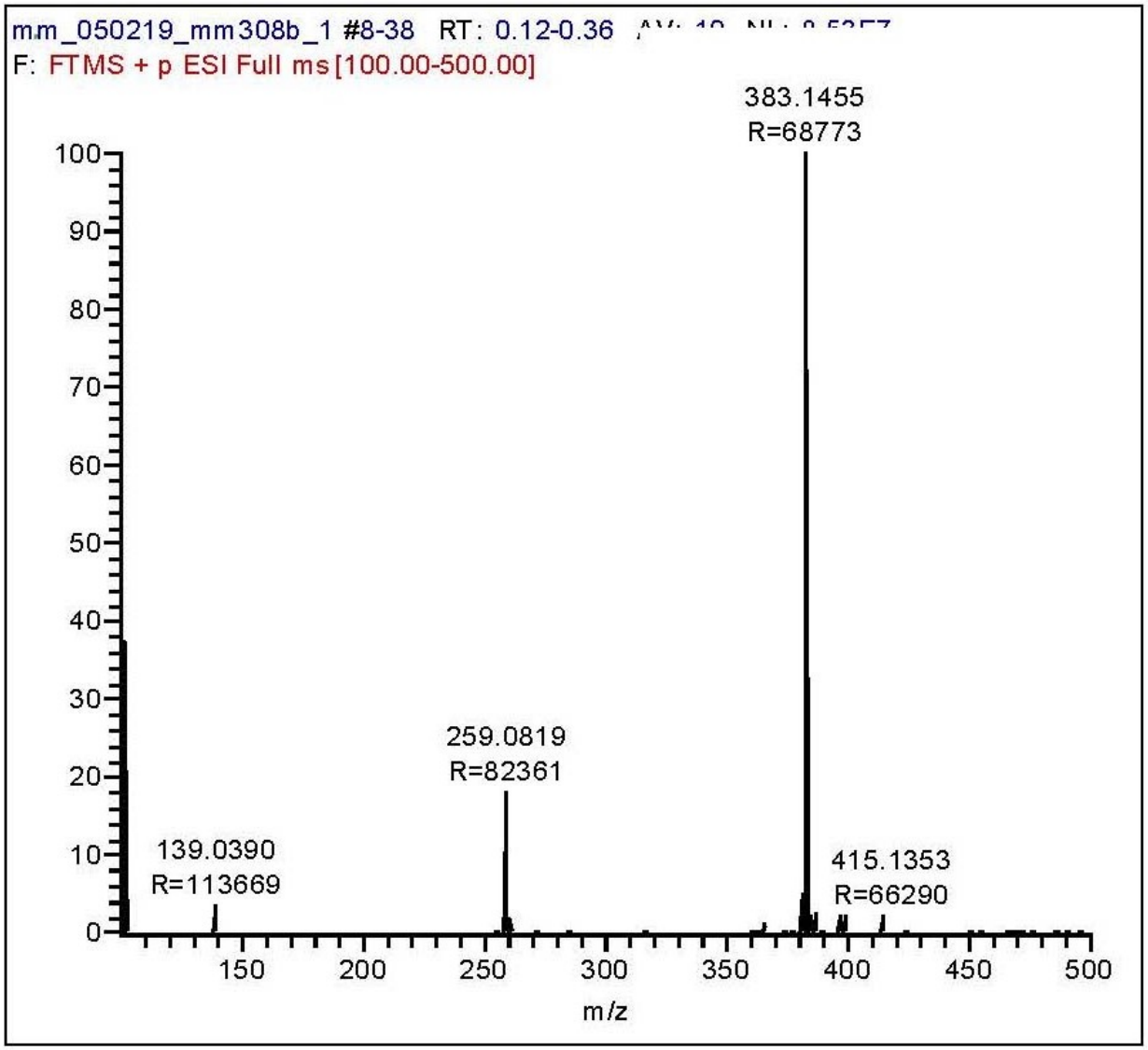

Fig. 36S HRMS (1:1 H_2O/ACN) of 1,6-NRH TA (**9**): full scan.

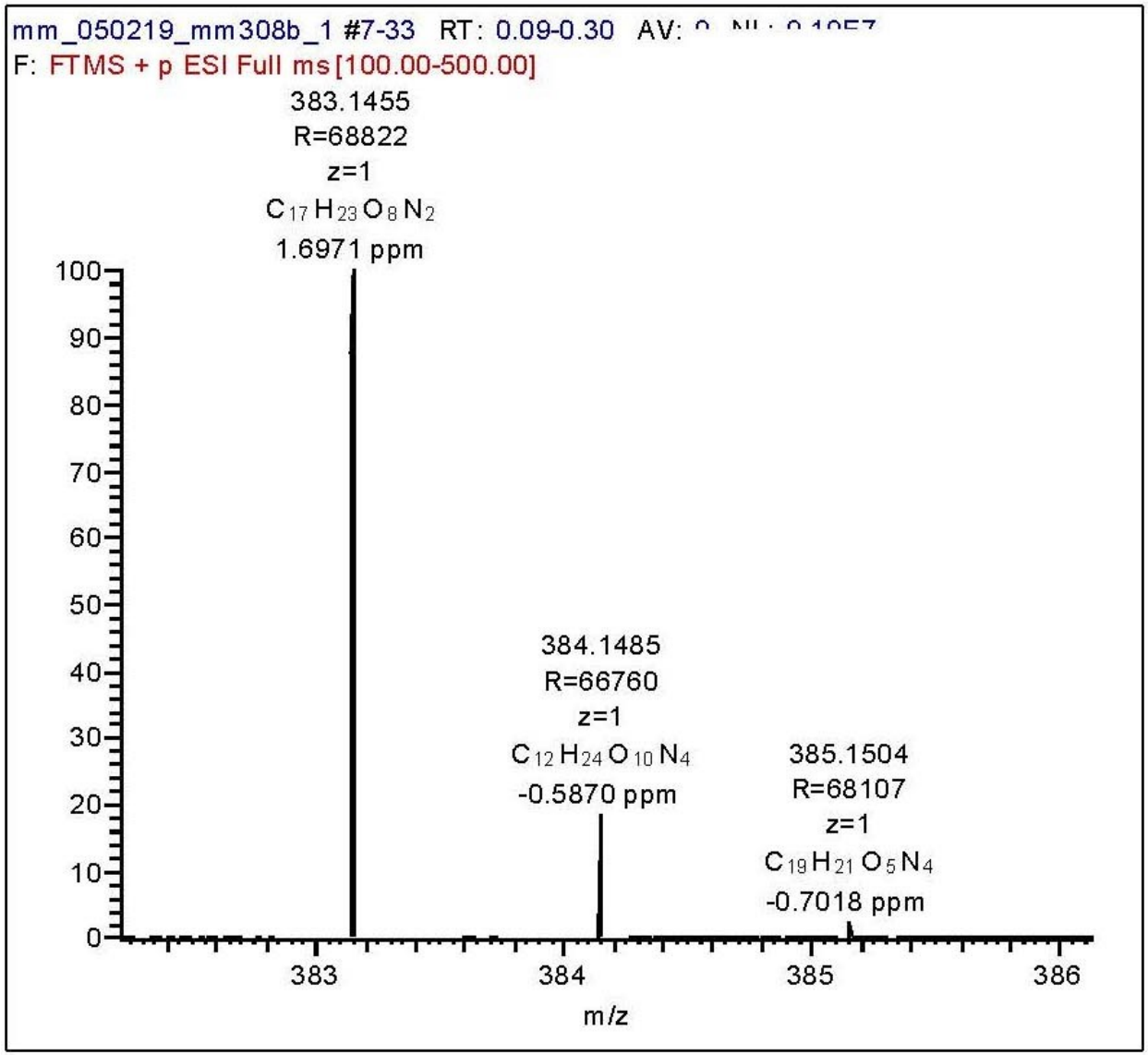

Fig. 37S HRMS (1:1 H_2O/ACN) of 1,6-NRH TA (**6**): parent peak.

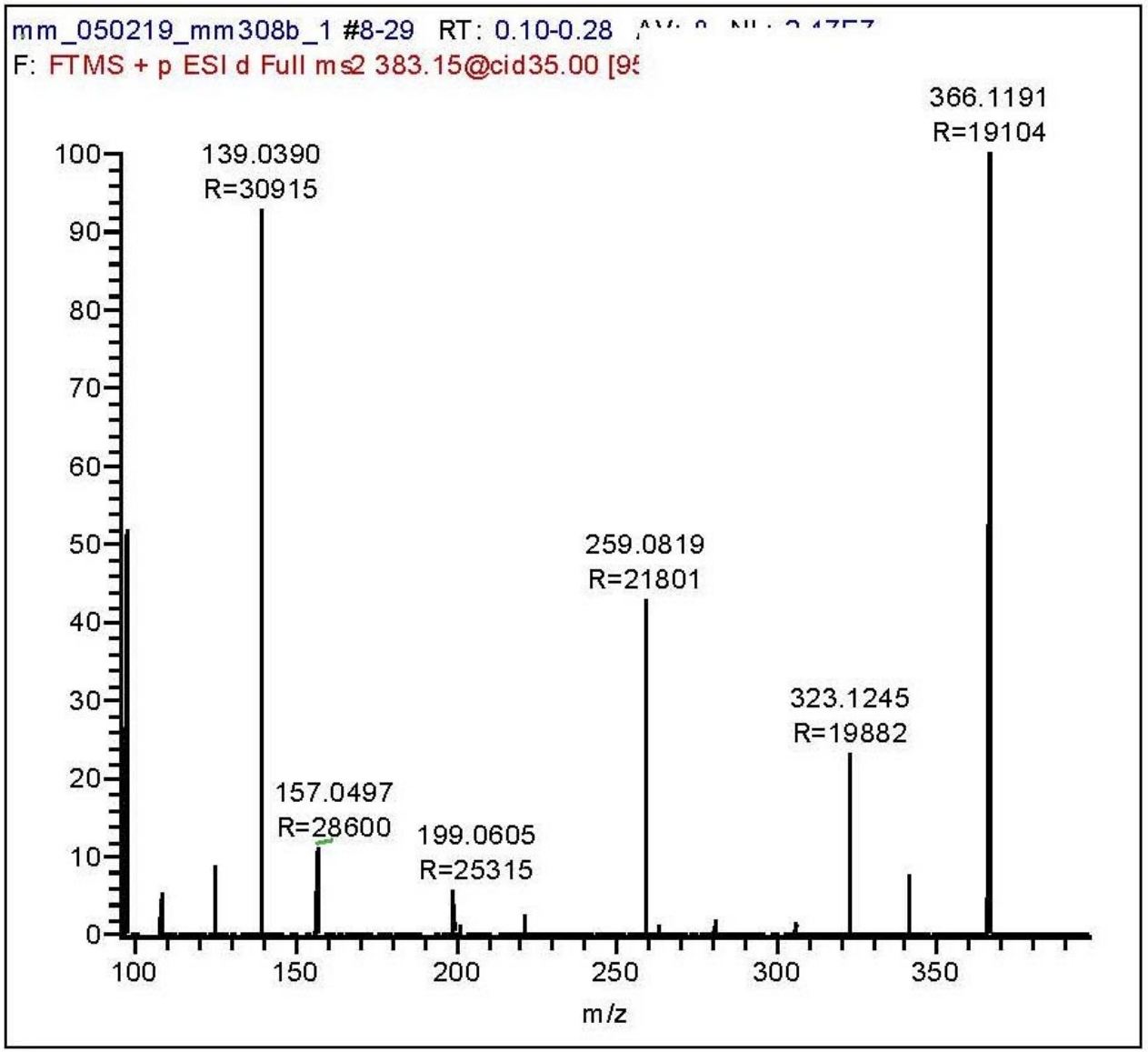

Fig. 38S HRMS (1:1 H_2O/ACN) of 1,6-NRH TA (**9**): fragmentation of parent peak.

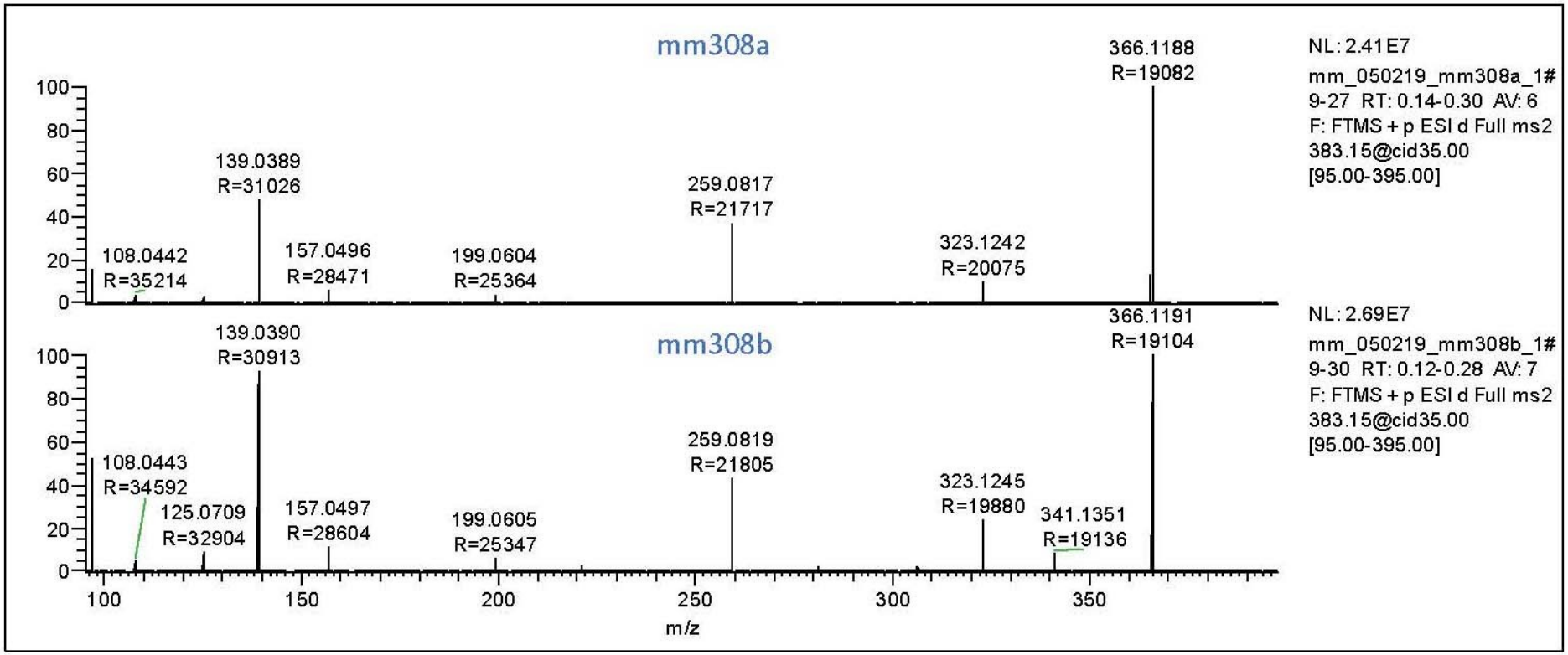

Fig. 39S Comparison of frafmentation of 1,2-NRH TA (**8**) (sample mm308a) and 1,6-NRH TA (**9**) (sample mm308b).

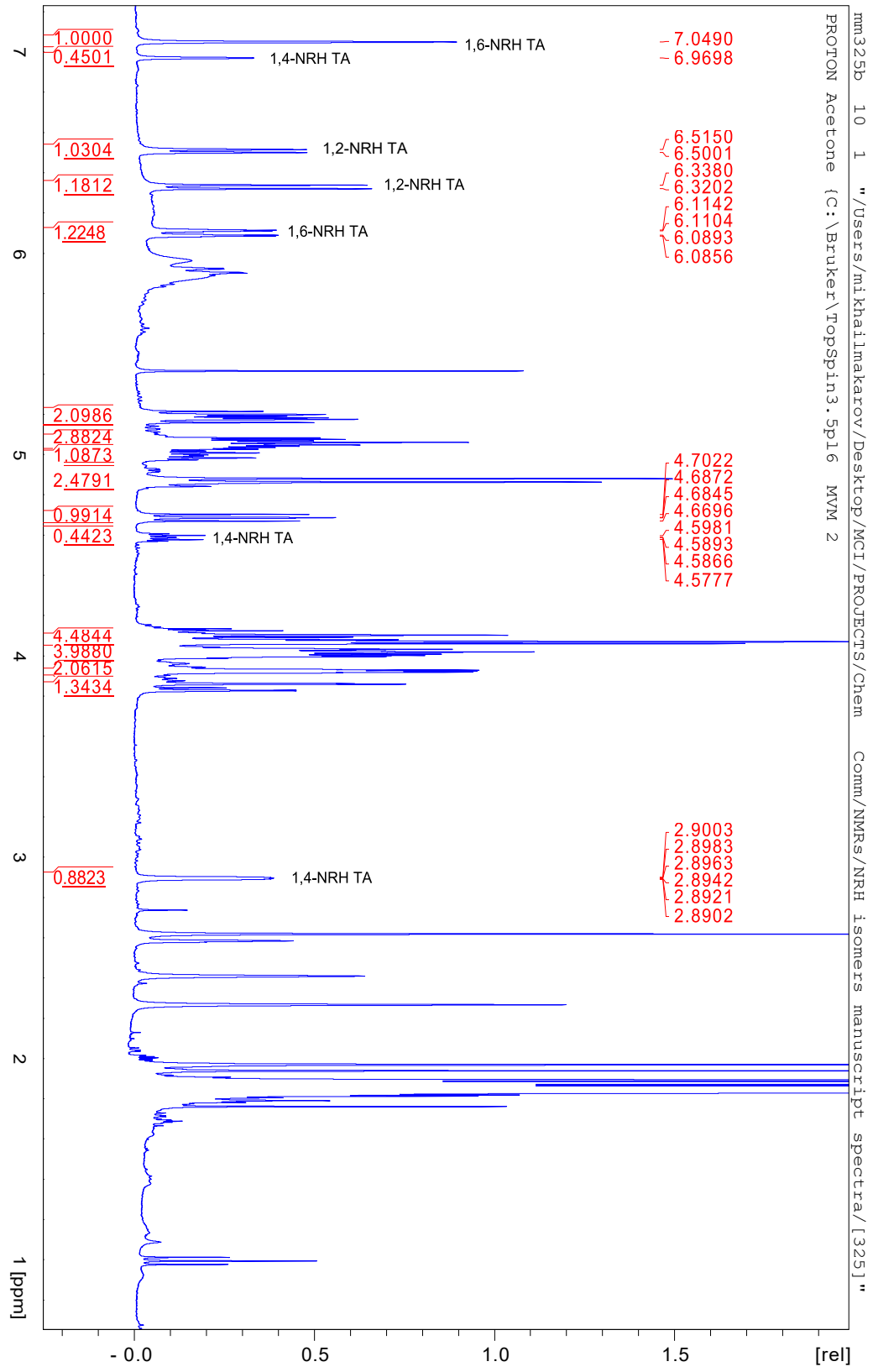

Fig. 40S ^{1}H NMR (acetone-d_6) of crude mixture of 1,2- (**8**), 1,4- (**7**), and 1,6-NRH TA (**9**) (reduction in DMF).

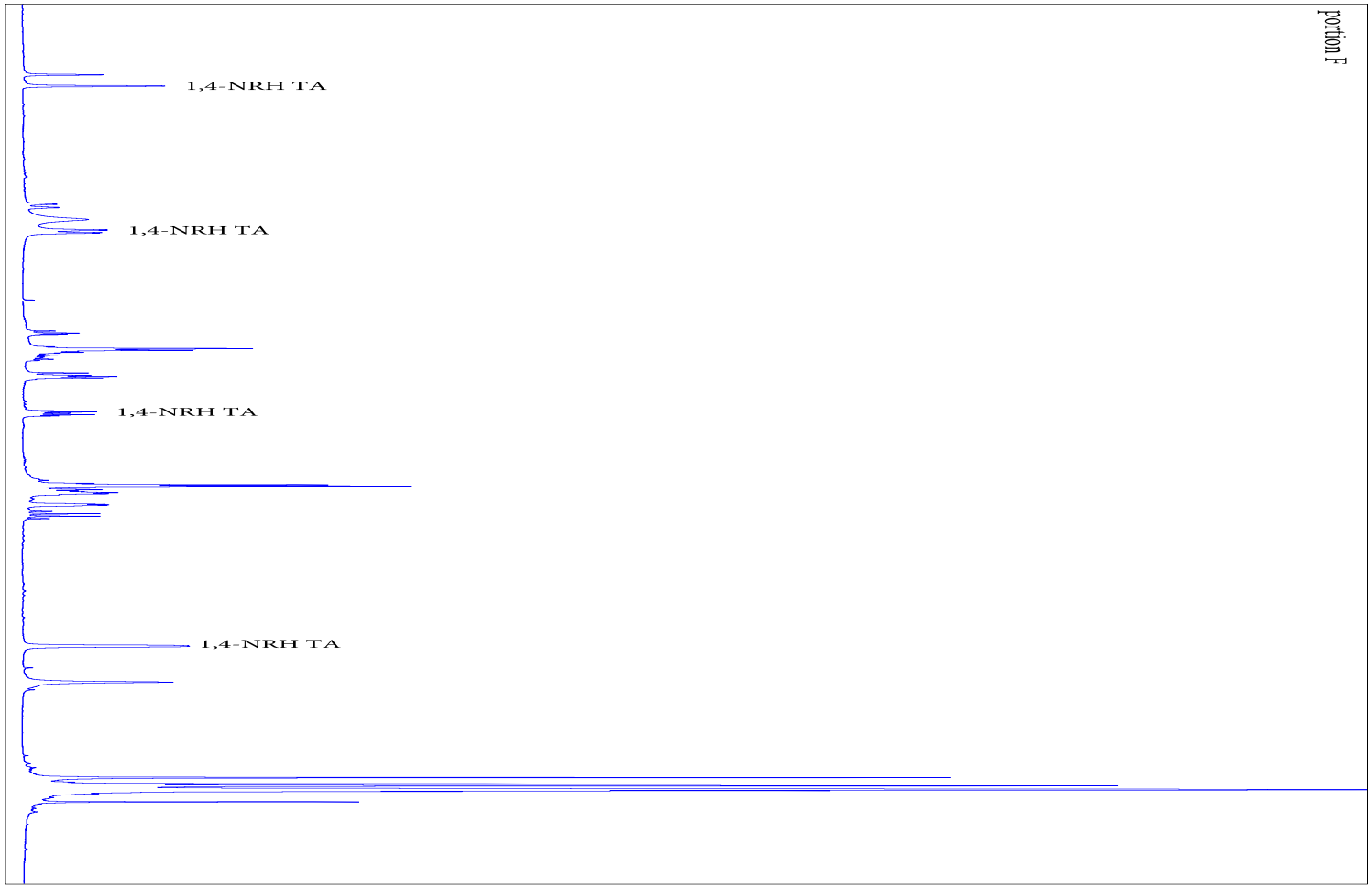

Fig. 41S Side-by-side comparison of ^{1}H NMRs (acetone-d_6) of portions C–F containg 1,6-NRH TA (**9**) and variable amounuts of 1,4-NRH TA (**7**) (reduction in DMF)

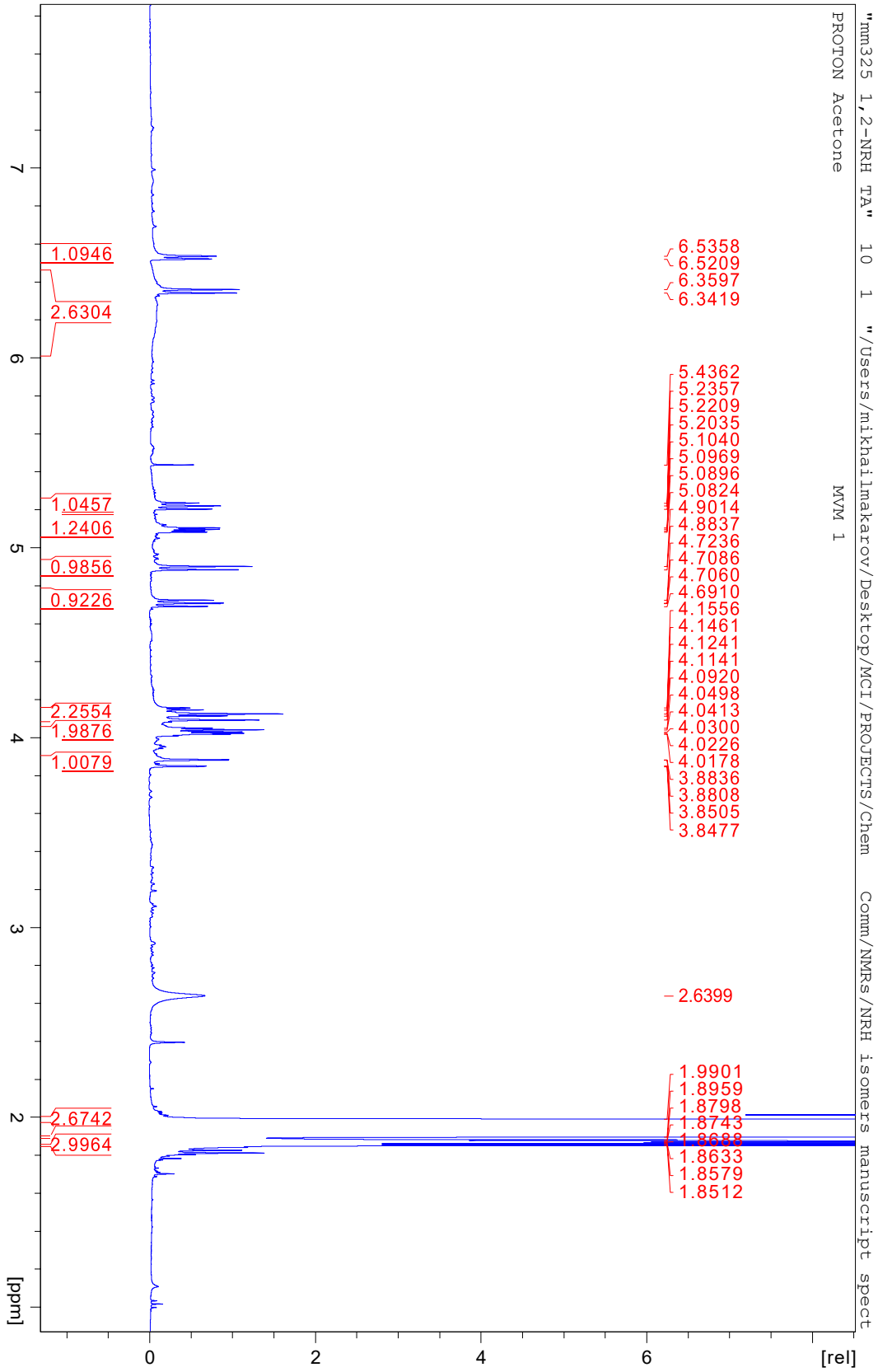

Fig. 42S ^{1}H NMR (acetone-d_6) of 1,2-NRH TA (**8**).

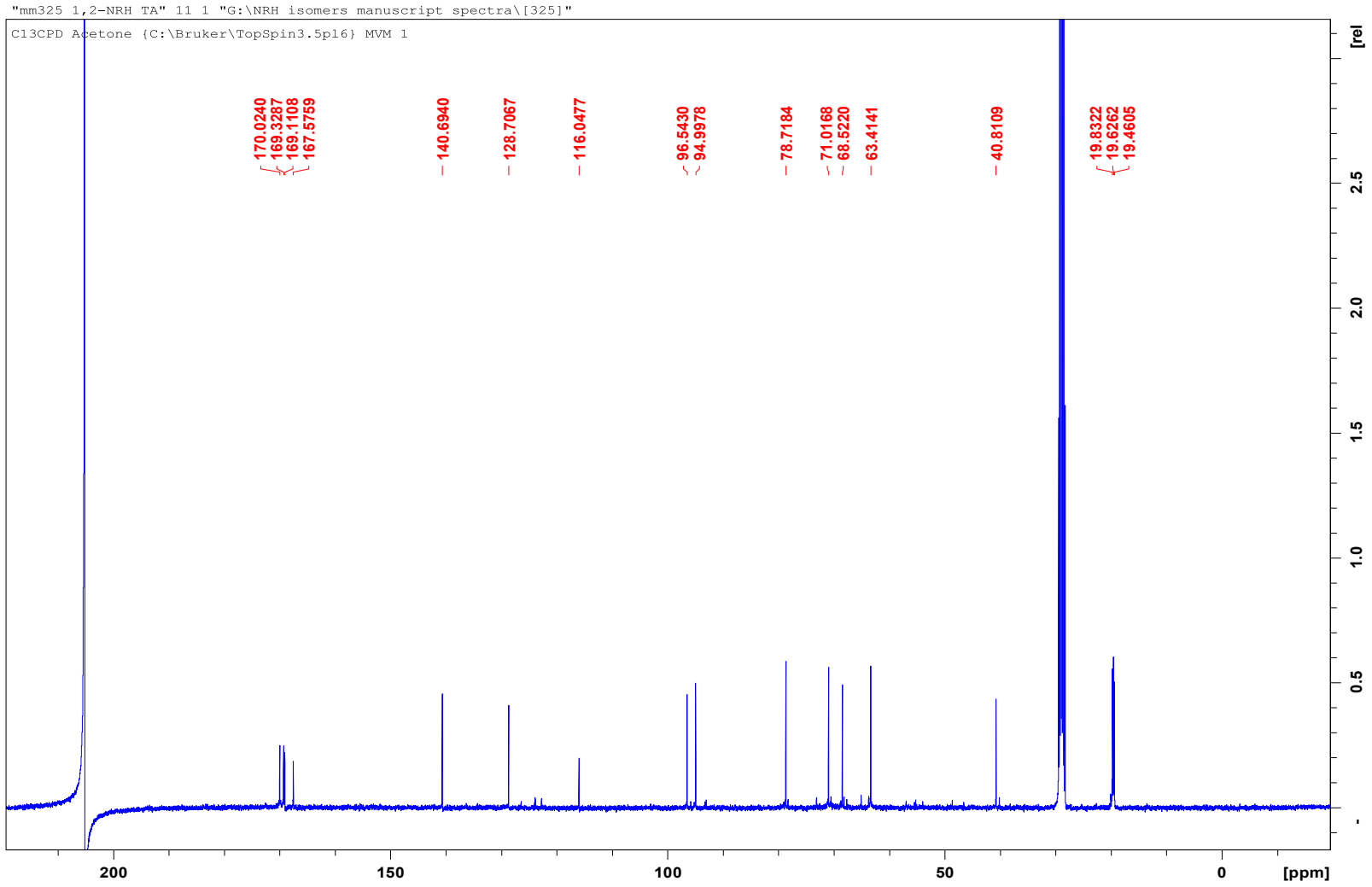

Fig. 43S ^{13}C NMR (acetone-d_6) of 1,2-NRH TA (**8**).

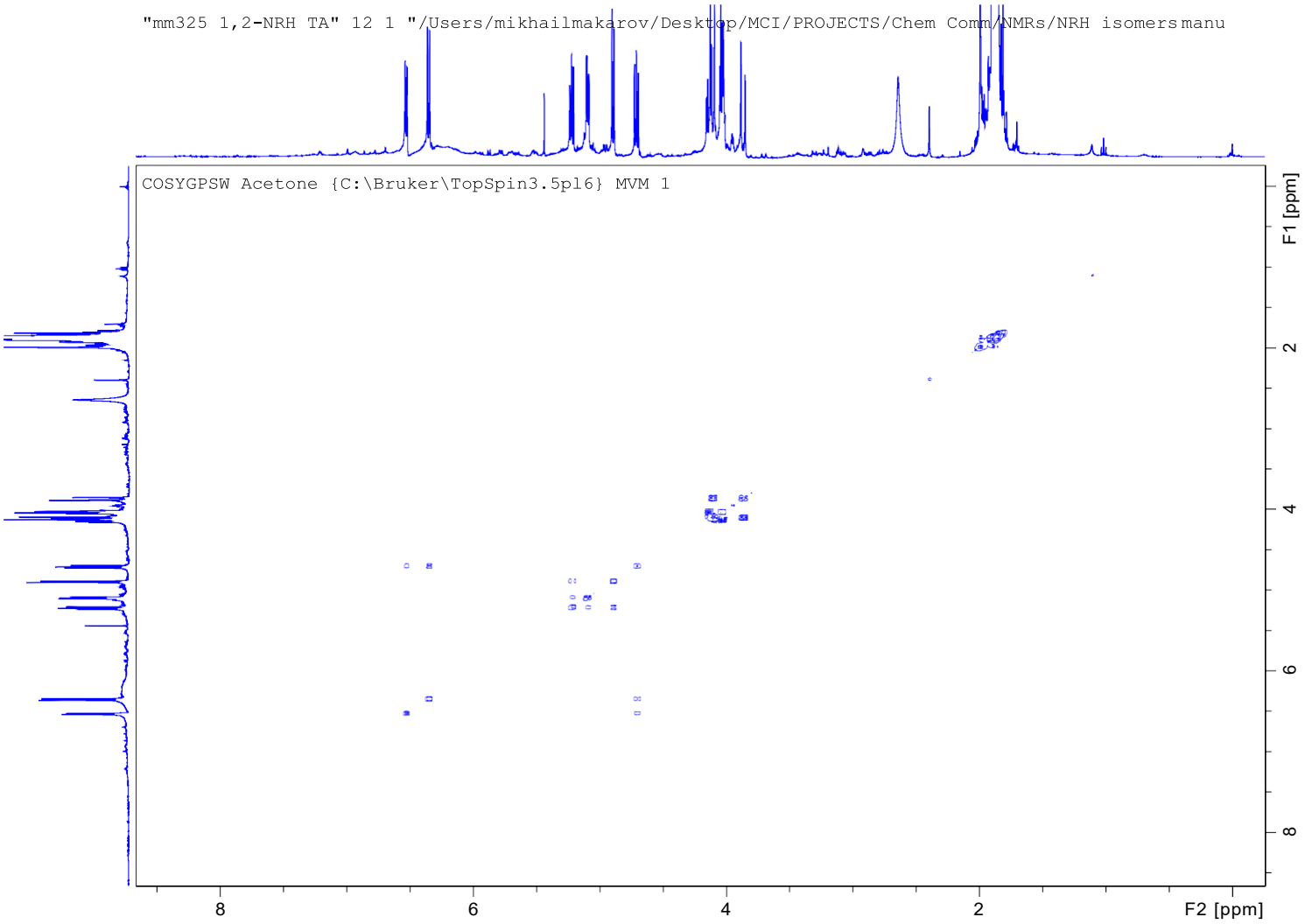

Fig. 44S ^{1}H-^{1}H correlation (COSY) NMR (acetone-d_6) of 1,2-NRH TA (**8**).

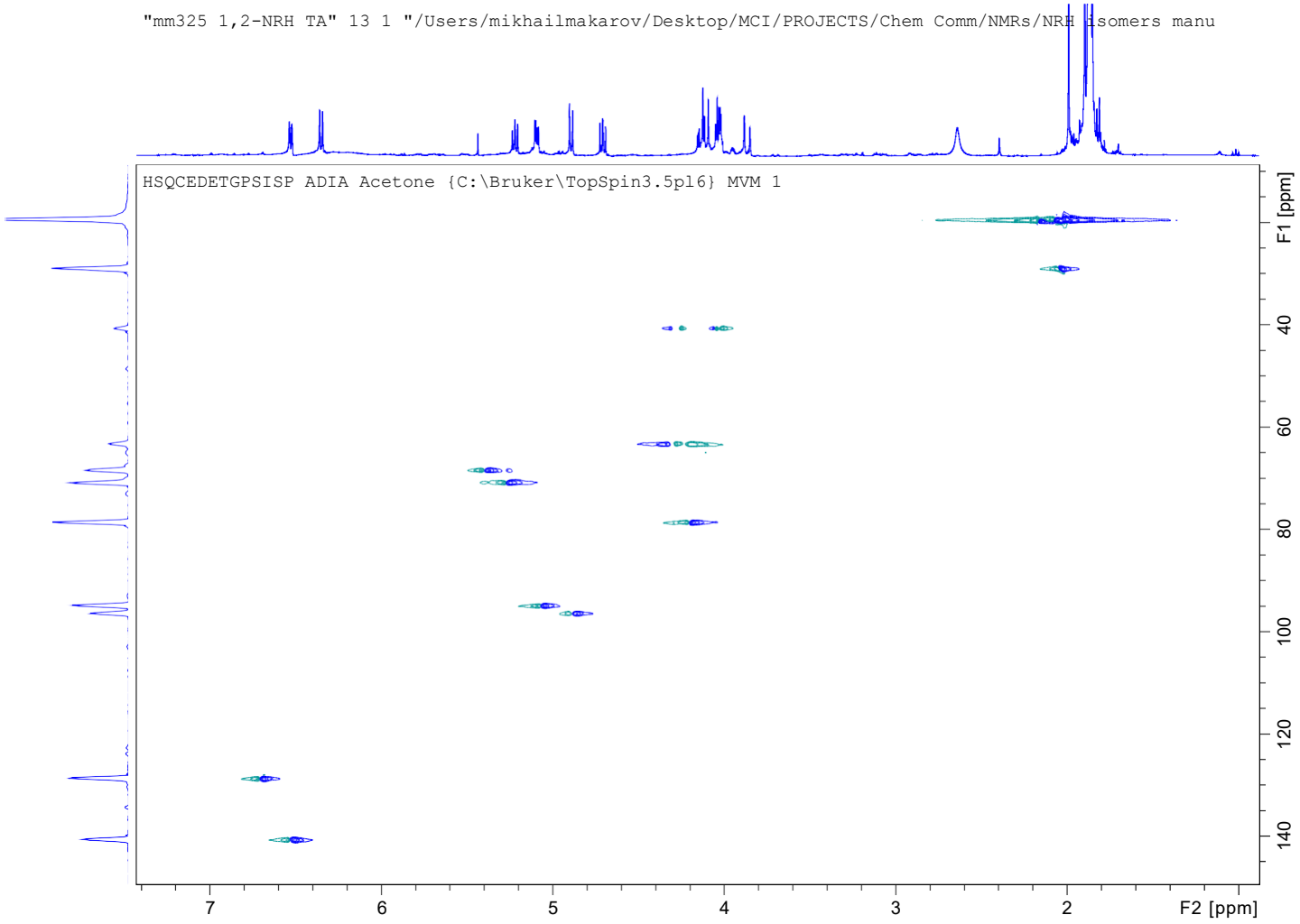

Fig. 45S ^{1}H-^{13}C correlation (HSQC) NMR (acetone-d_6) of 1,2-NRH TA (**8**).

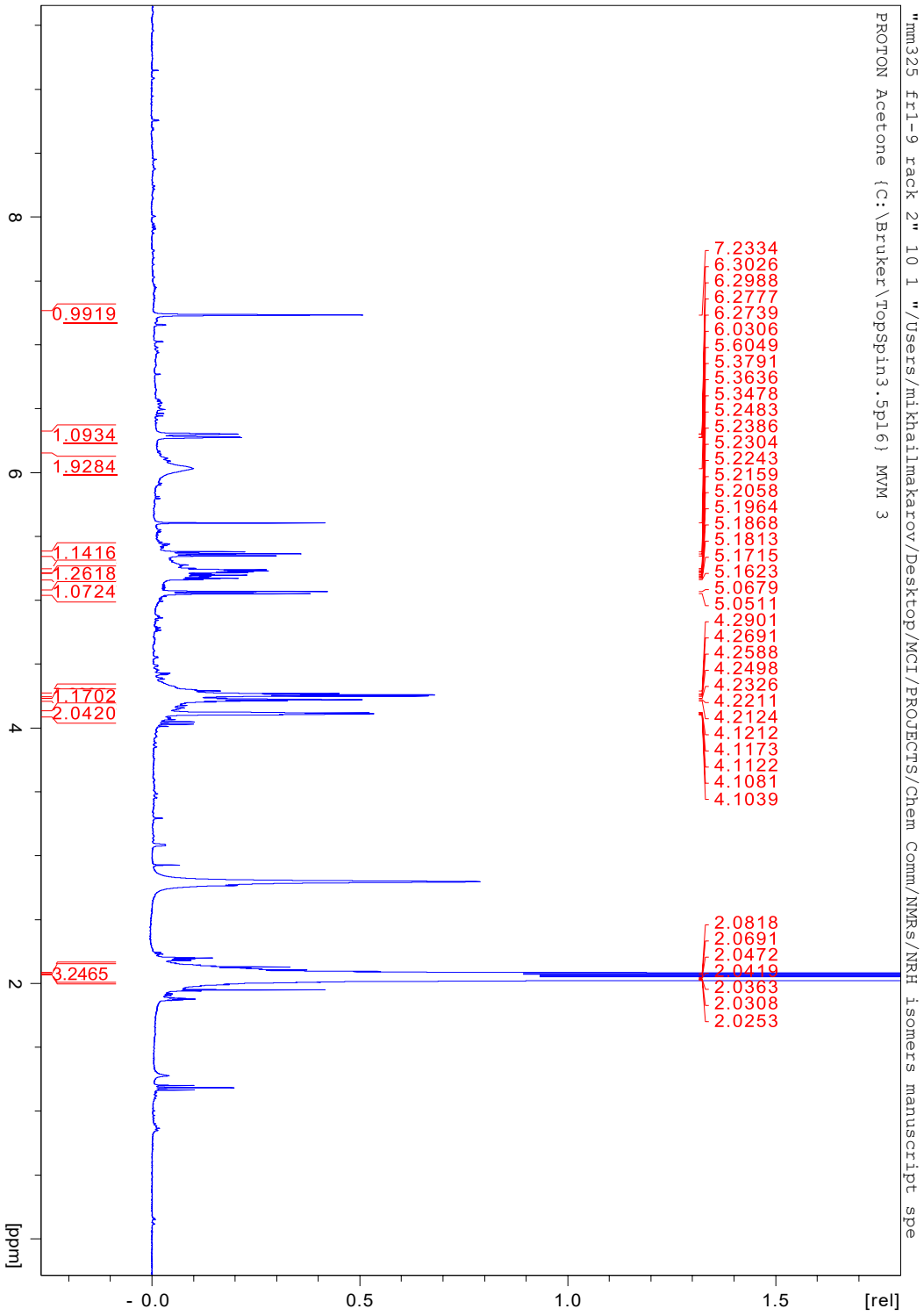

Fig. 46S ^{1}H full NMR(acetone-d_6) spectrum of 1,6-NRH TA (**9**).

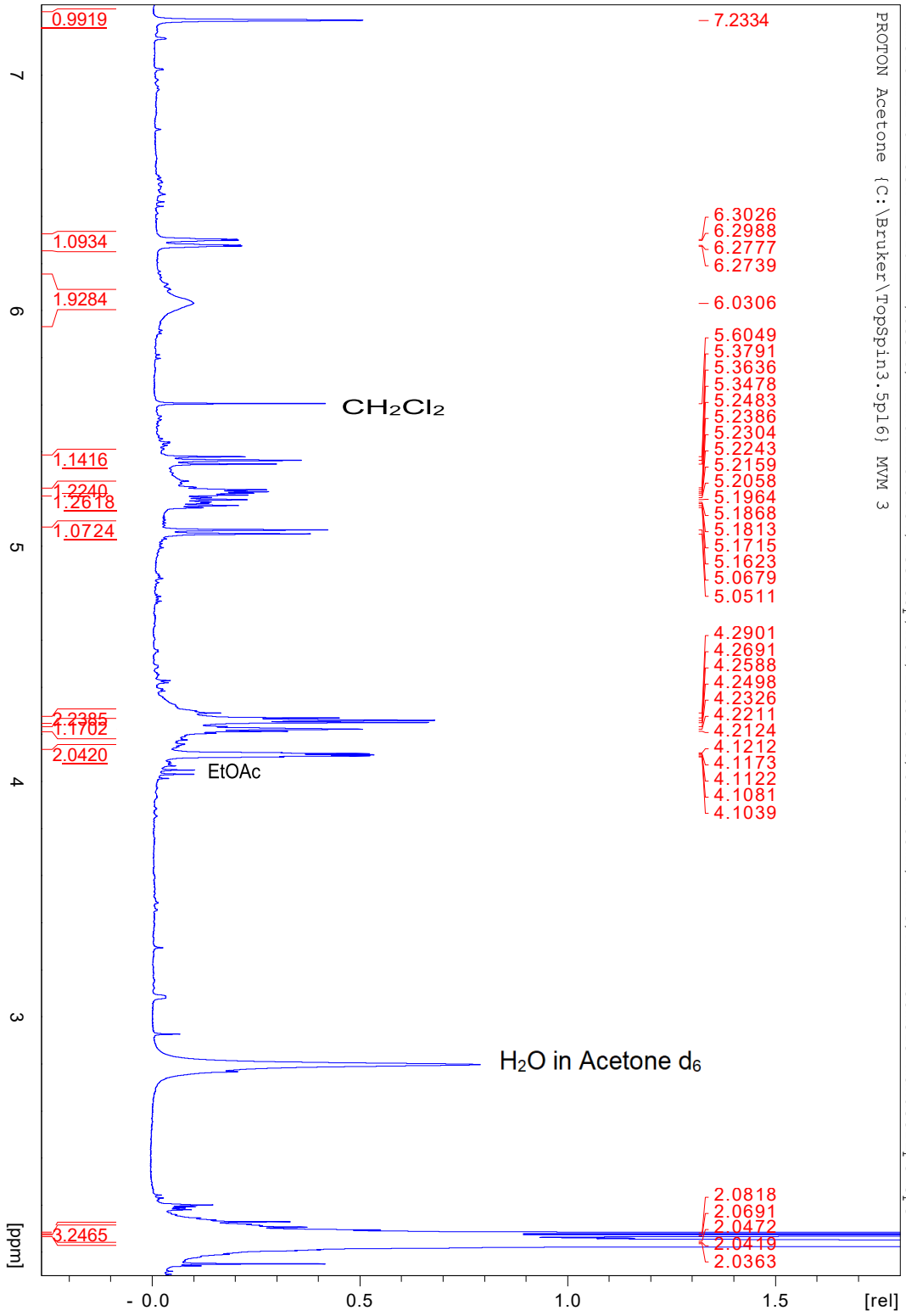

Fig. 47S ^{1}H zoomed NMR spectrum (acetone-d_6) of 1,6-NRH TA (**9**).

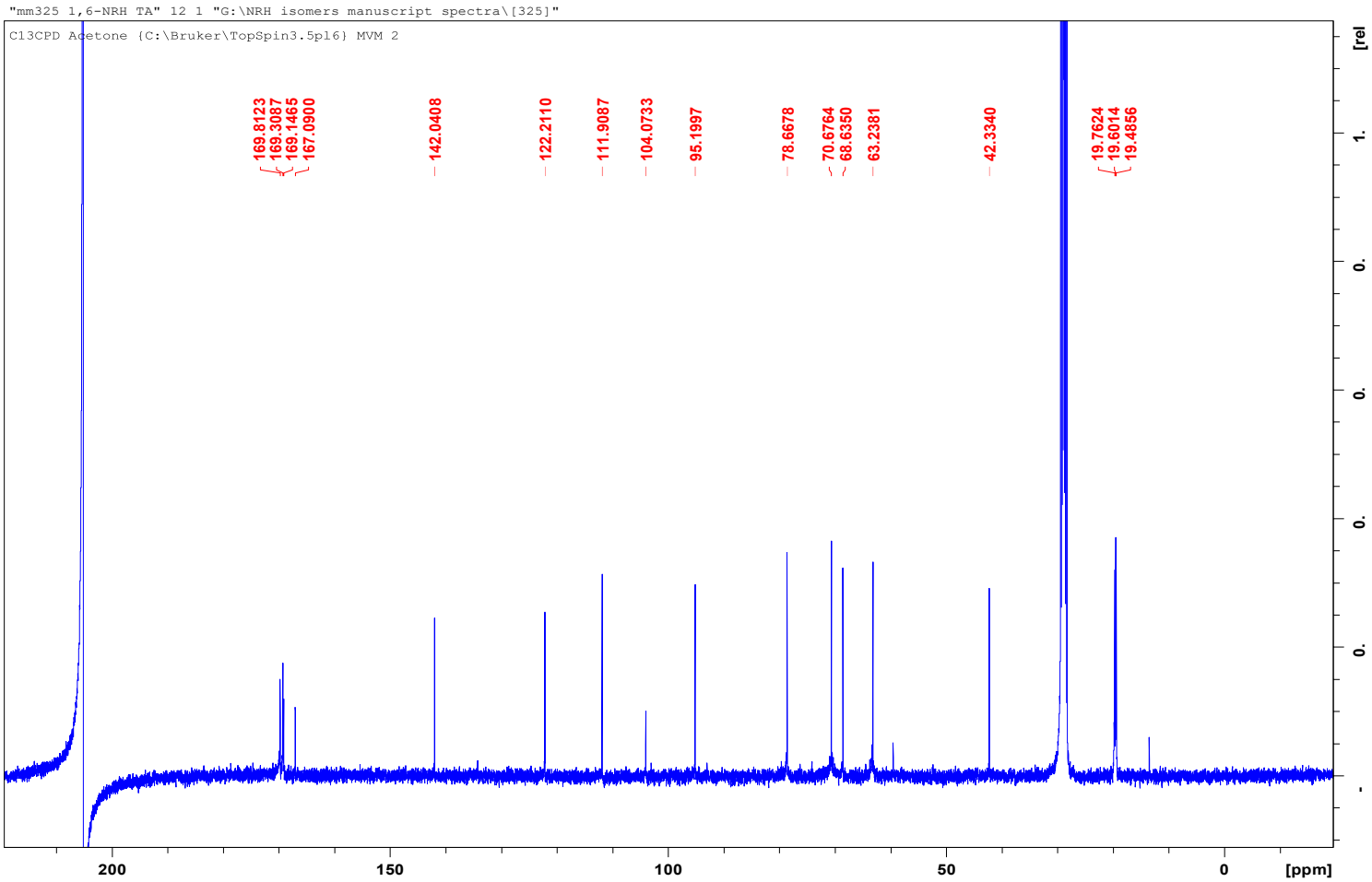

Fig. 48S ^{13}C NMR (acetone-d_6) of 1,6-NRH TA (**9**).

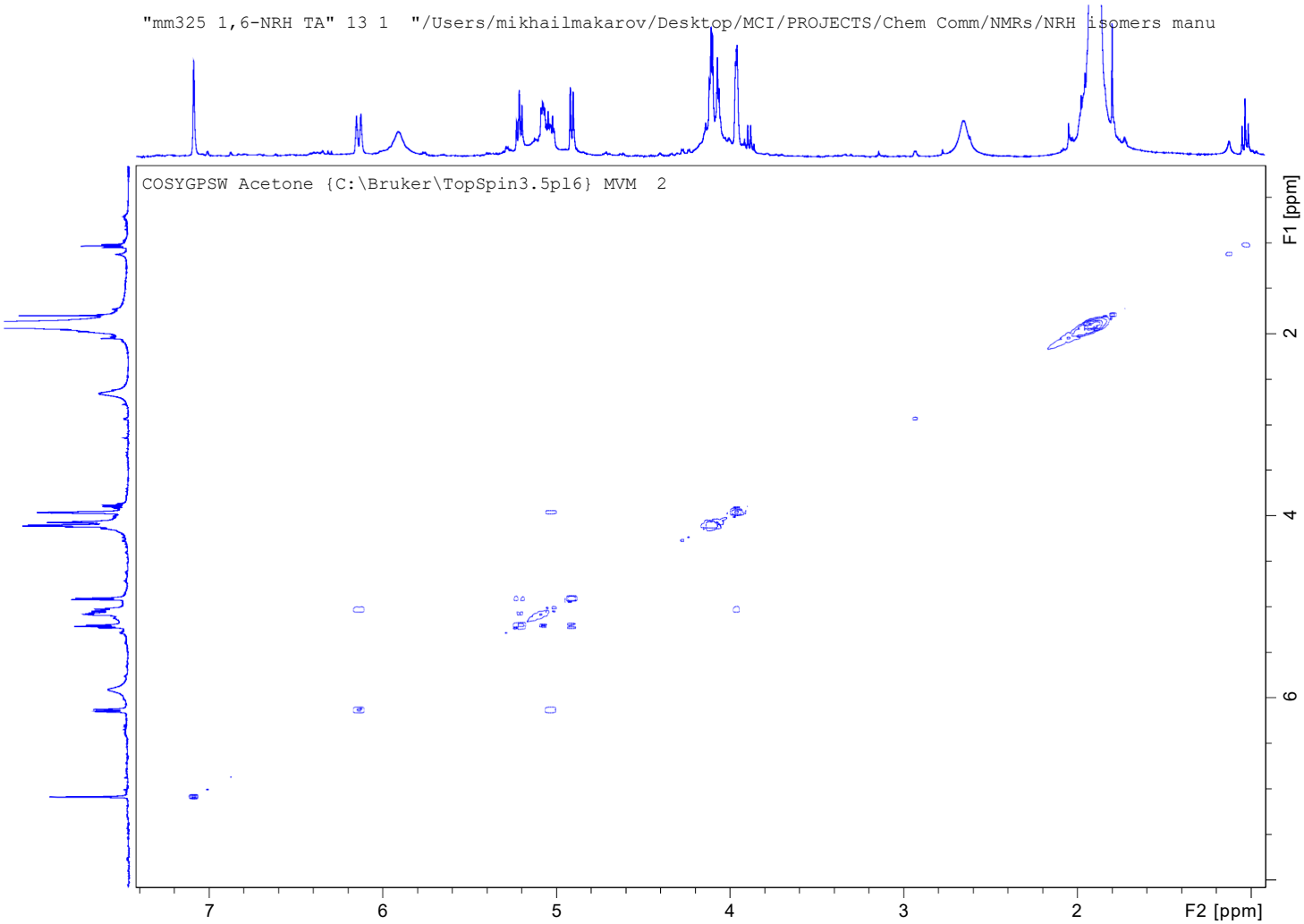

Fig. 49S ^{1}H-^{1}H correlation (COSY) NMR (acetone-d_6) of 1,6-NRH TA (**9**).

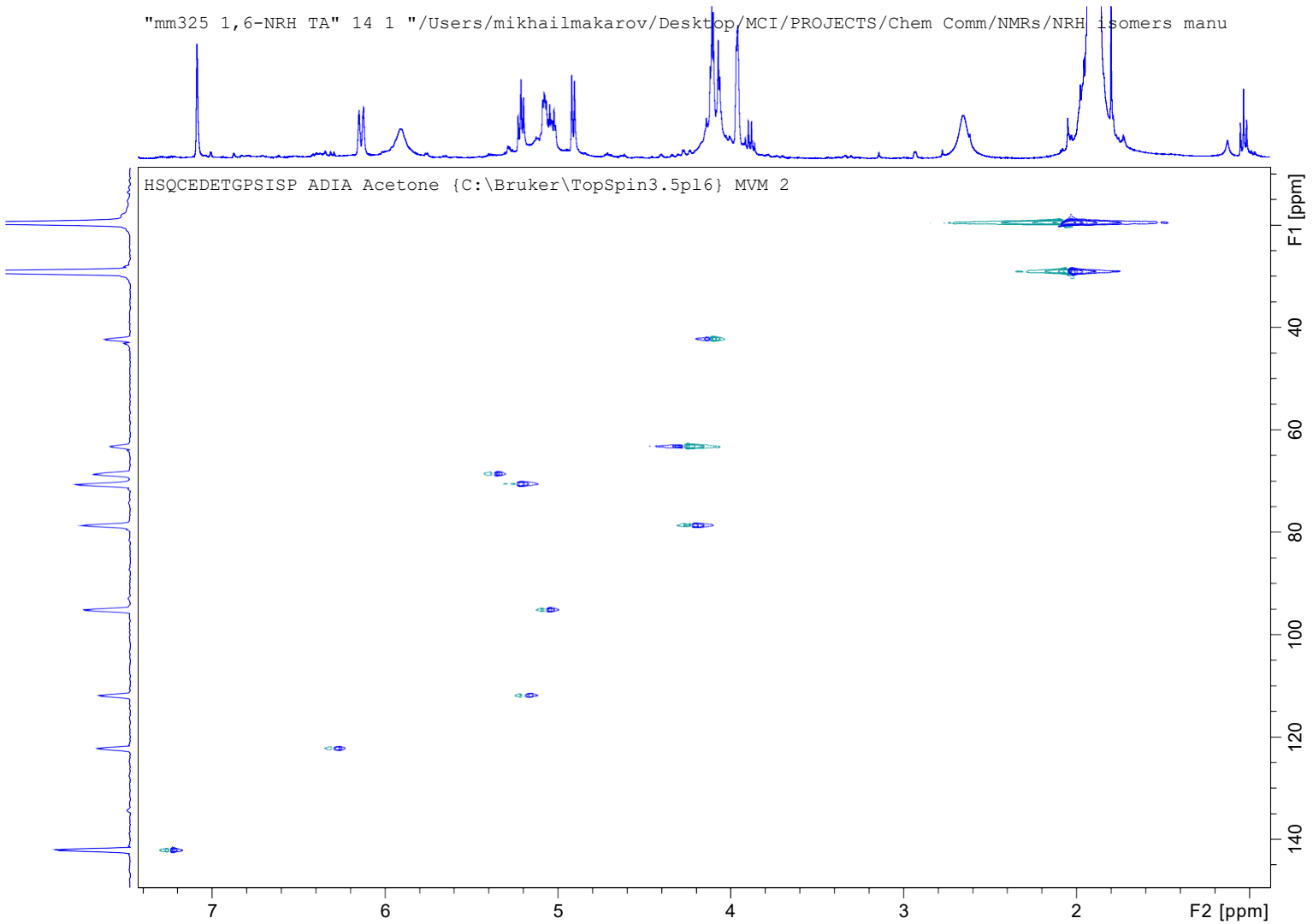

Fig. 50S ^{1}H-^{13}C correlation (HSQC) NMR (acetone-d_6) of 1,6-NRH TA (**9**).

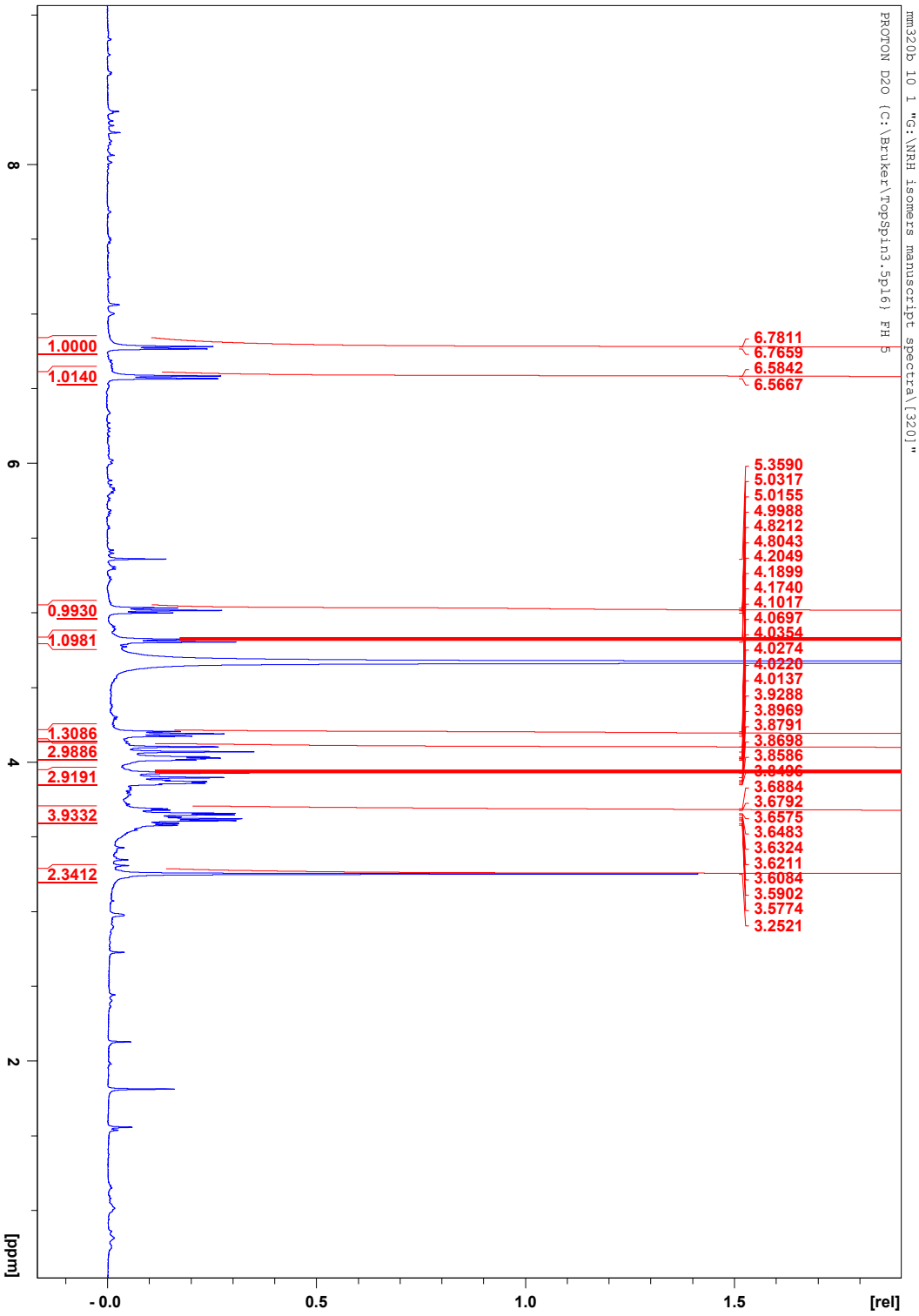

Fig. 51S ^{1}H full NMR (D_2O) spectrum of 1,2-NRH (**2**).

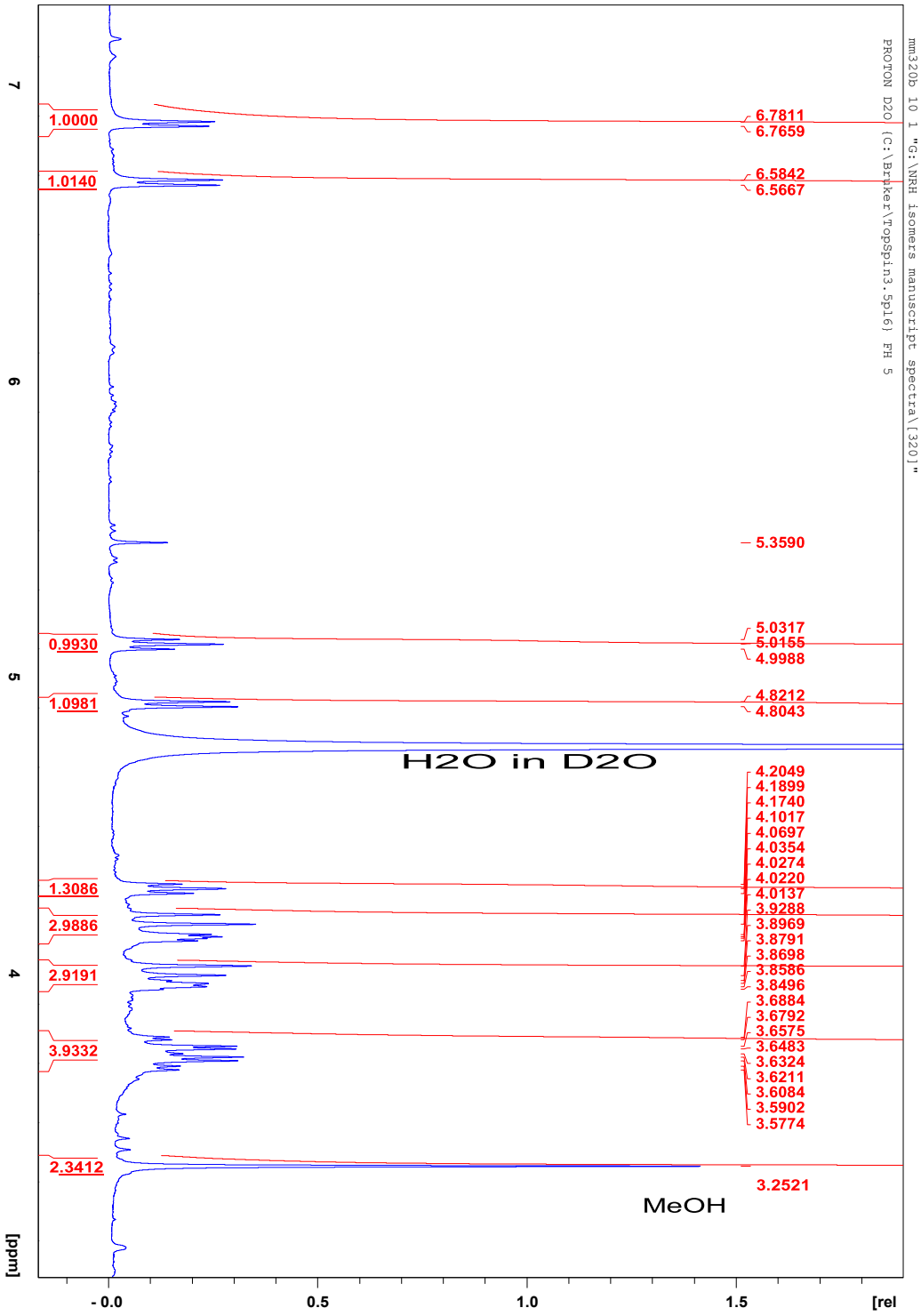

Fig. 52S ^{1}H zoomed NMR (D_2O) spectrum of 1,2-NRH (**2**).

mm320c 11 1 C:\Bruker\TopSpin3.5pl6\data\MVM\nmr Path=C:\Bruker\TopSpin3.5pl6\data\MVM\nmr\mm320c\11\pdata\1

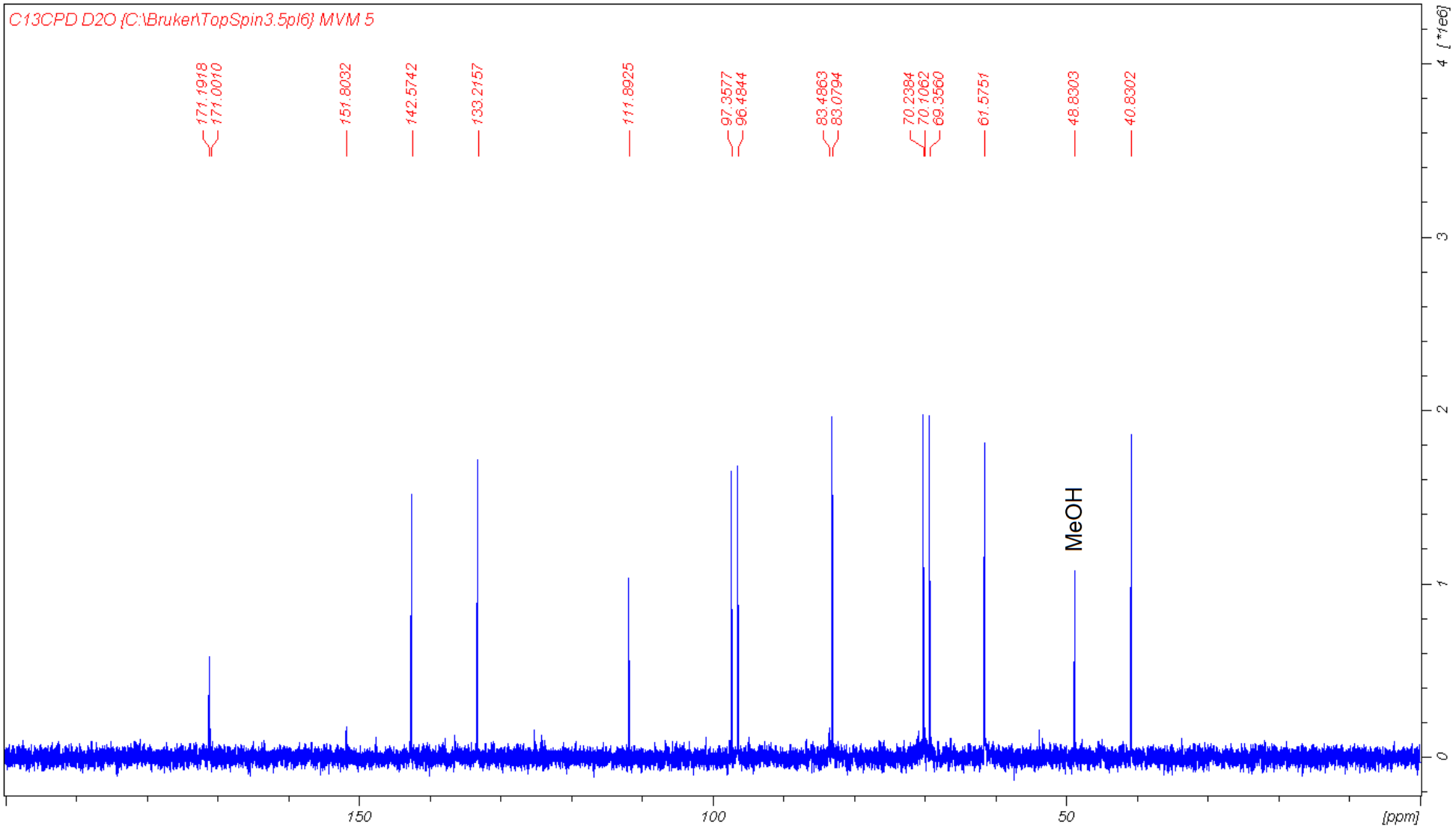

Fig. 53S ^{13}C NMR (D_2O) of 1,2-NRH (**2**).

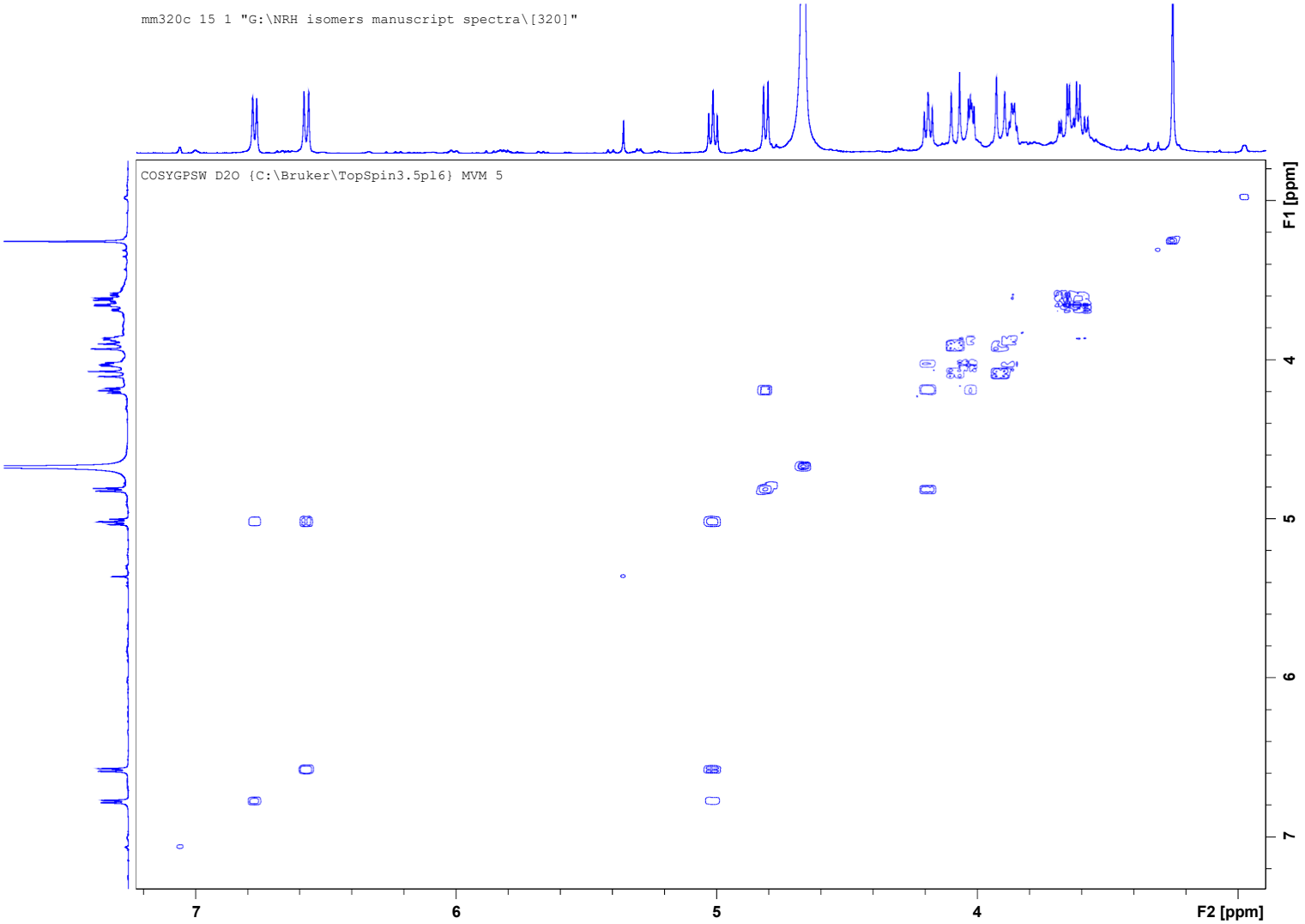

Fig. 54S ^{1}H-^{1}H correlation (COSY) NMR (D_2O) of 1,2-NRH (**2**).

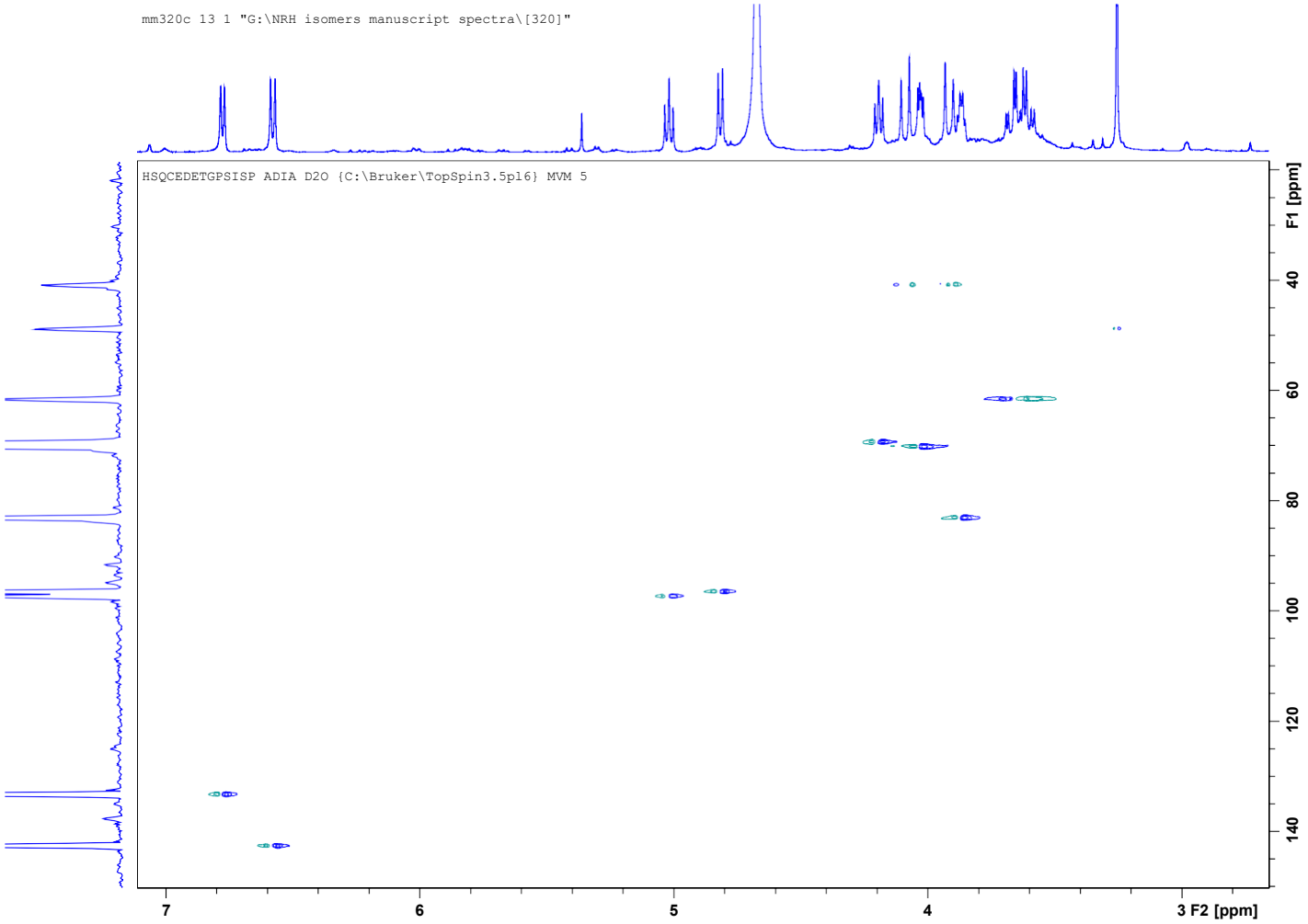

Fig. 55S ^{1}H-^{13}C correlation (HSQC) NMR (D_2O) of 1,2-NRH (**2**).

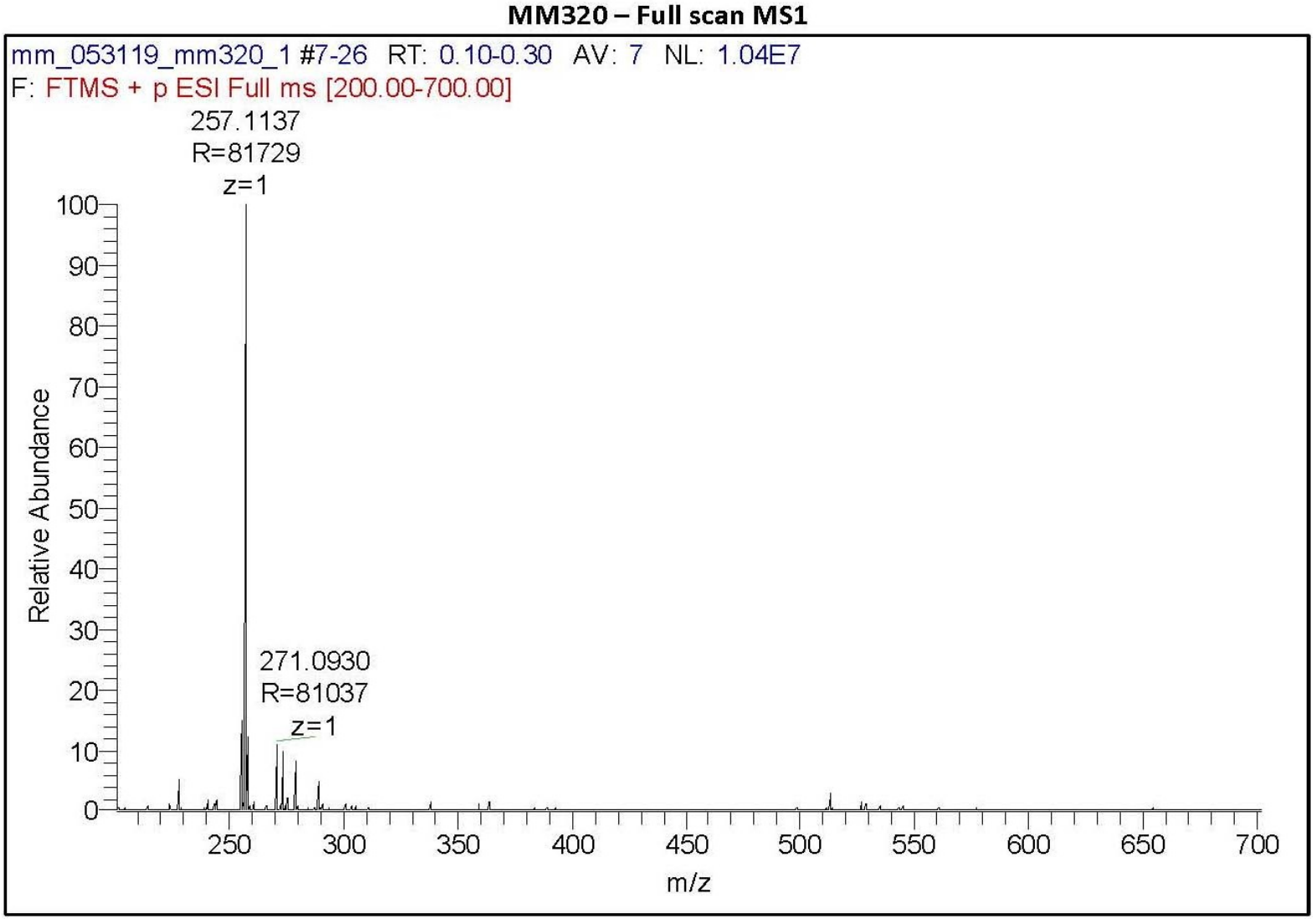

Fig. 56S HRMS (1:1 H_2O/ACN) of 1,2-NRH (**2**): full scan.

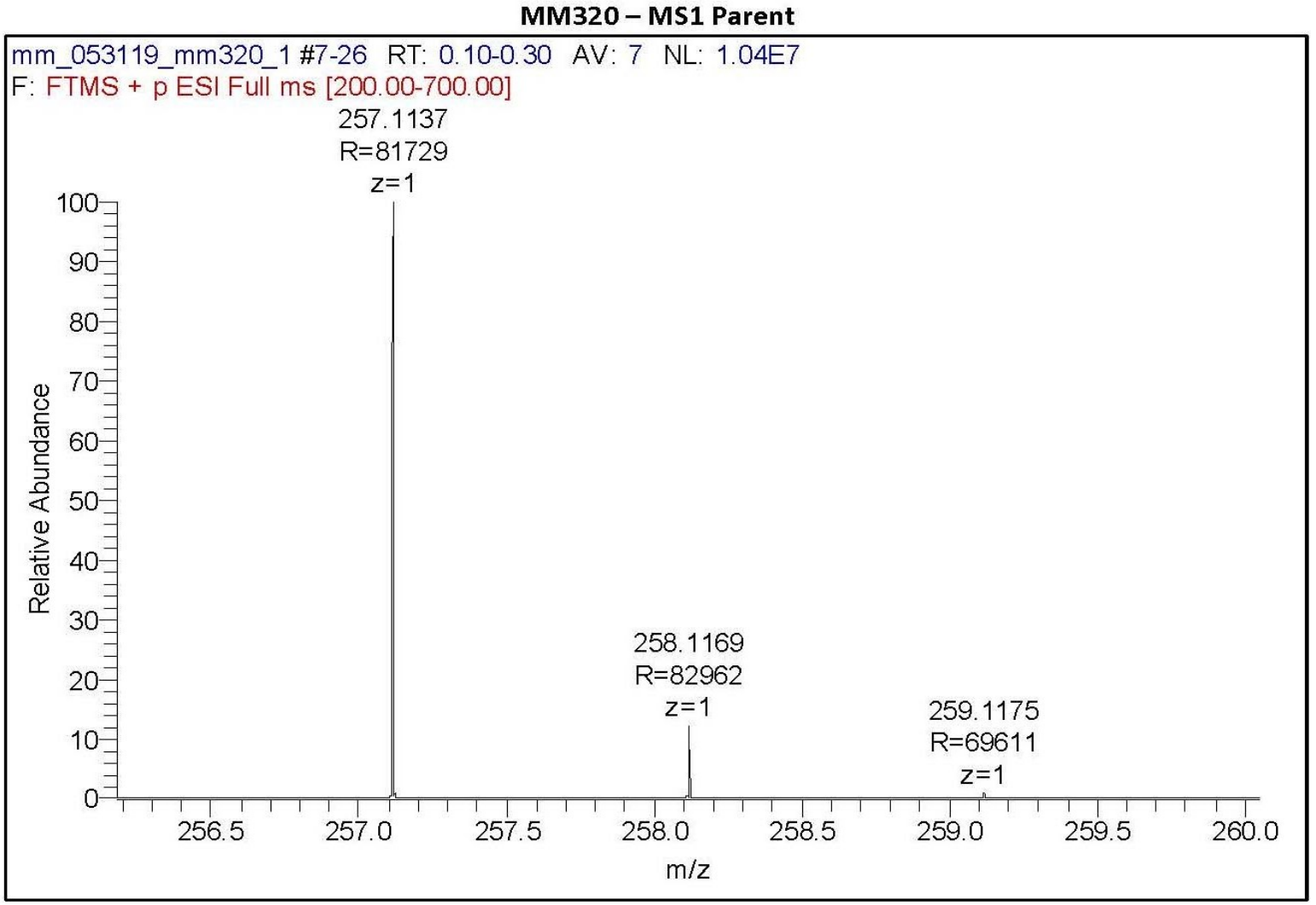

Fig. 57S HRMS (1:1 H_2O/ACN) of 1,2-NRH (**2**): parent peak.

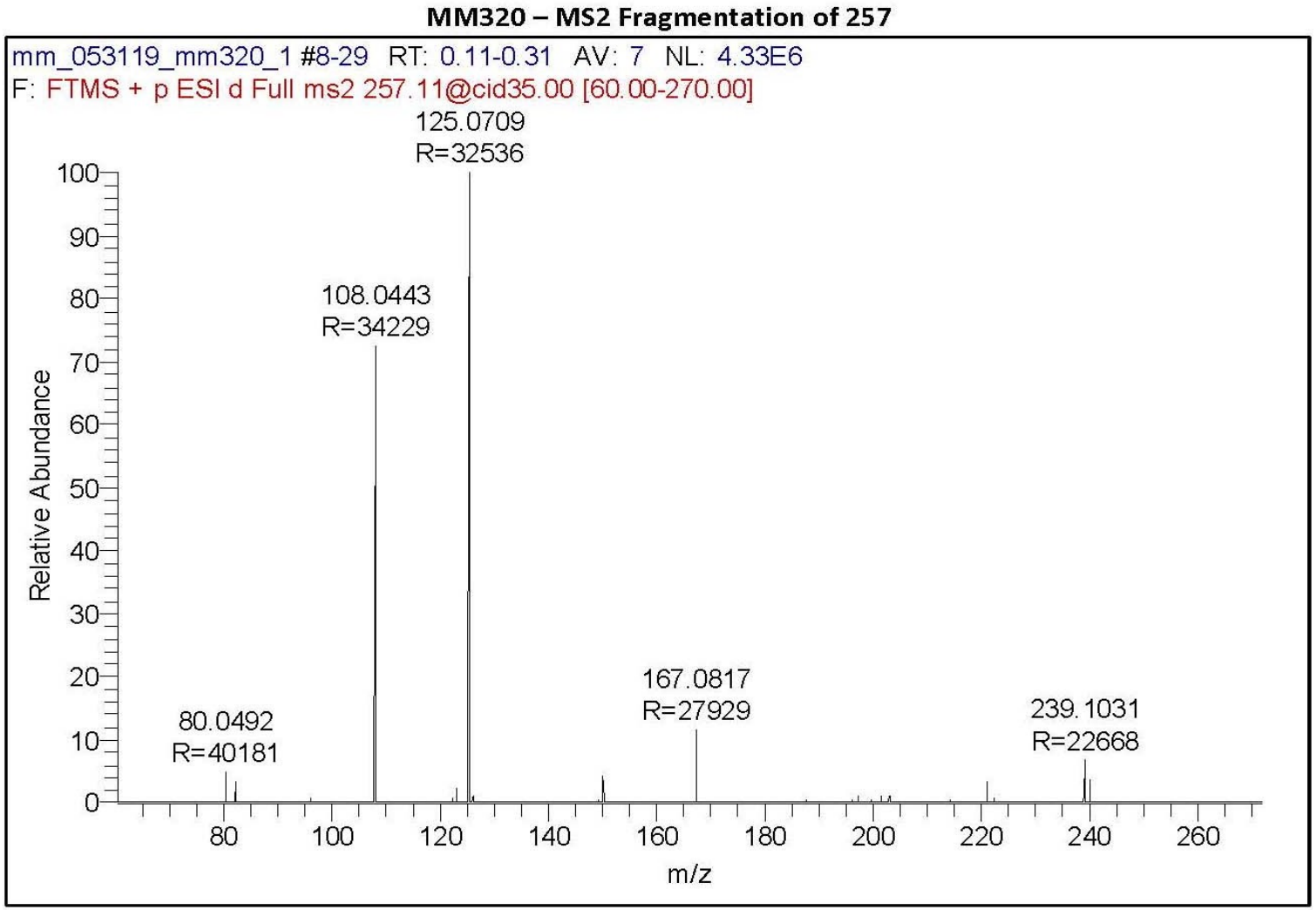

Fig. 58S HRMS (1:1 H_2O/ACN) of 1,2-NRH (**2**): fragmentation of parent peak.

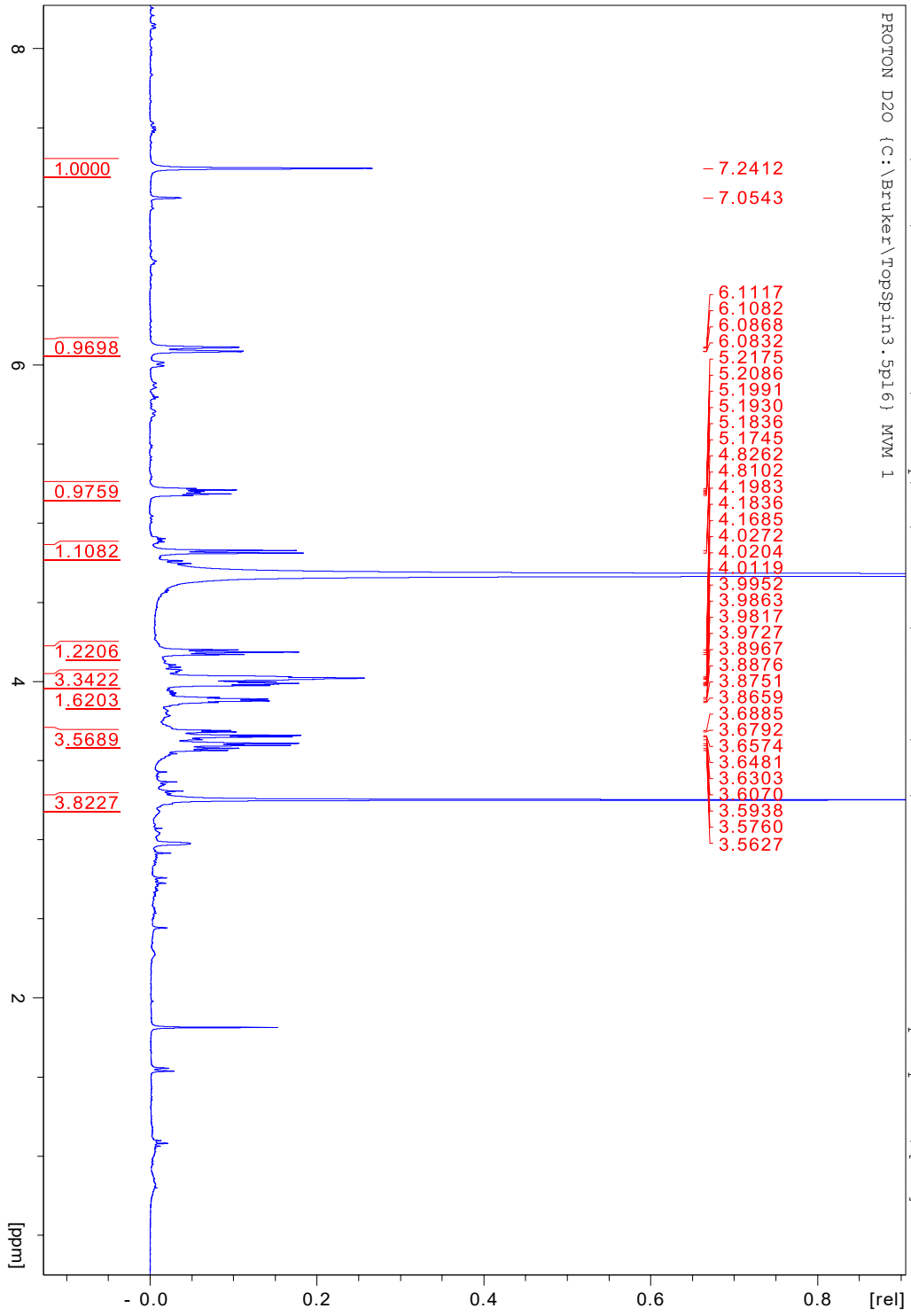

Fig. 59S ^{1}H full NMR (D_2O) spectrum of 1,6-NRH (**3**).

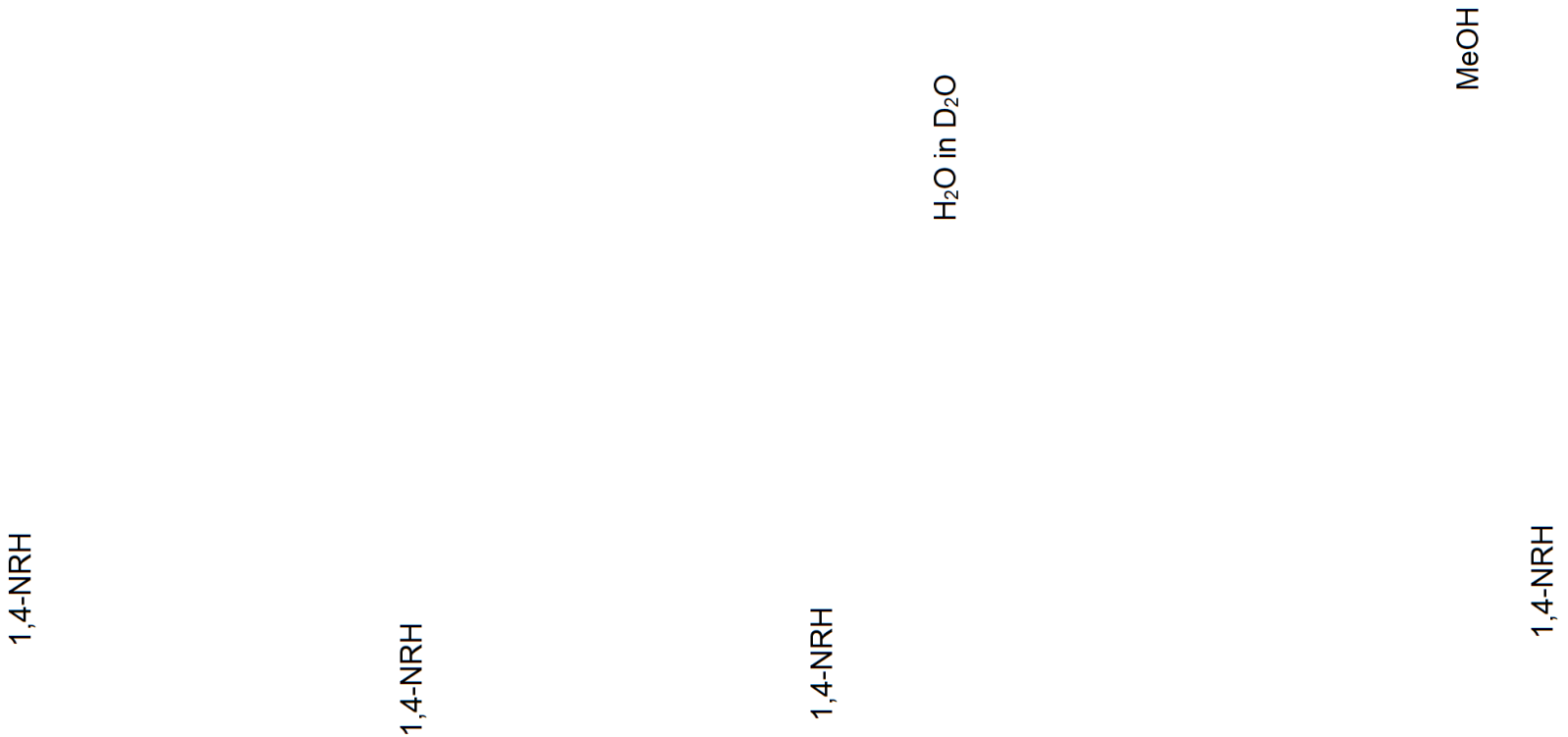

Fig. 60S ^{1}H zoomed NMR (D_2O) spectrum of 1,6-NRH (**3**).

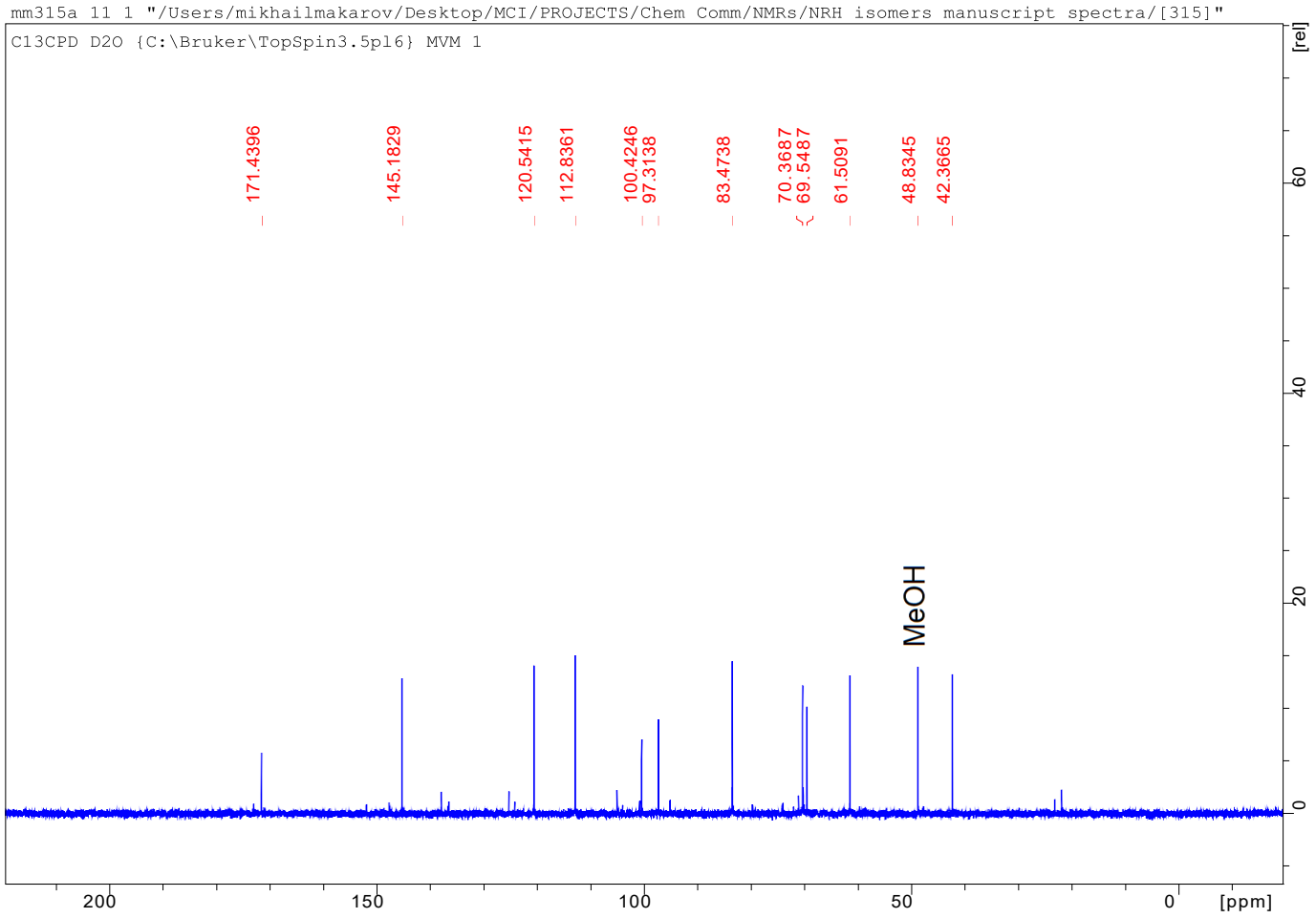

Fig. 61S ^{13}C NMR (D_2O) of 1,6-NRH (**3**).

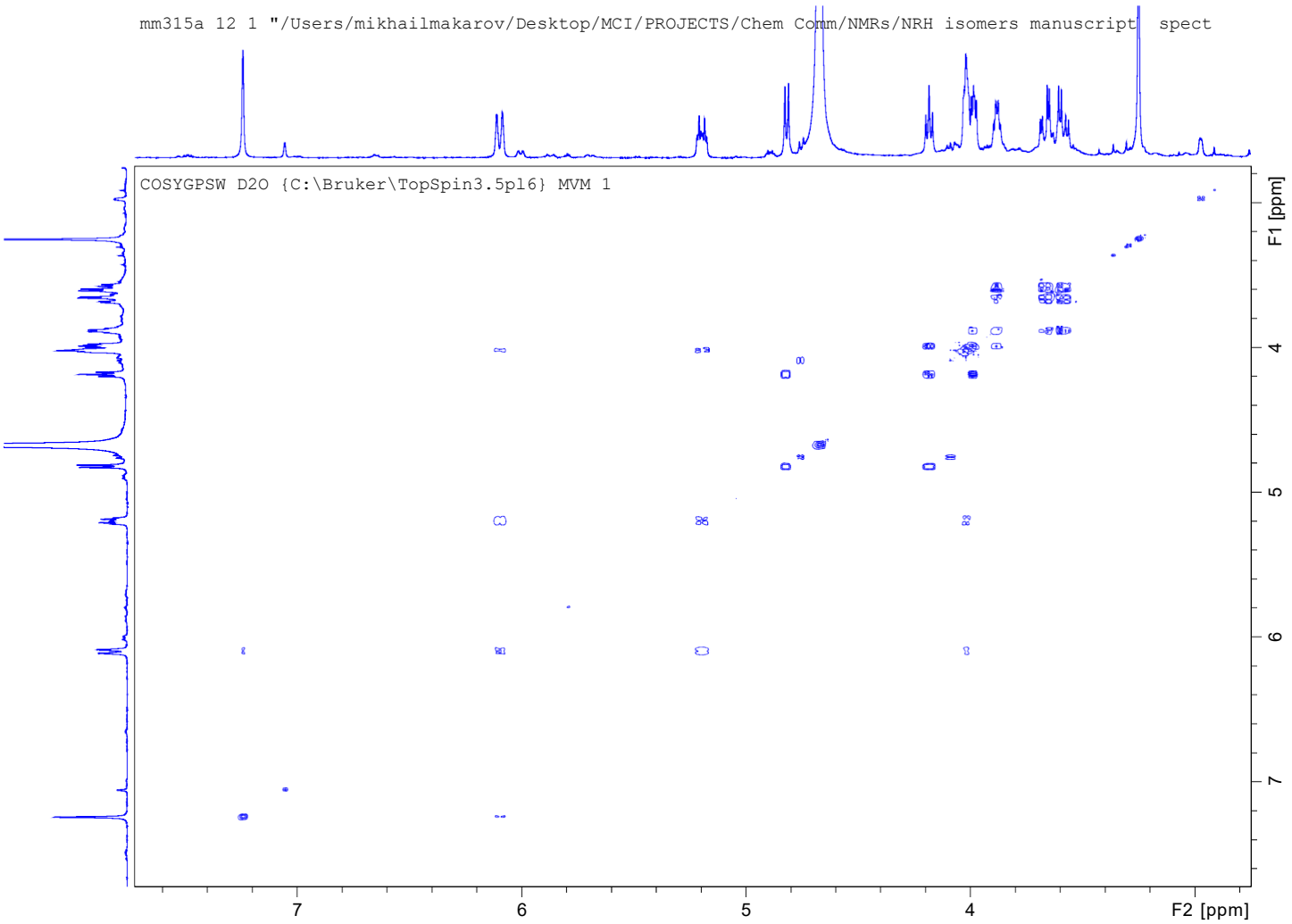

Fig. 62S ^{1}H-^{1}H correlation (COSY) NMR (D_2O) of 1,6-NRH (**3**).

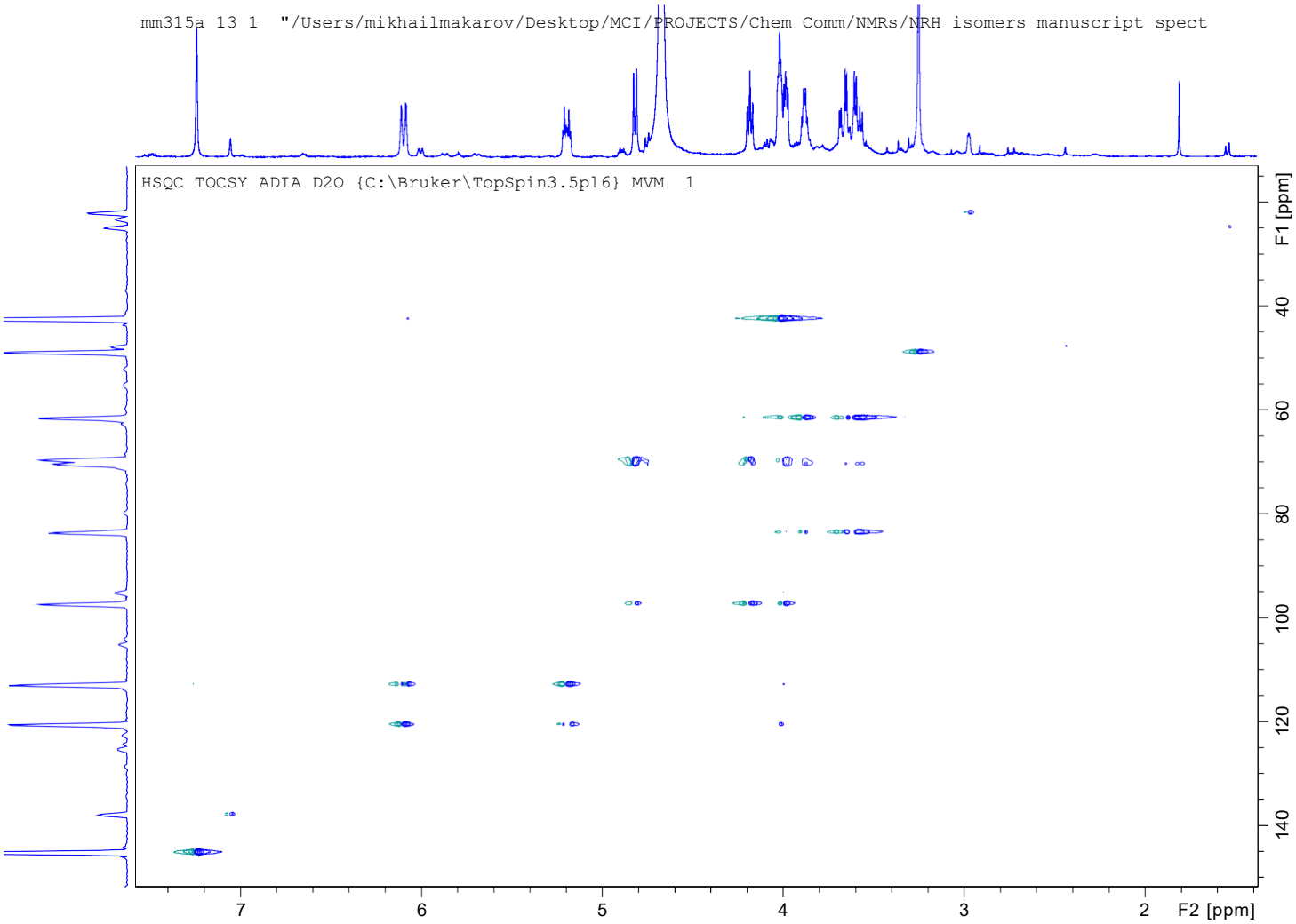

Fig. 63S ^{1}H-^{13}C correlation (HSQC) NMR (D_2O) of 1,6-NRH (**3**).

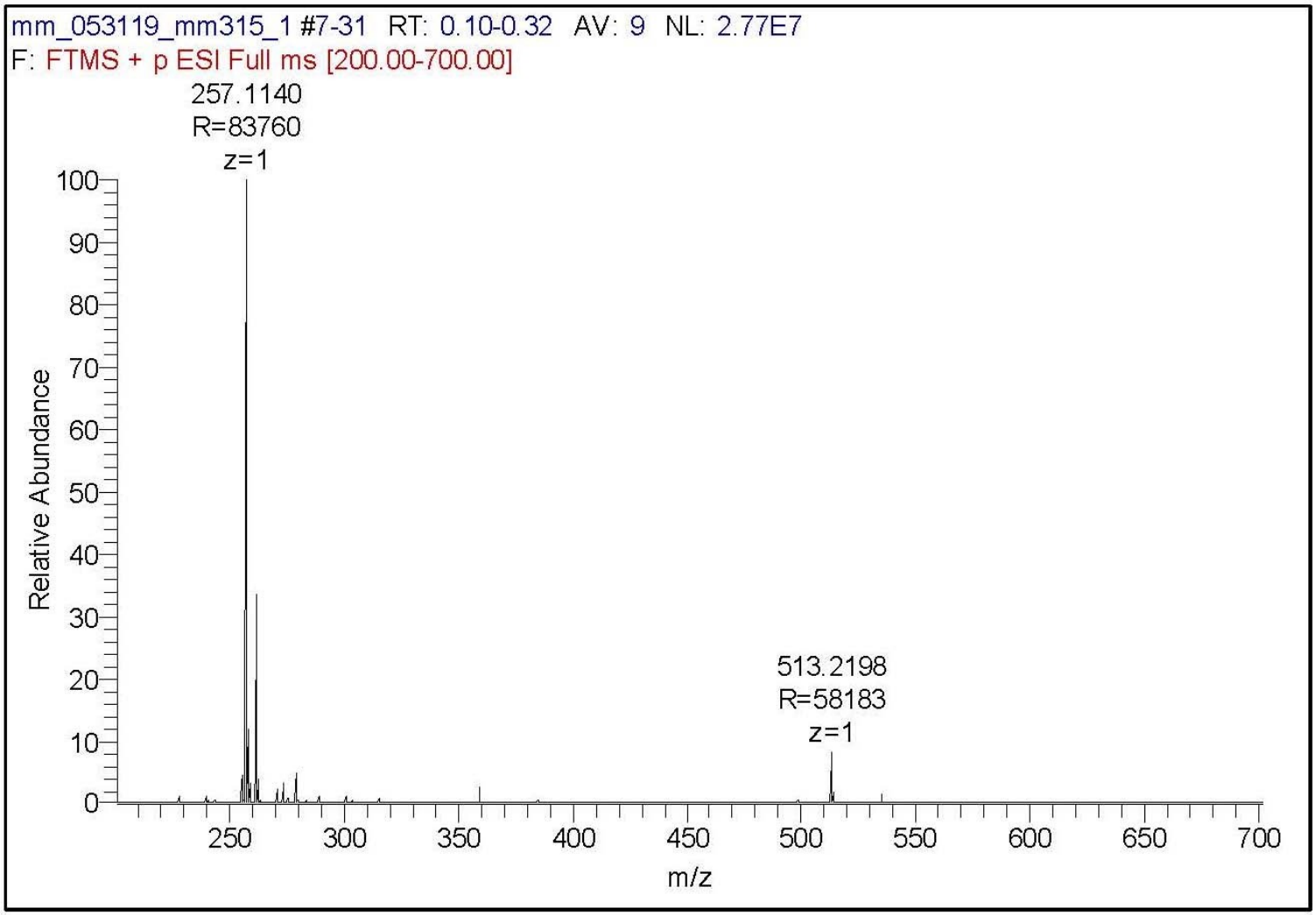

Fig. 64S HRMS (1:1 H_2O/ACN) of 1,6-NRH (**3**): full scan.

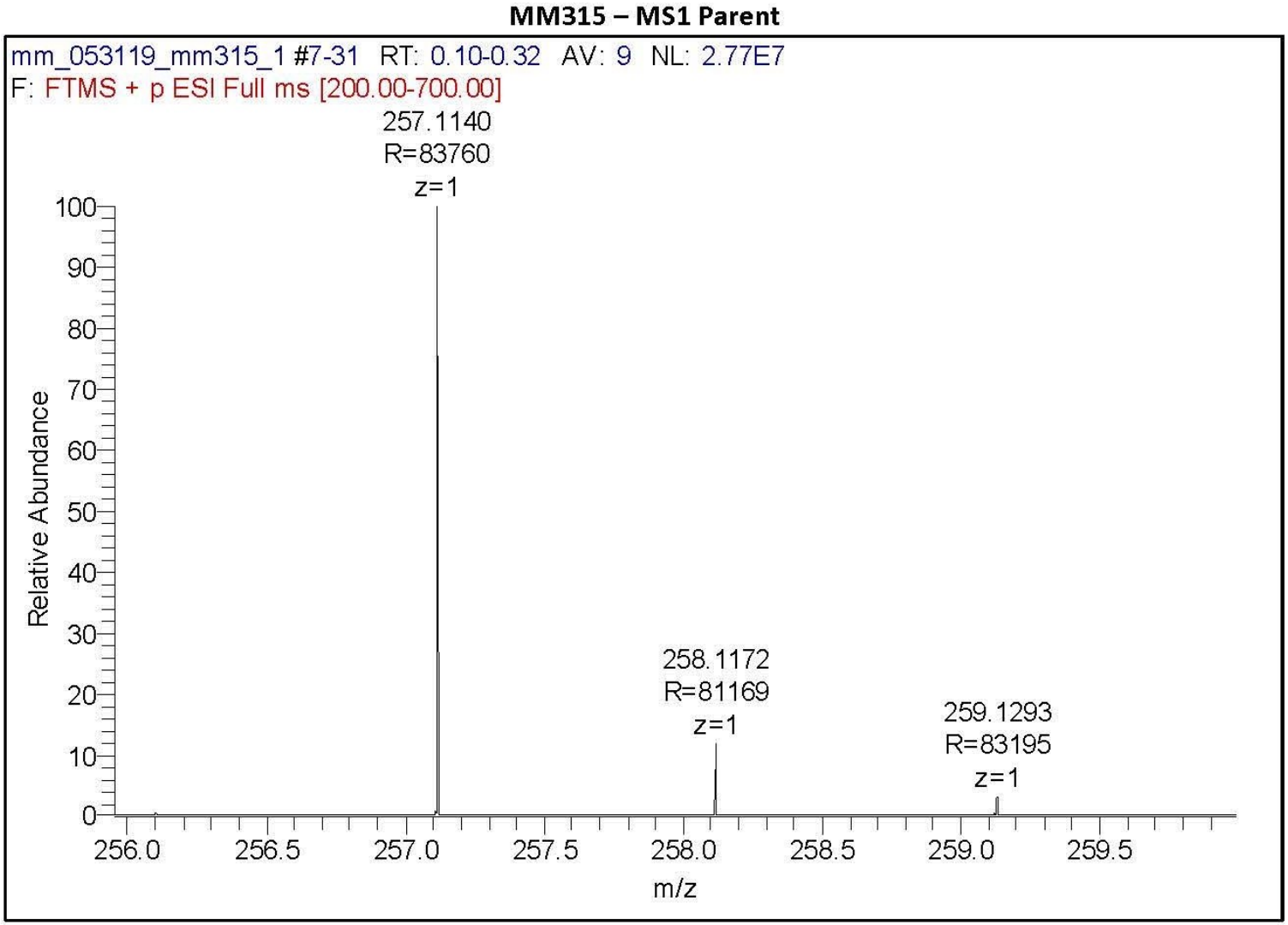

Fig. 65S HRMS (1:1 H_2O/ACN) of 1,6-NRH (**3**): parent peak.

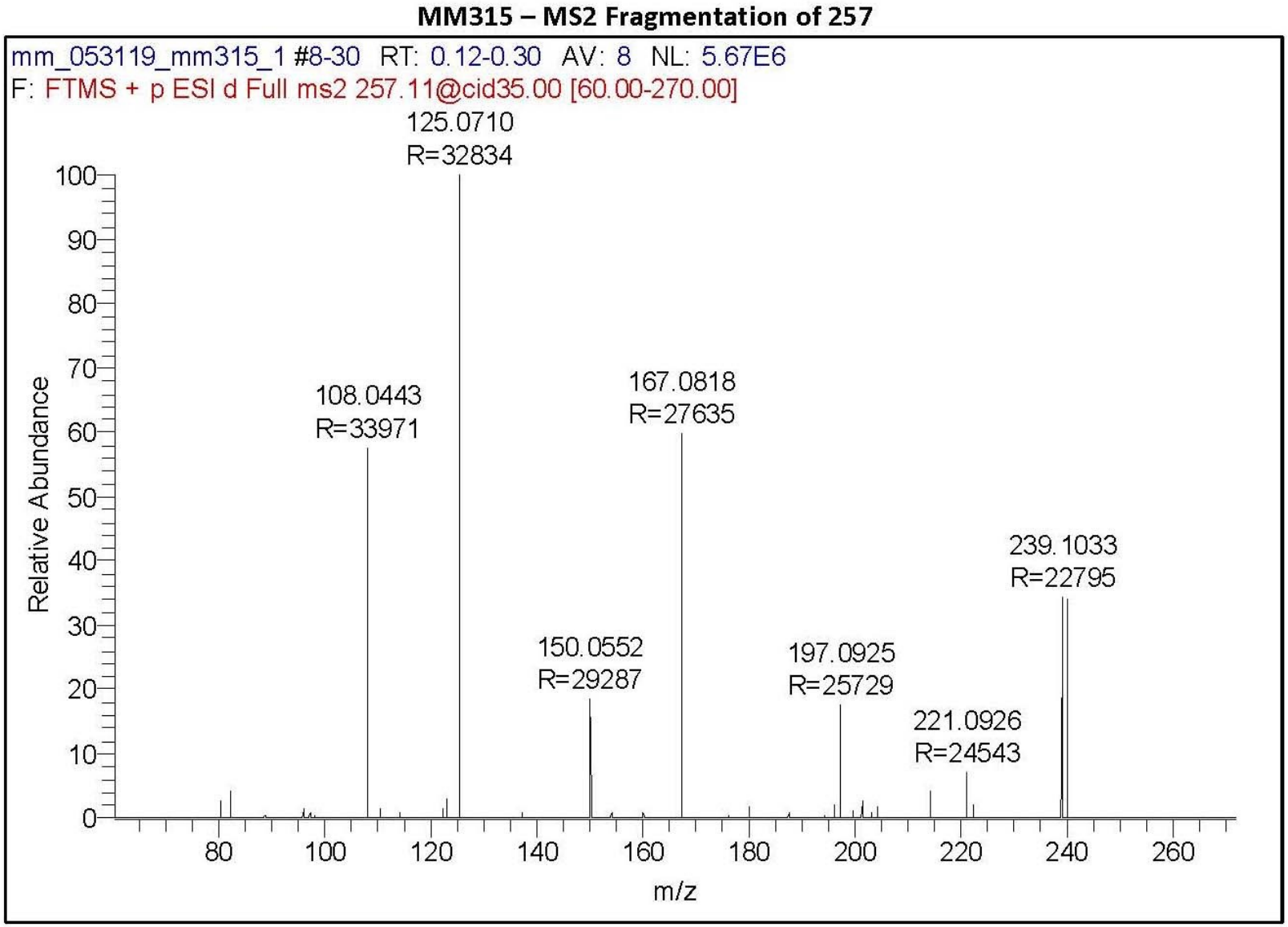

Fig. 66S HRMS (1:1 H_2O/ACN) of 1,6-NRH (**3**): fragmentation of parent peak.

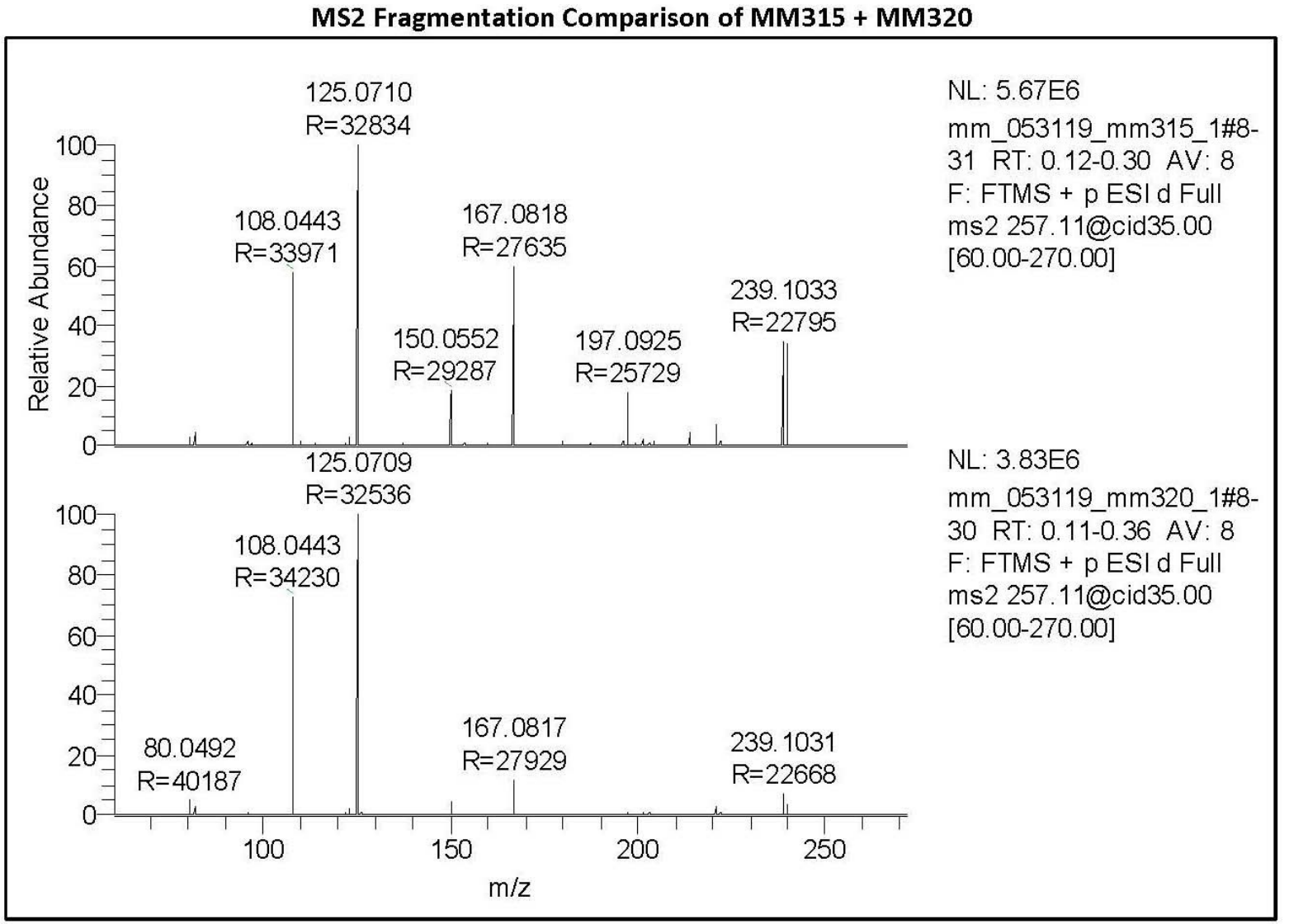

Fig. 67S Comparison of fragmentation of 1,2-NRH (**2**) (sample mm320) and 1,6-NRH (**3**) (sample mm315).